UNCLASSIFIED

[redacted]

NASA TECHNICAL MEMORANDUM

NASA TM X-856

NASA TM X-856

AERODYNAMIC AND STABILITY CHARACTERISTICS OF A PROPOSED HYPERSONIC GLIDER-BOOSTER COMBINATION AT MACH NUMBERS FROM 0.60 TO 3.52

by Norman J. Martin, Jules B. Dods, Jr., and Robert A. Taylor

Ames Research Center
Moffett Field, Calif.

NATIONAL AERONAUTICS AND SPACE ADMINISTRATION • WASHINGTON, D. C. • JUNE 1964

[redacted]

UNCLASSIFIED

UNCLASSIFIED
[redacted]

AERODYNAMIC AND STABILITY CHARACTERISTICS OF A PROPOSED HYPERSONIC GLIDER-BOOSTER COMBINATION AT MACH NUMBERS FROM 0.60 TO 3.52

By Norman J. Martin, Jules B. Dods, Jr.,
and Robert A. Taylor

Ames Research Center
Moffett Field, Calif.

GROUP 4
Downgraded at 3 year intervals;
declassified after 12 years

CLASSIFIED DOCUMENT—TITLE UNCLASSIFIED

This material contains information affecting the national defense of the United States within the meaning of the espionage laws, Title 18, U.S.C., Secs. 793 and 794, the transmission or revelation of which in any manner to an unauthorized person is prohibited by law.

NATIONAL AERONAUTICS AND SPACE ADMINISTRATION

[redacted]
UNCLASSIFIED

[redacted]

AERODYNAMIC AND STABILITY CHARACTERISTICS OF A PROPOSED HYPERSONIC GLIDER-BOOSTER COMBINATION AT MACH NUMBERS FROM 0.60 TO 3.52*

By Norman J. Martin, Jules B. Dods, Jr.,
and Robert A. Taylor

SUMMARY

The investigation was conducted to determine the static longitudinal and lateral aerodynamic characteristics of a proposed hypersonic glider-booster combination. This vehicle was tested at a Reynolds number of 3.0×10^6 per foot for all Mach numbers except 3.52; the Reynolds number for that Mach number was 2.5×10^6 per foot. The angle of attack varied from -8° to $+10^\circ$, and the angle of sideslip varied from -4° to $+8^\circ$.

The results indicate that for a typical trajectory the complete vehicle was longitudinally stable throughout the Mach number range investigated, and was directionally stable up to a Mach number of 2.6 at 0° and 5° angle of attack. Moderate directional instability occurred in the Mach number range from 2.6 to 3.5. At an angle of attack of -5°, directional stability was maintained only up to a Mach number of 2.2. The vehicle had a stable dihedral effect at 5° angle of attack, but an unstable effect at zero and negative angles of attack throughout the Mach number range. The dihedral effect at 0° angle of attack became stable when the deflection of the glider elevons was reduced from -10° to 0°. Differential deflection of the elevons was relatively ineffective in providing roll control of the vehicle.

Adding a skirt extension to the base of the booster provided moderate increases in both the longitudinal and lateral stability. Blast-vent openings located near the engines of the second stage of the booster had a negligible effect upon the aerodynamic characteristics.

INTRODUCTION

A continuing effort is being made to evaluate the aerodynamic characteristics of hypersonic glider and booster combinations. Results have been presented in reference 1, for the transonic speed range, for a proposed glider with several booster combinations. The present investigation, which was conducted in the Ames 11- by 11-foot, 9- by 7-foot, and 8- by 7-foot wind tunnels, provides data on a later version of the complete vehicle at Mach numbers from 0.60 to 3.52. In addition to the determination of the basic stability and aerodynamic characteristics, the secondary purposes of the investigation were to determine the effects of adding a skirt extension to the base of the booster, the effect of blast vent

*Title, Unclassified

[redacted]

openings near the engines of the second stage of the booster, the effectiveness of the glider elevons, and the effect of changes in the incidence of the glider.

NOTATION

A	aspect ratio of glider wing
b	span of glider
b_f	span of booster fins
c	chord of the glider wing
c_f	chord of the booster fins
$\bar{c}$	mean aerodynamic chord of the glider wing
$\bar{c}_f$	mean aerodynamic chord of the booster fins
c.g.	center of gravity of complete vehicle
C_A	forebody axial force coefficient, $\frac{\text{(total axial force)} - \text{(base axial force)}}{q_\infty S}$
C_{H_f}	fin hinge-moment coefficient, $\frac{\text{fin hinge moment}}{q_\infty S_f \bar{c}_f}$
C_l	rolling-moment coefficient, $\frac{\text{rolling moment}}{q_\infty S b}$
C_{l_β}	rate of change of rolling-moment coefficient with angle of sideslip measured through $\beta = 0^\circ$, $\frac{\partial C_l}{\partial \beta}$, per deg
C_{l_f}	fin root-bending-moment coefficient, $\frac{\text{root bending moment}}{q_\infty S_f b_f}$
C_m	pitching-moment coefficient, $\frac{\text{pitching moment}}{q_\infty S \bar{c}}$
C_{m_o}	pitching-moment coefficient at zero normal force
$C_{m_{\delta_e}}$	rate of change of pitching moment with angle of elevon deflection, $\frac{\partial C_m}{\partial \delta_e}$, per deg
C_n	yawing-moment coefficient, $\frac{\text{yawing moment}}{q_\infty S b}$

C_{n_β} rate of change of yawing-moment coefficient with angle of sideslip measured through $\beta = 0^\circ$, $\frac{\partial C_n}{\partial \beta}$, per deg

C_N normal-force coefficient, $\frac{\text{normal force}}{q_\infty S}$

C_{N_α} rate of change of normal-force coefficient with angle of attack measured through $\alpha = 0^\circ$, $\frac{\partial C_N}{\partial \alpha}$, per deg

C_{N_f} fin normal-force coefficient, $\frac{\text{fin normal force}}{q_\infty S_f}$

C_Y side-force coefficient, $\frac{\text{side force}}{q_\infty S}$

C_{Y_β} rate of change of side-force coefficient with angle of sideslip measured through $\beta = 0^\circ$, $\frac{\partial C_Y}{\partial \beta}$, per deg

d spanwise distance to fin mean aerodynamic chord, in.

i_g incidence of glider (wing lower surface) with respect to the booster center line, deg

l vehicle length from model station 5.219 to 62.797 (57.578 in.)

M_∞ free-stream Mach number

q_∞ free-stream dynamic pressure

S glider wing area, ft^2

S_e elevon area of glider wing (total), ft^2

S_v vertical fin area of glider (total), ft^2

S_f booster fin area (each fin), ft^2

t thickness, in.

α angle of attack, deg (referred to booster center line)

β angle of sideslip (referred to booster center line), deg

δ_e elevon deflection, deg

δ_H nominal horizontal fin deflections (See table III for measured fin deflections.)

δ_V nominal vertical fin deflections (See table III for measured fin deflections.)

ϵ downwash angle, deg

Λ angle of sweepback of leading edge of glider, deg

Subscripts

r root

t tip

R right

L left

APPARATUS AND MODEL

The tests were conducted in the 11- by 11-foot, 9- by 7-foot, and the 8- by 7-foot wind tunnels, which are closed-circuit, variable-pressure type tunnels, and which have Mach number ranges from 0.60 to 1.40, 1.55 to 2.51, and 2.48 to 3.52, respectively.

The basic model configuration (fig. 1) was a 0.04-scale hypersonic glider mounted on a finned two-stage booster, with blast-vent openings near the engines of the second stage. The aspect ratios of the vertical and horizontal fins of the booster were 2.0 and 3.0, respectively. Modifications to the model consisted of adding a skirt extension to the base of the booster, closing the blast vents, changing the basic glider elevon deflection, changing the incidence of the glider, and increasing the aspect ratio of the vertical fin from 2.0 to 3.0. The geometric characteristics of the model and booster fin are given in tables I and II.

The model was sting mounted on a 6-component, 2-inch-diameter, strain-gage balance. Forces and moments were also measured on the left horizontal booster fin and on the upper vertical booster fin (aspect ratio 3 only) by the use of strain gages mounted on the root of the fin. A typical installation of the model in one of the wind tunnels (9 by 7 foot) is shown in figure 2.

TEST PROCEDURE

The wind-tunnel tests were made throughout the Mach number range for angles of attack from -8° to $+10^{\circ}$ and angles of sideslip from -4° to $+8^{\circ}$. A constant Reynolds number of 3.0×10^{6} per foot was maintained up to a Mach number of 3.05. The Reynolds number for $M_{\infty} = 3.52$ was reduced to 2.5×10^{6} per foot because of power limitations.

The complete vehicle was tested with the elevons deflected to -10°, 0°, and differentially with the right elevon deflected 20° and the left elevon deflected

-20°. Incidence was changed by rotating the glider so that the lower surface of the glider wing was at an angle of -1° and $+3^{\circ}$ with respect to the booster center line. Unless specifically noted, the elevon deflection was -10° and the incidence of the glider was 1°.

All tests were made with fixed transition on the glider wings, vertical fins, and nose, aft of the pilot canopy, and on the vertical and horizontal booster fins. The method of fixing transition conformed to the procedures found by previous experience in the individual wind tunnels to be the most satisfactory. For the 11- by 11-foot wind tunnel, number 80 carborundum grains were set in adhesive bands 0.25 inch wide at each location. For both of the supersonic test sections small triangles of tape, approximately 0.10 inch on a side, were used. These triangles were 0.014 inch thick for tests in the 9- by 7-foot wind tunnel and 0.035 inch thick for tests in the 8- by 7-foot wind tunnel.

MEASUREMENTS AND ACCURACY

The aerodynamic force and moment coefficients for the complete vehicle were based upon the glider wing dimensions and were referred to the body-axes system. The pitching moments were referred to model station 45.932 (see fig. 1). The angles of attack and sideslip of the vehicle were referred to the booster center line. The force and moment coefficients of the booster fins were based on the individual fin dimensions. The fin hinge moments were taken about the fin center line (M.S. 61.052), and the root bending moments were taken about the fin root chord. The axial-force coefficient has been adjusted for the difference between the booster base pressure and free-stream static pressure, and the angles of attack and sideslip have been corrected for sting deflection and air-stream inclination. A comparison of the data at several Mach numbers over a range of Reynolds numbers indicated that there were no significant Reynolds number effects.

The estimated precision of the data is as follows:

$C_N = \pm 0.05$	$C_l = \pm 0.005$
$C_m = \pm 0.02$	$\alpha = \pm 0.2^{\circ}$
$C_A = \pm 0.02$	$\beta = \pm 0.2^{\circ}$
$C_Y = \pm 0.02$	$M_{\infty} = \pm 0.02$
$C_n = \pm 0.01$	

The values of the nominal and the measured angles of fin deflection are given in table III.

RESULTS AND DISCUSSION

The basic longitudinal and lateral aerodynamic characteristics of the vehicle with and without booster fins are presented in figures 3 and 4, respectively. The variations of the force and stability parameters derived from these figures as a function of the Mach number are summarized in figure 5. The effect of the base-skirt extension is shown in figure 6. The effect of blast-vent openings is shown in figures 7 and 8. The effects of glider elevon deflection are summarized in figure 9. Figure 10 illustrates the effect of glider incidence upon the pitching moment at zero normal force. The downwash characteristics are shown in figure 11. Figure 12 presents the aerodynamic coefficients of the left horizontal booster fin and figure 13 presents the aerodynamic coefficients of the aspect ratio 3 upper vertical fin. The centers of pressure for these fins are given in figures 14 and 15.

Longitudinal and Lateral Aerodynamic Characteristics

Characteristics of the basic configuration.- The basic longitudinal and lateral stability data presented in figures 3 and 4, and summarized in figure 5, are for the pitching- and yawing-moment coefficients referred to a point at 70.7 percent of the vehicle length (M.S. 45.932). These data were used to calculate the longitudinal and lateral center-of-pressure positions in terms of the vehicle length, l, as a function of the Mach number. In order to evaluate the stability of the vehicle, these center-of-pressure positions are compared to the center-of-gravity positions for a typical trajectory in figures 5(f) and (g).

Figure 5(g) shows that the vehicle had a positive longitudinal stability margin throughout the Mach number range investigated, but the amount of the margin was reduced with increasing Mach number. The stability margin was also reduced in the subsonic and low supersonic Mach number range by increasing the angle of sideslip. This effect is not significant, however, because the stability margin for the assumed trajectory is relatively large in these regions. At the higher Mach numbers there was no effect due to sideslip.

As shown in figures 5(a) and (b) the axial-force coefficient and the normal-force curve slope were insensitive to changes in the angle of sideslip throughout the Mach number range.

As shown in figure 5(f), a positive directional stability margin was maintained up to a Mach number of about 2.6 for the vehicle at 0° and 5° angle of attack, with moderate instability occurring in the Mach number range from 2.6 to 3.5. At an angle of attack of -5°, however, directional stability was maintained only up to a Mach number of 2.2.

The vehicle had a stable dihedral effect at an angle of attack of 5°, but it was unstable at 0° and -5° (fig. 5(e)).

Effect of base-skirt extension.- The base-skirt extension (see fig. 1) was added to the booster to compensate for the extension of the fins beyond the base.

It was reasoned that the addition of this cylindrical structure would provide an end plate for each fin, thereby increasing their effectiveness. As shown in figure 6(b), this modification does provide an increased longitudinal stability margin in the low supersonic Mach number range (the center of pressure was displaced rearward by about 3 percent at a Mach number of 1.3), but the increased stability effect decreases at the higher Mach numbers.

The lateral stability margin was also increased as shown in figure 6(a). For Mach numbers greater than about 1.5, the lateral center of pressure was shifted rearward about 2 percent.

Effect of blast vents.- No appreciable effect on the longitudinal or the lateral aerodynamic characteristics was measured through the Mach number range from 0.60 to 2.51. Typical data for the extremes of the Mach number range for which tests were made are presented in figures 7 and 8.

Effect of elevon deflection.- A limited amount of data was obtained to investigate the effectiveness of the elevons on the glider wing in providing pitching- and rolling-moment control of the complete vehicle. As shown in figure 9(a), changing the elevon deflection from the basic -10° to 0° deflection caused a stable dihedral effect. Differential deflection of the elevons was relatively ineffective in providing rolling-moment control. The pitching-moment effectiveness parameter, $C_{m_{\delta_e}}$, which was evaluated using the data for 0° and -10° elevon deflection, decreased rapidly with increasing Mach number (fig. 9(b)).

Effect of glider incidence.- The effects of glider incidence on the pitching-moment coefficient at zero normal-force coefficient, C_{m_0}, are shown in figures 10(a) and (b). A glider incidence of about 1.8° is required for a $C_{m_0} = 0$ in the low supersonic Mach number range (1.3 to 1.5) for the rigid vehicle, while values of about 2.9° are required for either subsonic or higher supersonic Mach numbers. (A rigid vehicle is specified because the choice of the glider incidence would also depend upon aeroelastic, and possibly, thermoelastic effects.)

Downwash effects.- The downwash characteristics throughout the Mach number range tested are shown in figures 11(a) through (k). The downwash angle was evaluated from the equation

$$\epsilon = \frac{\Delta C_m}{\left(C_{m_{\delta_H}}\right)_{\alpha=0}} \tag{1}$$

where ΔC_m is the incremental pitching moment due to the effective downwash at the tail, and $\left(C_{m_{\delta_H}}\right)_{\alpha=0}$ is the fin-effectiveness parameter. To evaluate the increment ΔC_m the pitching-moment coefficients with the tail on and off were compared with those produced by incremental fin deflections. The downwash angle obtained by this procedure is termed an effective angle since some secondary interference effects on the tail are not accounted for.

The rate of change of downwash angle with angle of attack, $d\epsilon/d\alpha$, was negative (decreasing downwash with increasing angle of attack) throughout the Mach number range, and, above a Mach number of 1.3, $d\epsilon/d\alpha$ became progressively more negative. In the subsonic and transonic range, however, rather large and erratic variations of $d\epsilon/d\alpha$ with Mach number were observed.

Aerodynamic Characteristics of the Booster Fins

Horizontal fins.- The normal-force, hinge-moment, and root-bending-moment coefficients of the left horizontal booster fin for various Mach numbers are presented in figure 12. These data have been used to compute the chordwise and spanwise center-of-pressure positions at 0° angle of attack. The results, summarized in figure 14, show the shift in the center of pressure with Mach number and with angle of sideslip. In general, the center of pressure shifted rearward by about 25-percent $\bar{c}_f$ between the subsonic and supersonic Mach numbers, regardless of the angle of sideslip. The effect of 6° angle of sideslip was to shift the spanwise center of pressure outboard by between 5- and 14-percent b_f from subsonic to low supersonic Mach numbers (1.55) and from 3 to 21 percent in the Mach number range from 2 to 3.5. The variation of these spanwise shifts due to sideslip was not a linear function of the Mach number, however, and would be difficult to predict analytically.

As mentioned previously, the effect of blast vents upon the longitudinal and lateral aerodynamic characteristics of the vehicle was negligible. Similarly, the fin aerodynamic characteristics were not affected by the blast vent openings. The substantiating data, which were obtained only up to a Mach number of 2.5, have been omitted from figure 12 in the interests of clarity.

Vertical fins.- As shown in figure 1(c), the aspect ratio of the vertical fins was 2.0 for the basic configuration. Although no inidividual forces and moments were measured upon these fins because they were not instrumented, a limited test program was conducted with an instrumented upper vertical fin of aspect ratio 3.0. The test results are presented in figure 13, and the center-of-pressure locations computed from these data for the intermediate Mach number range are presented in figure 15.

Ames Research Center
National Aeronautics and Space Administration
Moffett Field, Calif., Nov. 12, 1963

REFERENCE

1. Bielat, Ralph P.: A Transonic Wind-Tunnel Investigation of the Static Longitudinal and Lateral Aerodynamic Characteristics of a Proposed Hypersonic Glider With Several Booster Configurations. NASA TM X-345, 1960.

[redacted]

TABLE I.- MODEL GEOMETRIC CHARACTERISTICS

A	1.2
b, ft	0.809
$\bar{c}$, ft	0.820
S, ft^2	0.546
S_e, ft^2	0.076
S_v, ft^2	0.099
Λ, deg	73.0
Area of glider base, ft^2	0.039
Distance of glider nose (actual) to beginning $\bar{c}$, ft	0.430
Distance of glider center line to $\bar{c}$, ft	0.149
Glider c.g., percent $\bar{c}$	45.0
Area of booster base, ft^2	0.126
Diameter of booster, ft	0.40

[redacted]

TABLE II.- BOOSTER FIN GEOMETRY

	Normal configuration		Alternate
	A=2 vertical	A=3 horizontal	A=3 vertical
$\bar{c}_f$, ft	0.382	0.488	0.312
t/c_f	.060	.060	.060
c_{f_t}/c_{f_r}	.500	.500	.500
S_f, ft^2	.136	.332	.136
c_{f_t}, in.	2.940	3.764	2.409
c_{f_r}, in.	5.880	7.527	4.818
b_f, in.	4.440	8.468	5.420
d, in.	2.468	3.764	2.409
t_t, in.	.176	.226	.145
t_r, in.	.356	.452	.289

TABLE III.- NOMINAL AND MEASURED FIN DEFLECTIONS

δ_H, deg	Right fin, deg	Left fin, deg
-6	-6.01	-5.91
-2	-1.90	-1.96
0	.03	.07
1	1.05	1.13
4	4.11	4.03
6	6.03	6.16
δ_V, deg	Upper fin, deg	Lower fin, deg
-1	-1.00	-1.02
0	.02	.06
2	1.97	2.04
4	4.01	4.01

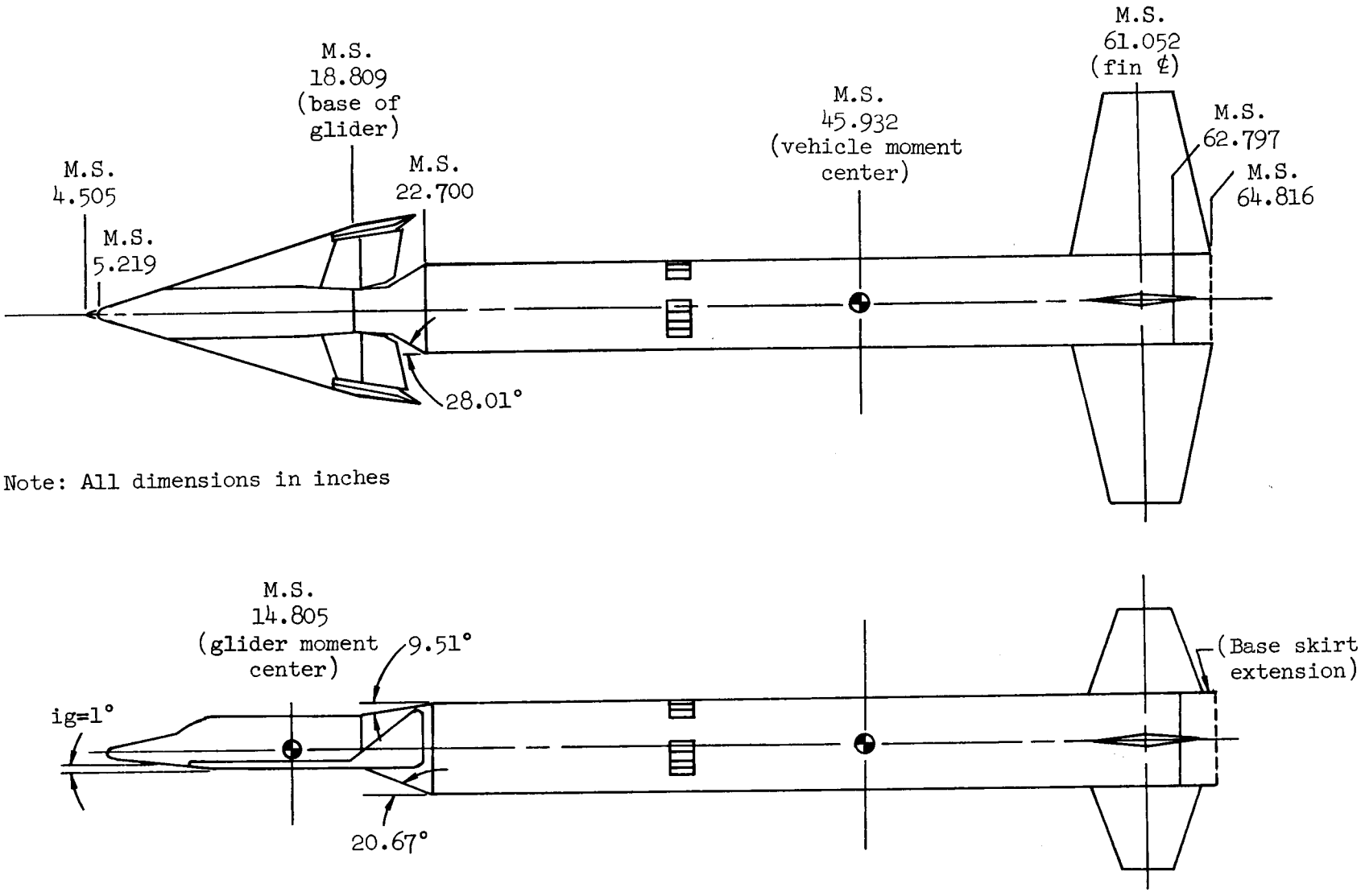

(a) Plan and elevation view of an 0.04-scale model of the vehicle.

Figure 1.- Model arrangement and details of an 0.04-scale model of the vehicle.

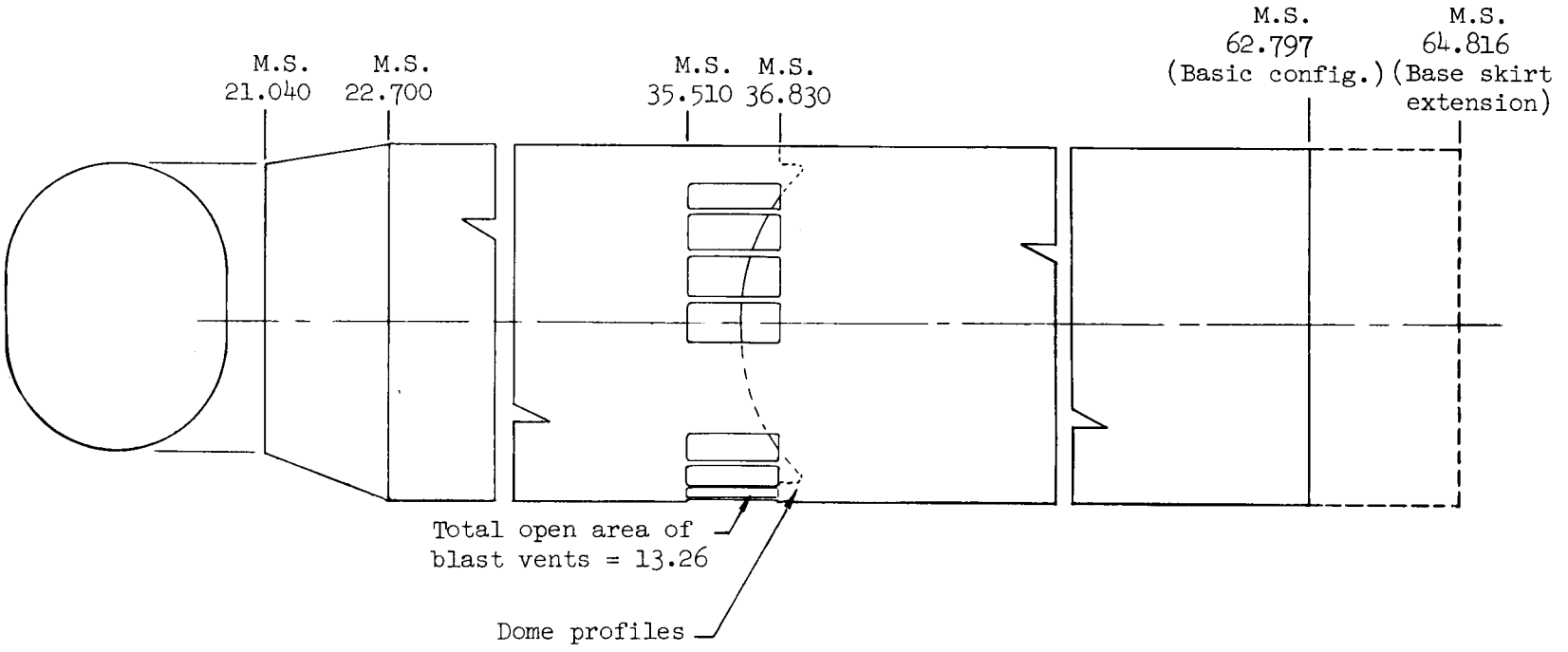

Note: All dimensions in inches

(b) Booster details.

Figure 1.- Continued.

[redacted]

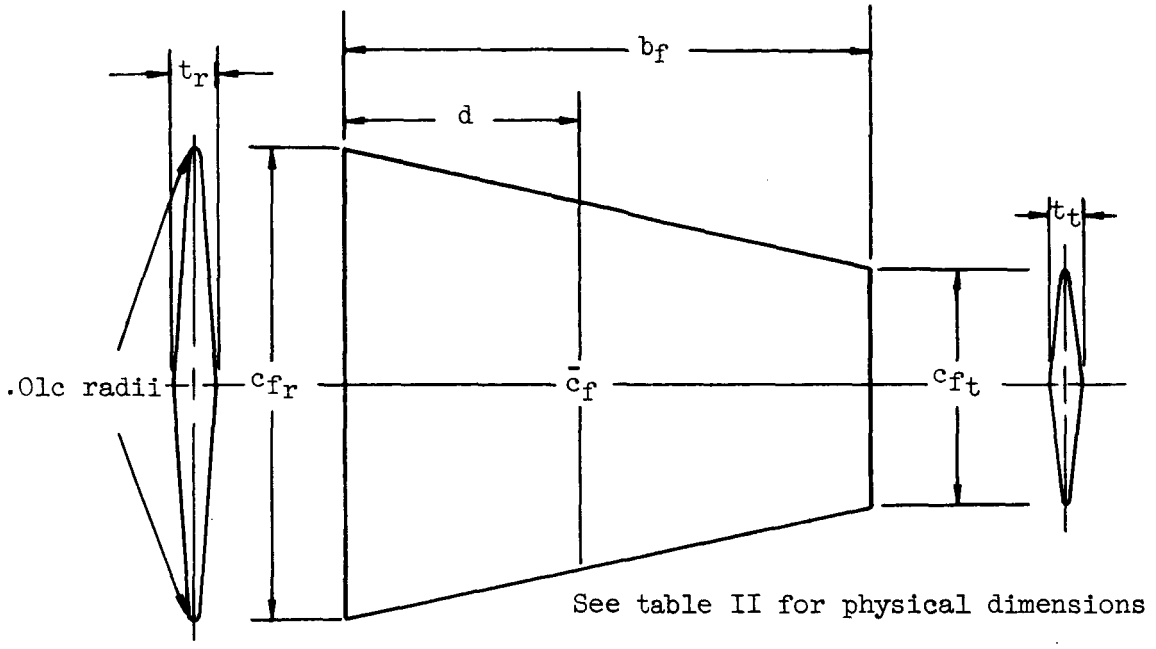

(c) Booster fin geometry.

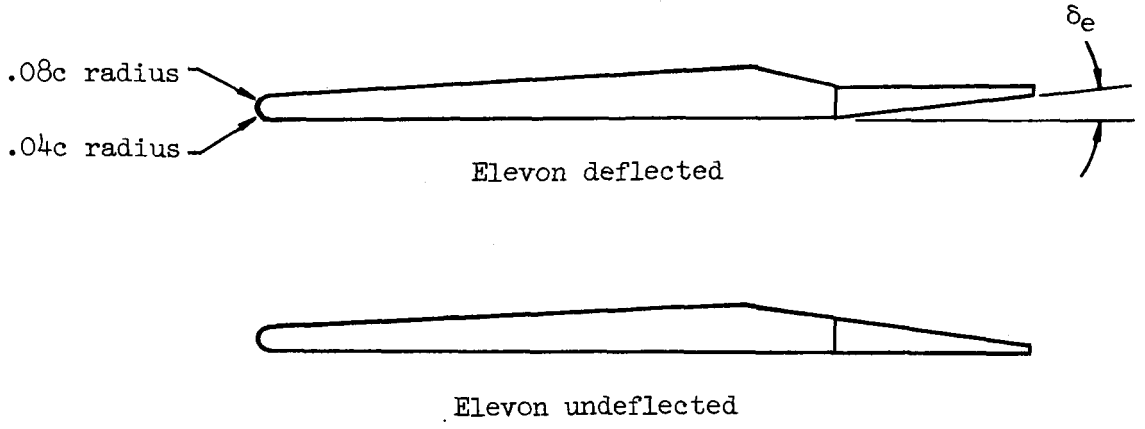

(d) Glider wing profile showing reference for elevon deflection.

Figure 1.- Concluded.

[redacted]

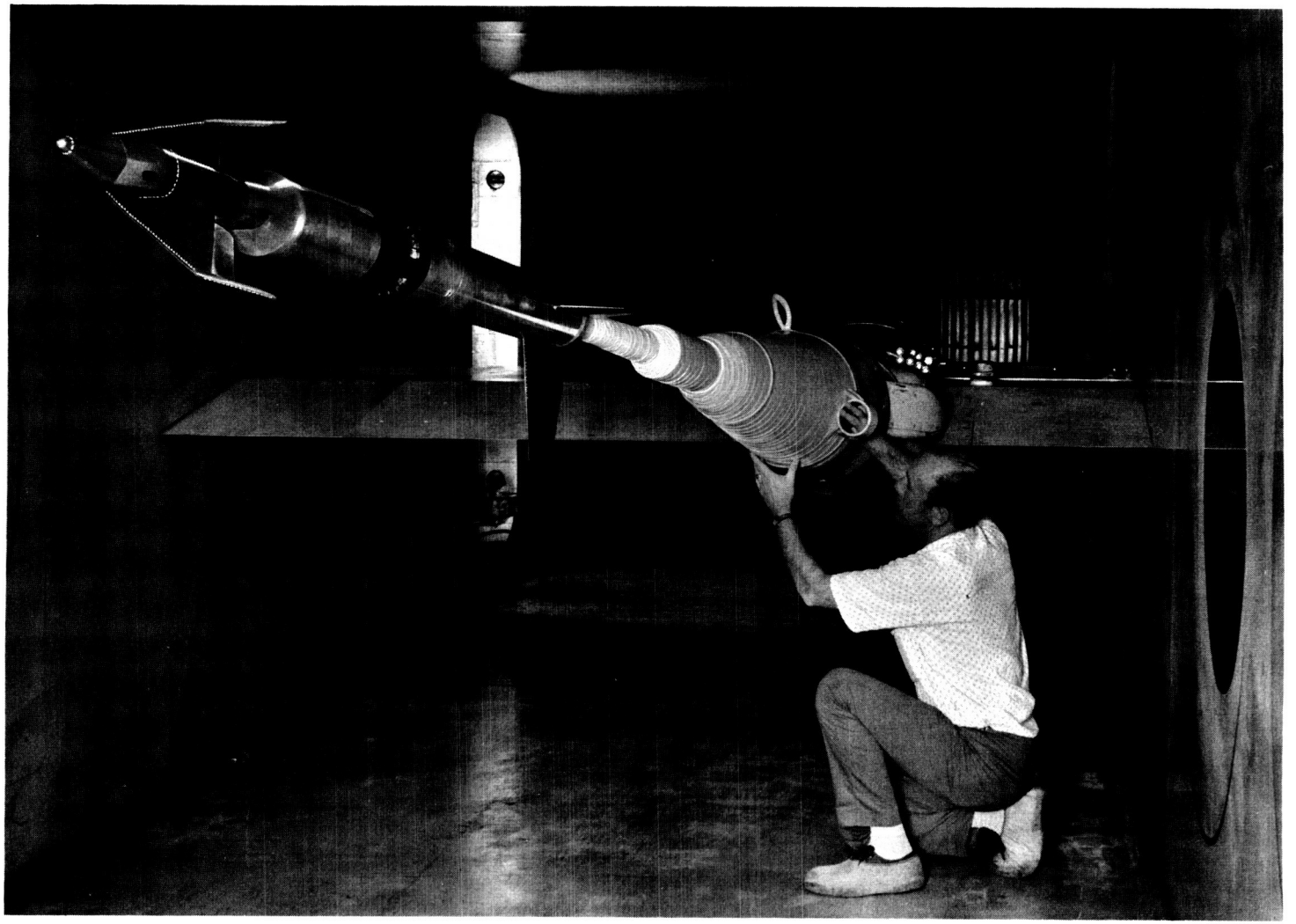

A-27822

(a) Top view.

Figure 2.- View of the 0.04-scale model of the vehicle mounted in the tunnel.

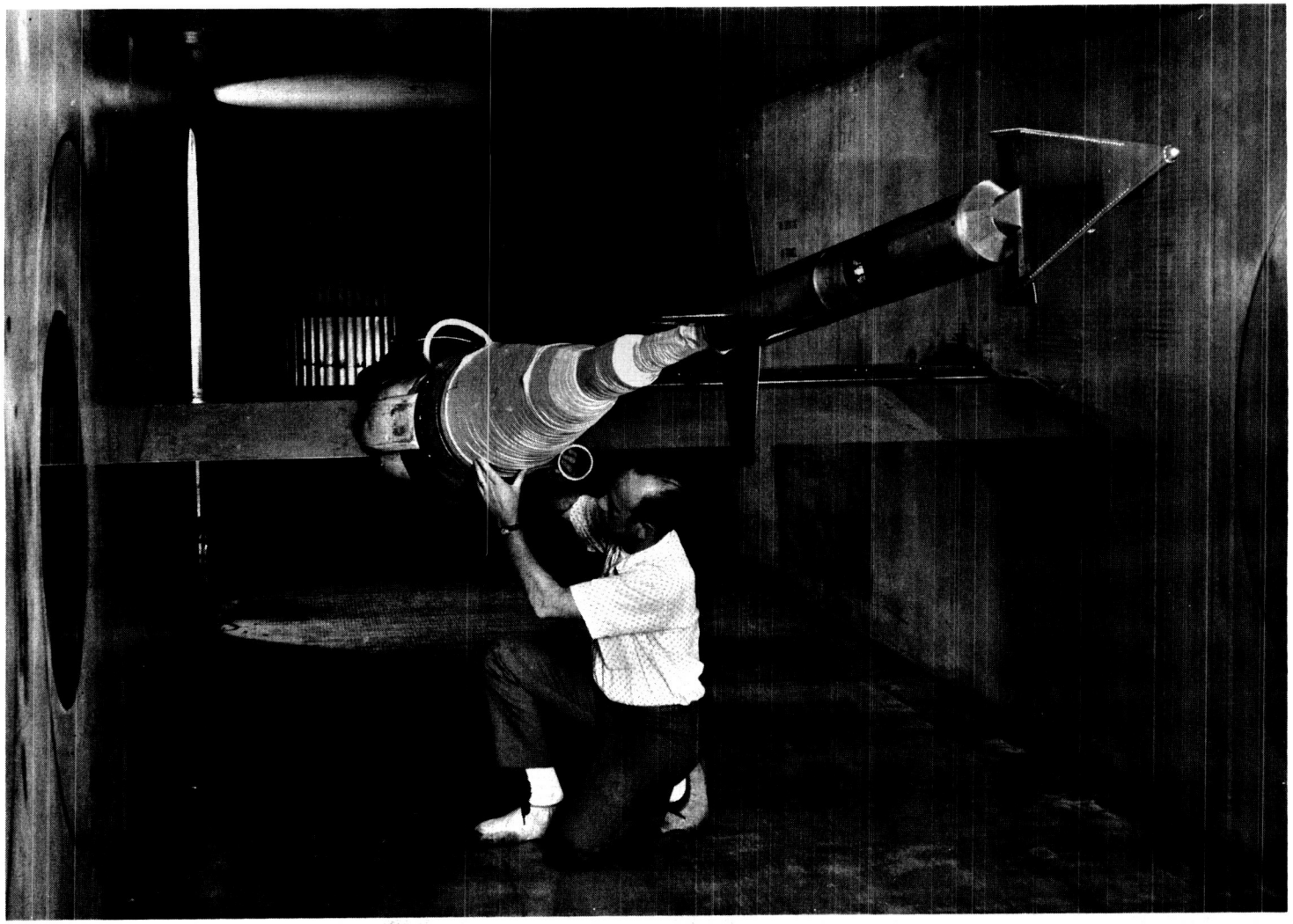

A-27823

(b) Bottom view.

Figure 2.- Concluded.

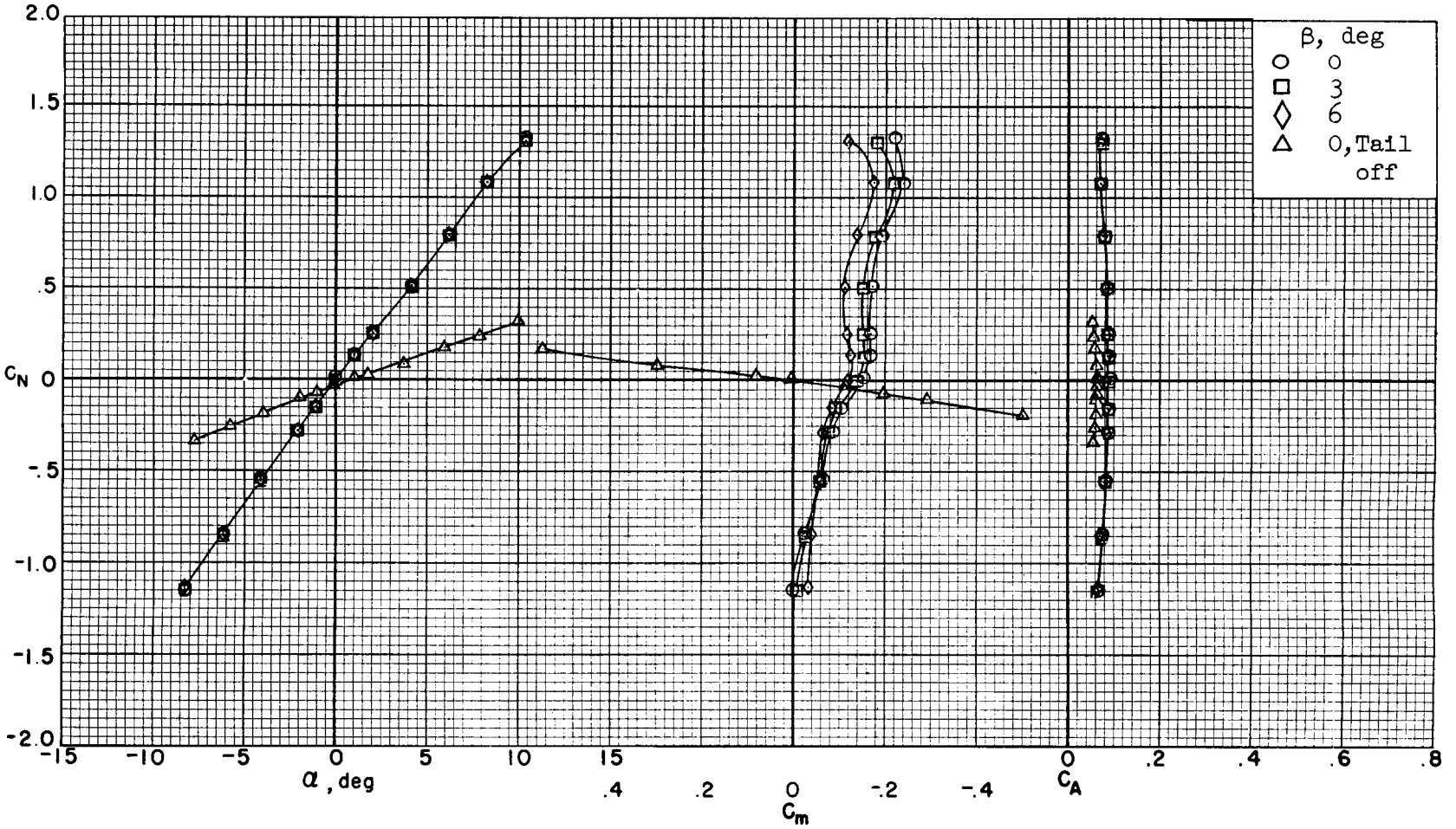

(a) $M_\infty = 0.60$

Figure 3.- The longitudinal aerodynamic characteristics of the vehicle at several free-stream Mach numbers.

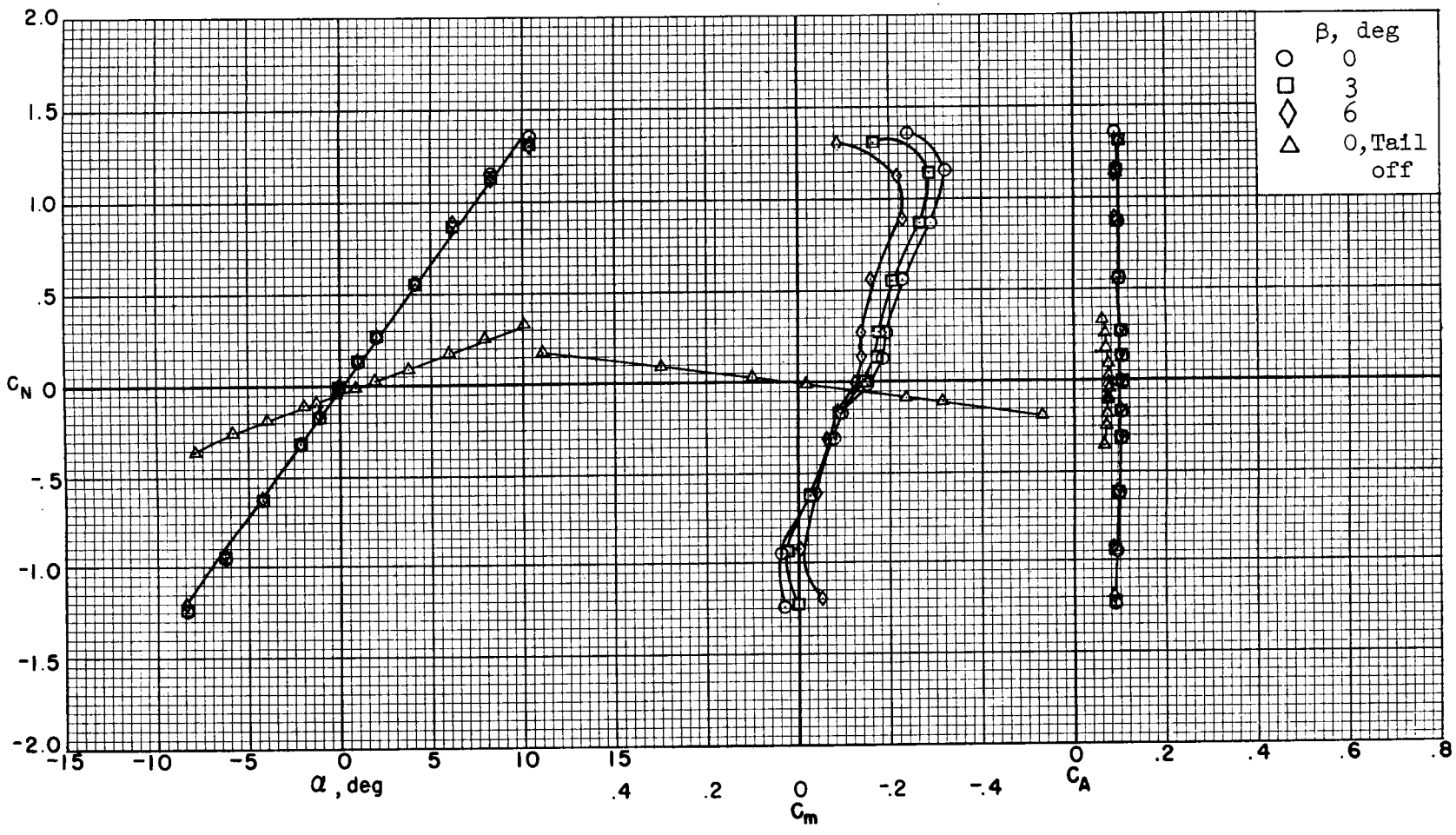

(b) $M_\infty = 0.80$

Figure 3.- Continued.

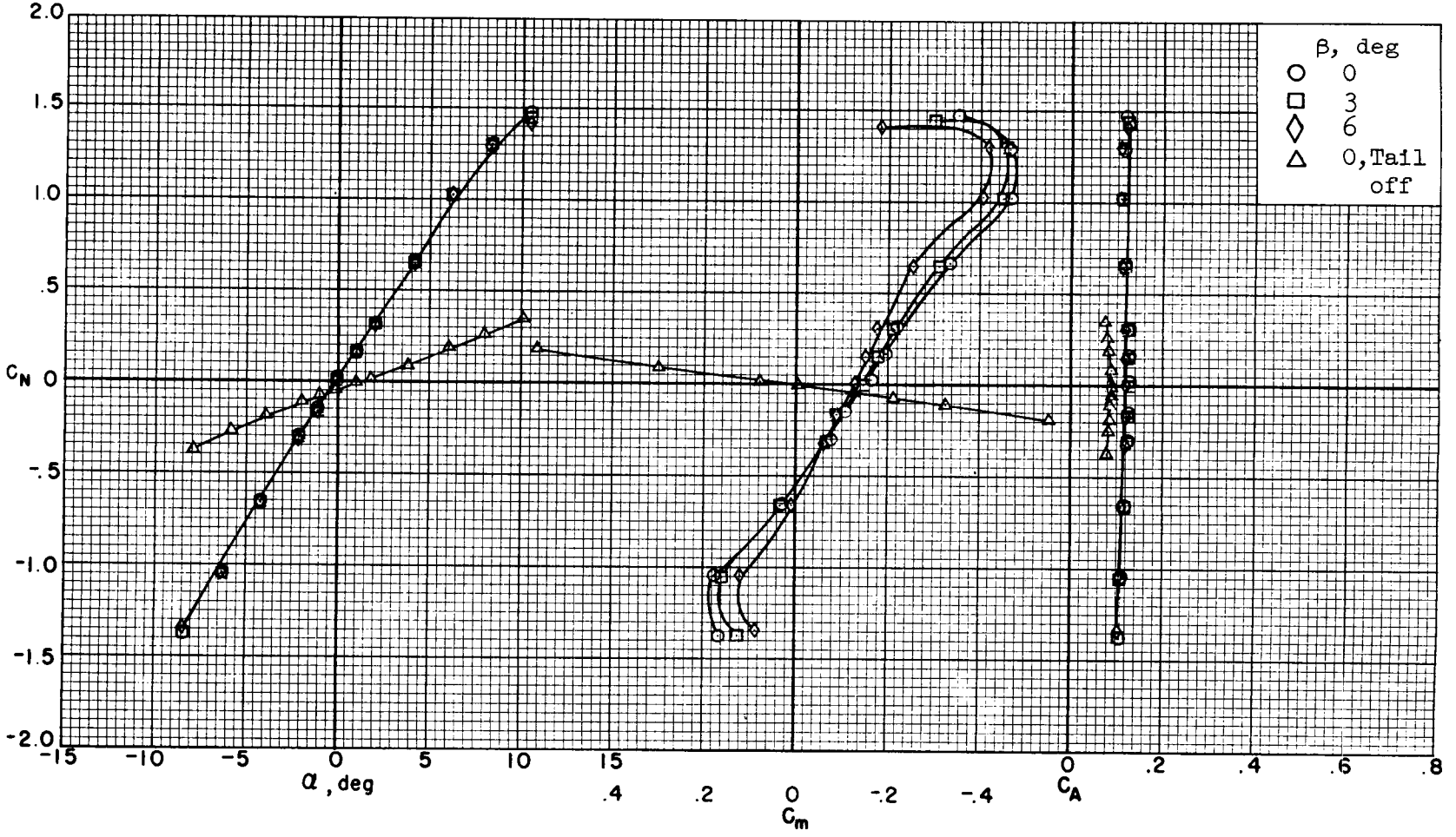

(c) $M_\infty = 0.90$

Figure 3.- Continued.

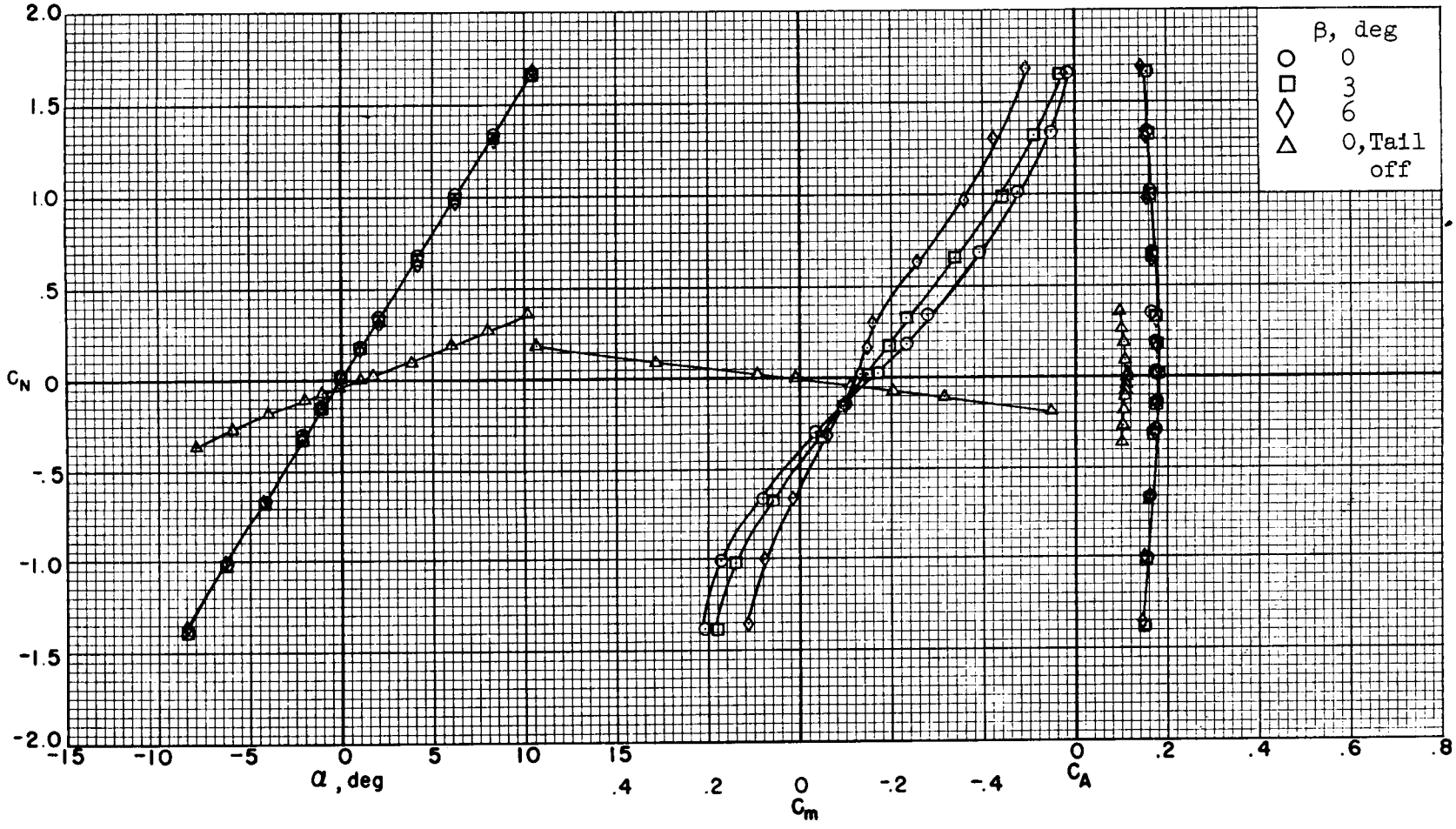

(d) $M_\infty = 1.00$

Figure 3.- Continued.

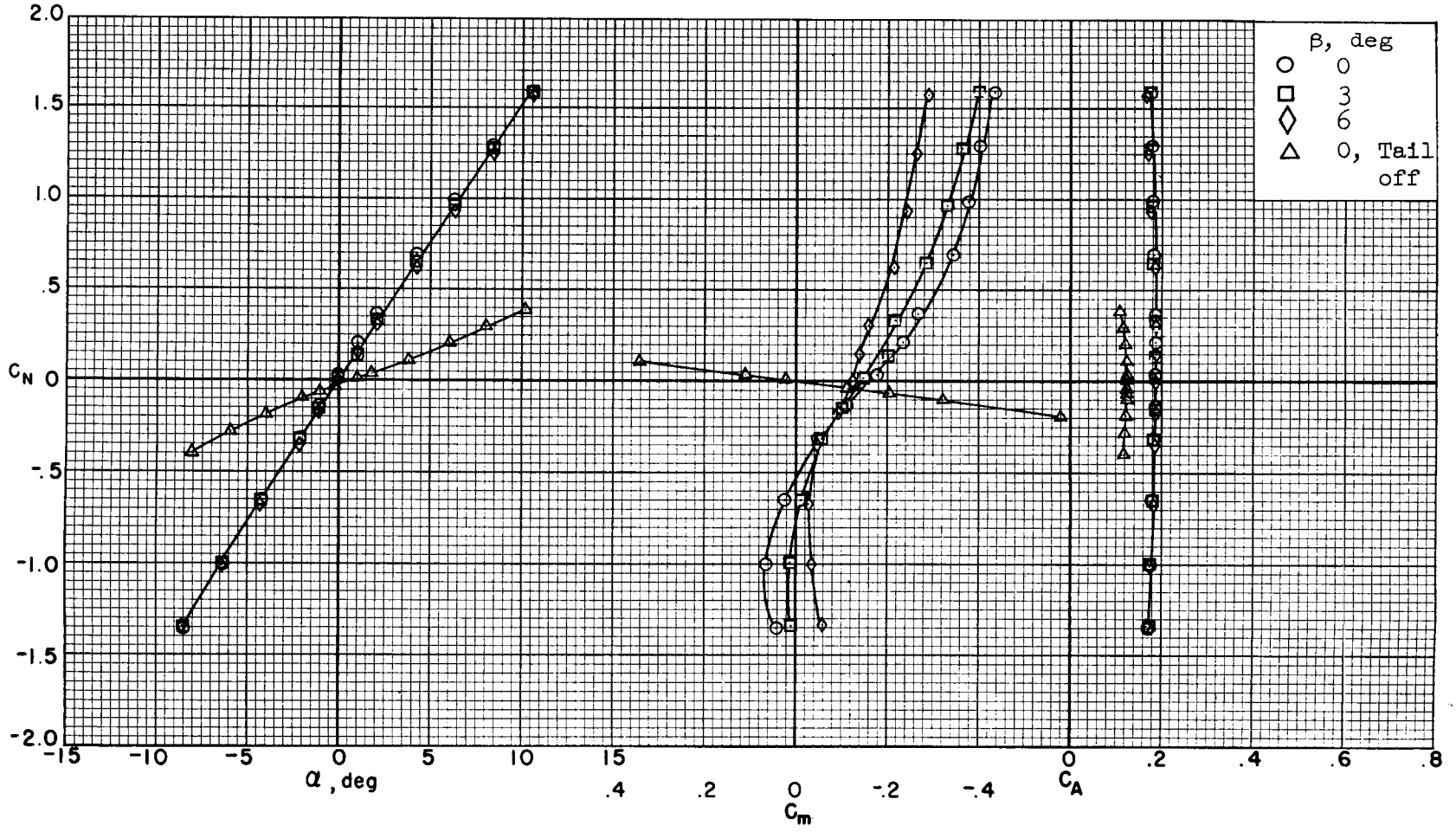

(e) $M_\infty = 1.10$

Figure 3.- Continued.

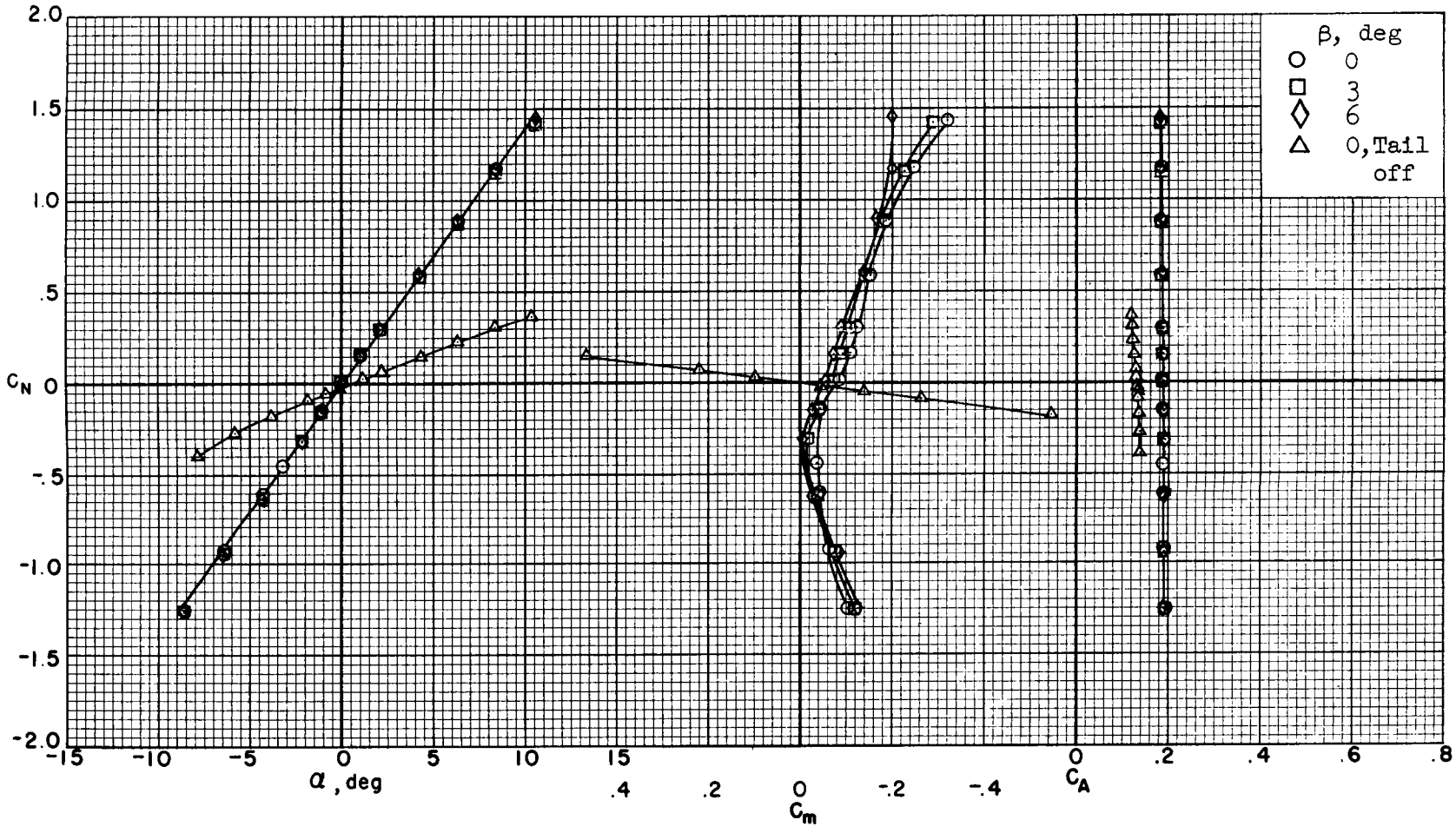

(f) $M_\infty = 1.30$

Figure 3.- Continued.

[redacted]

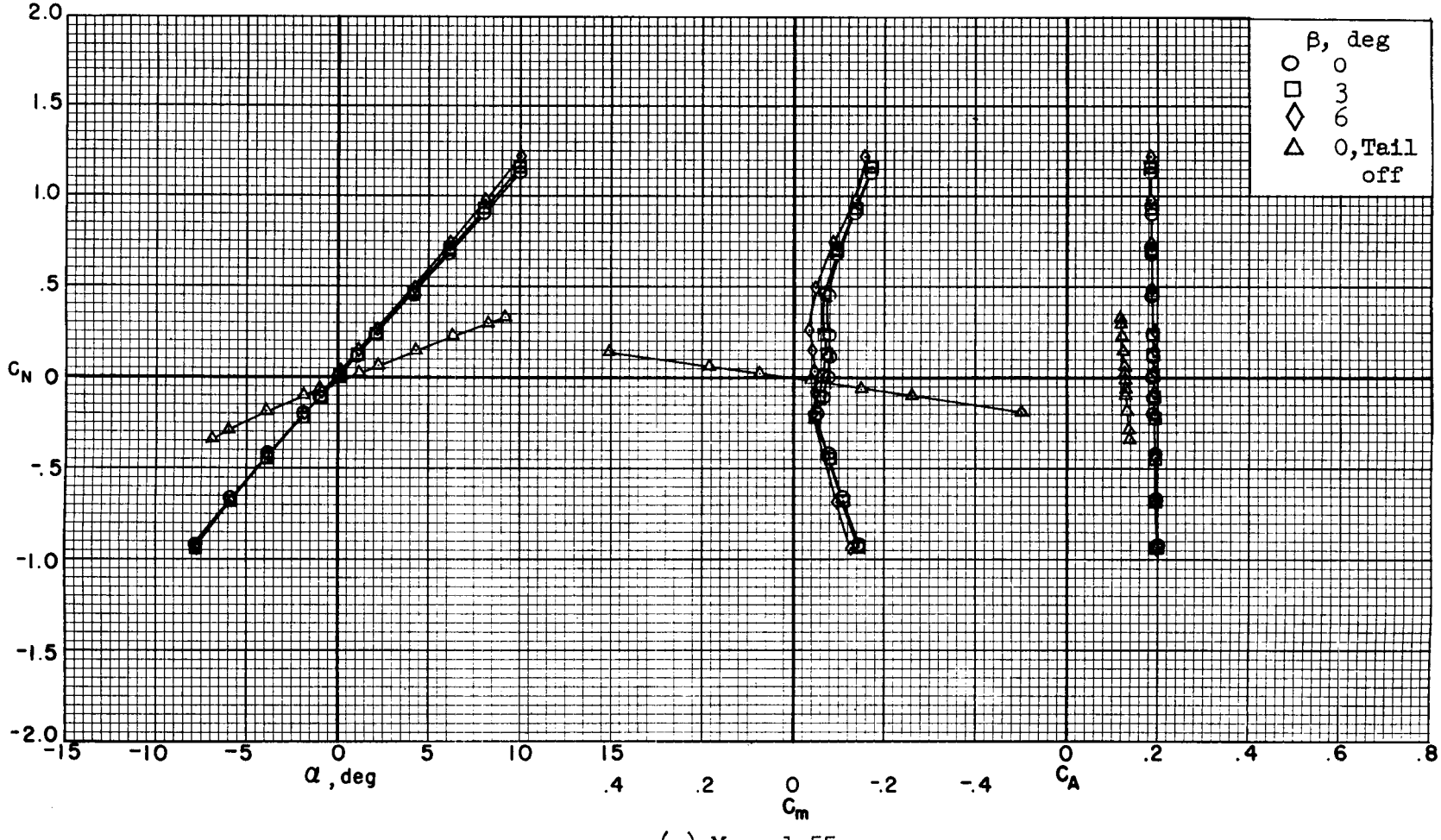

[redacted]

(g) $M_\infty = 1.55$

Figure 3.- Continued.

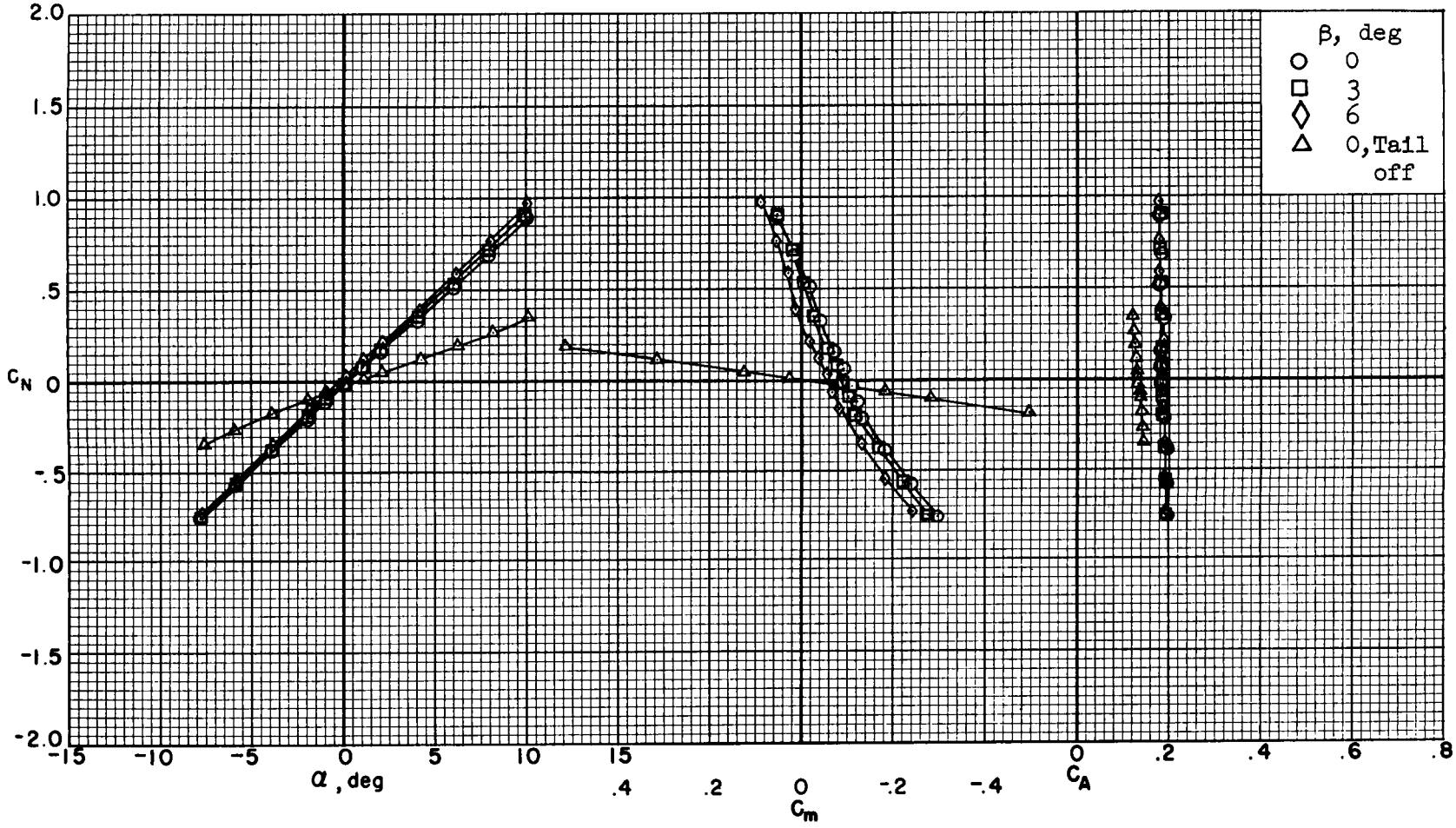

(h) $M_\infty = 2.01$

Figure 3.- Continued.

[redacted]

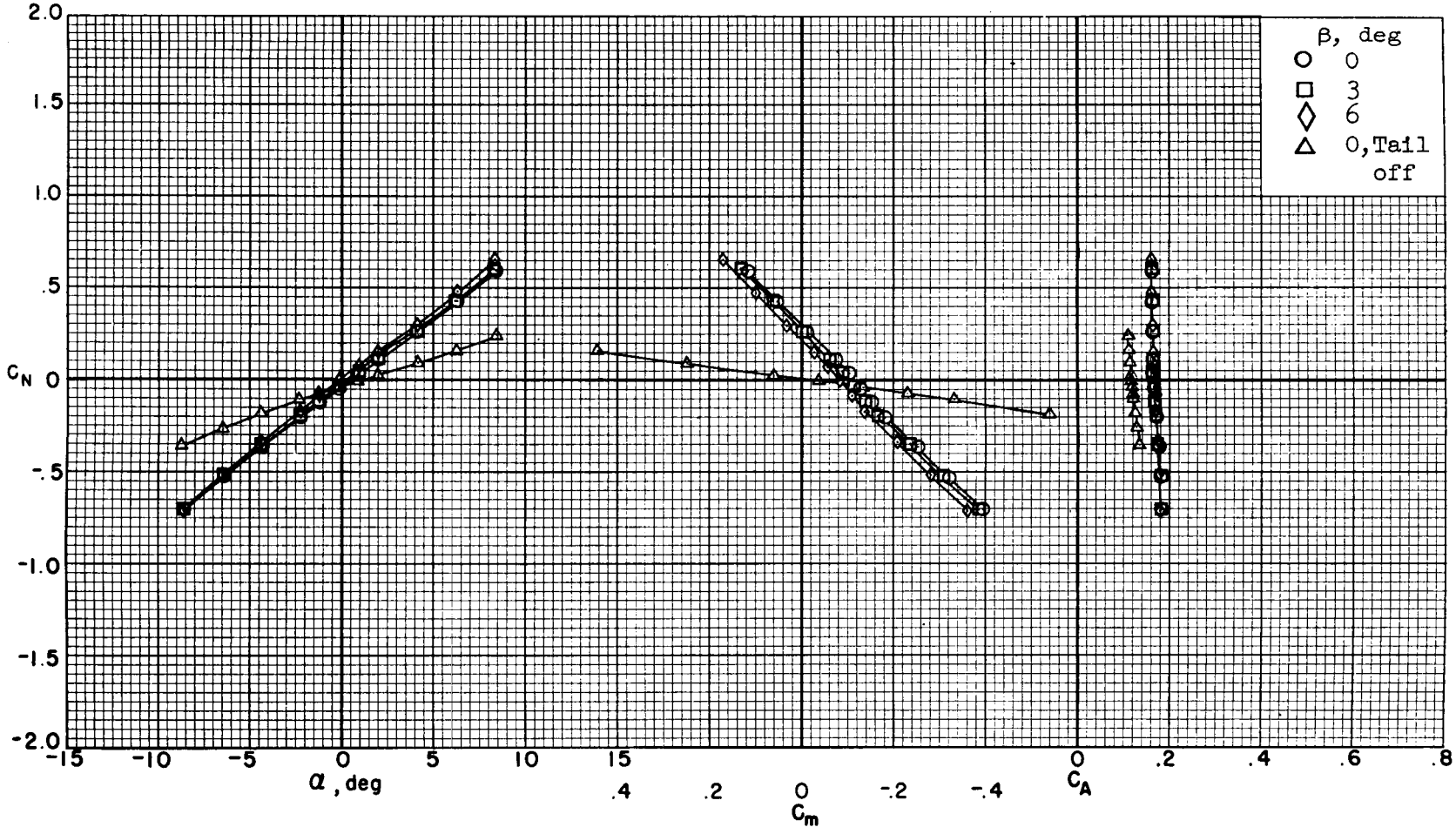

(i) $M_\infty = 2.48$

Figure 3.- Continued.

[redacted]

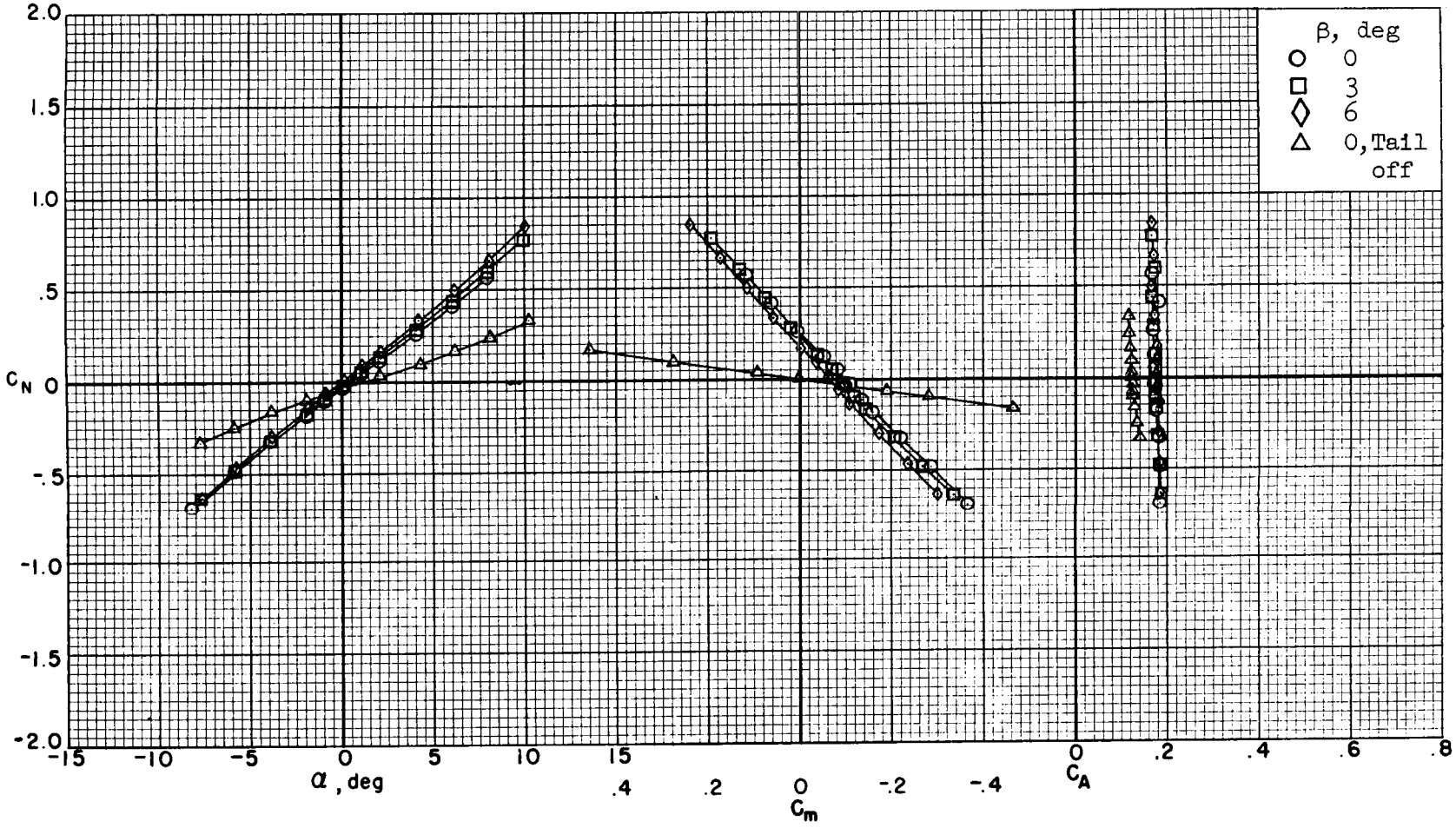

(j) $M_\infty = 2.51$

Figure 3.- Continued.

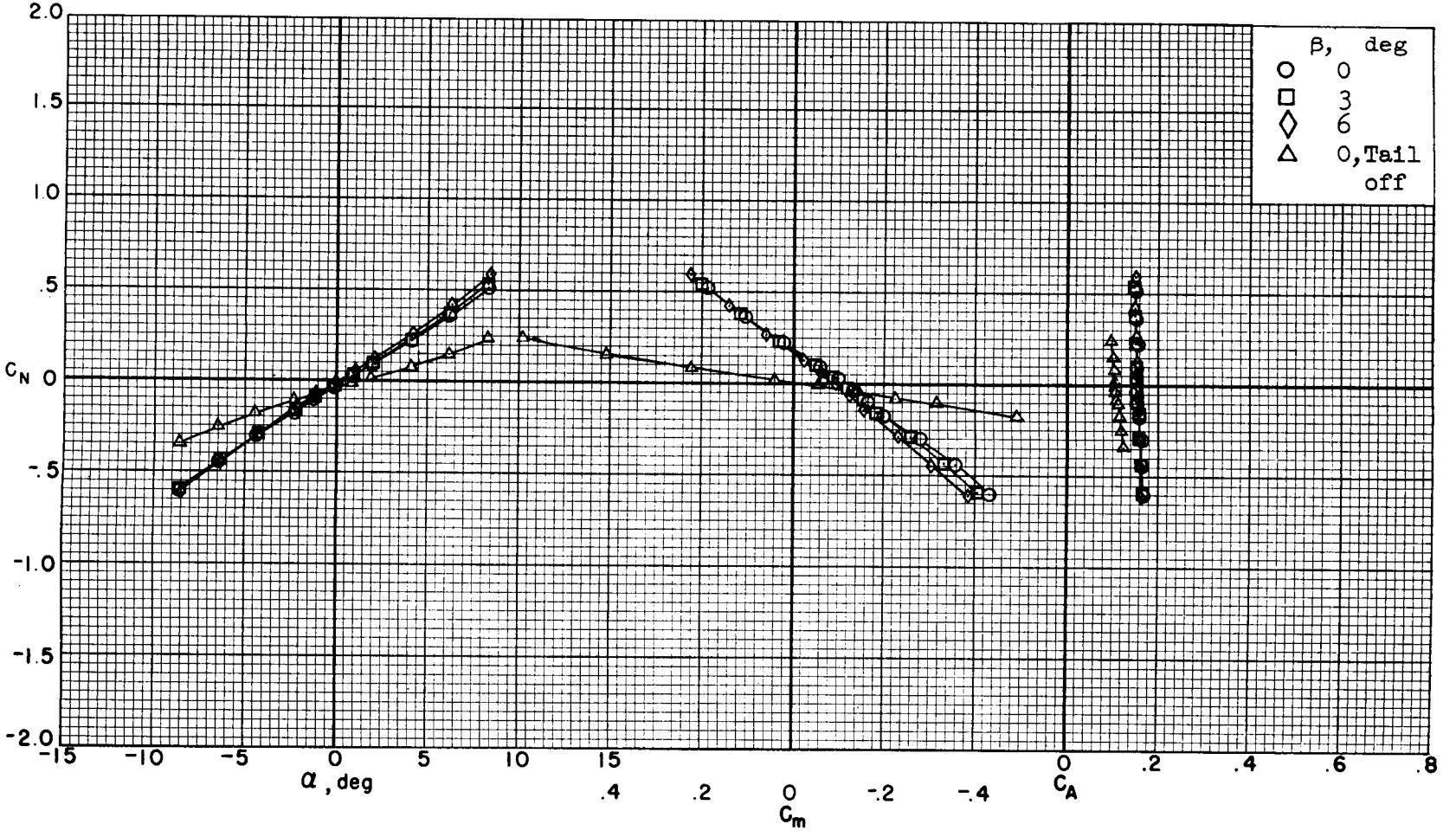

(k) $M_\infty = 3.05$

Figure 3.- Continued.

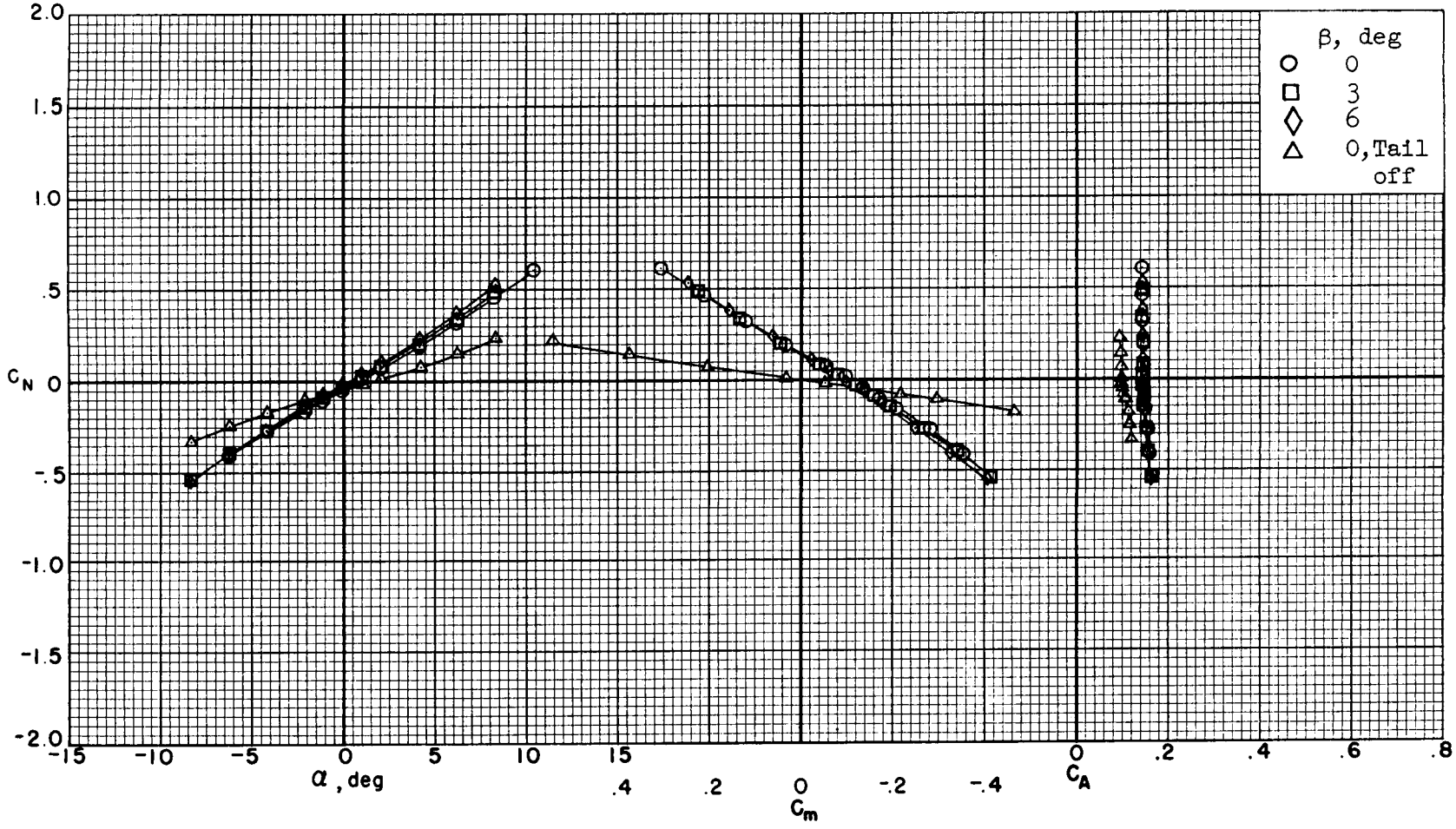

(1) $M_\infty = 3.52$

Figure 3.- Concluded.

[redacted]

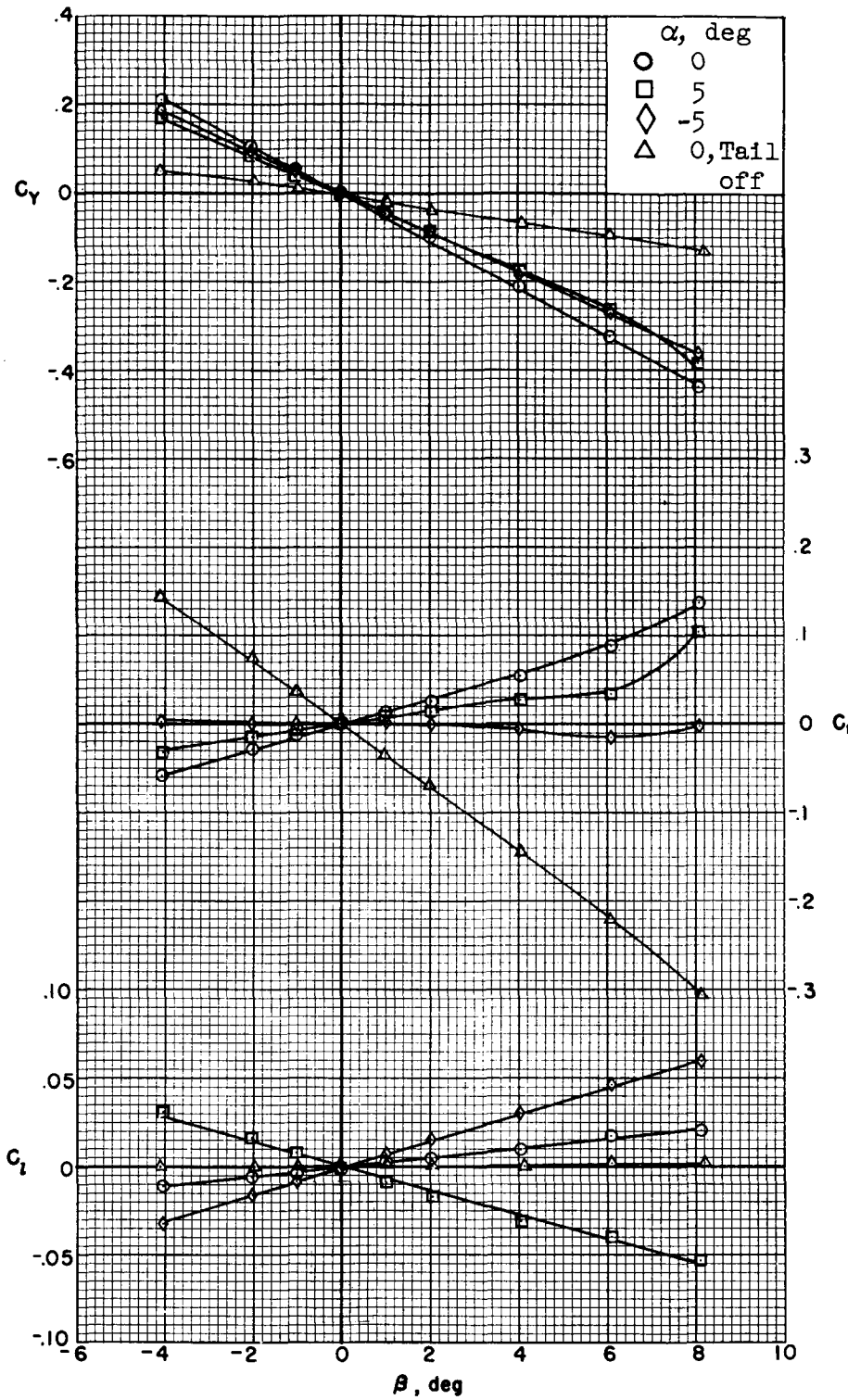

(a) $M_\infty = 0.60$

Figure 4.- The lateral aerodynamic characteristics of the vehicle at several free-stream Mach numbers.

[redacted]

[redacted]

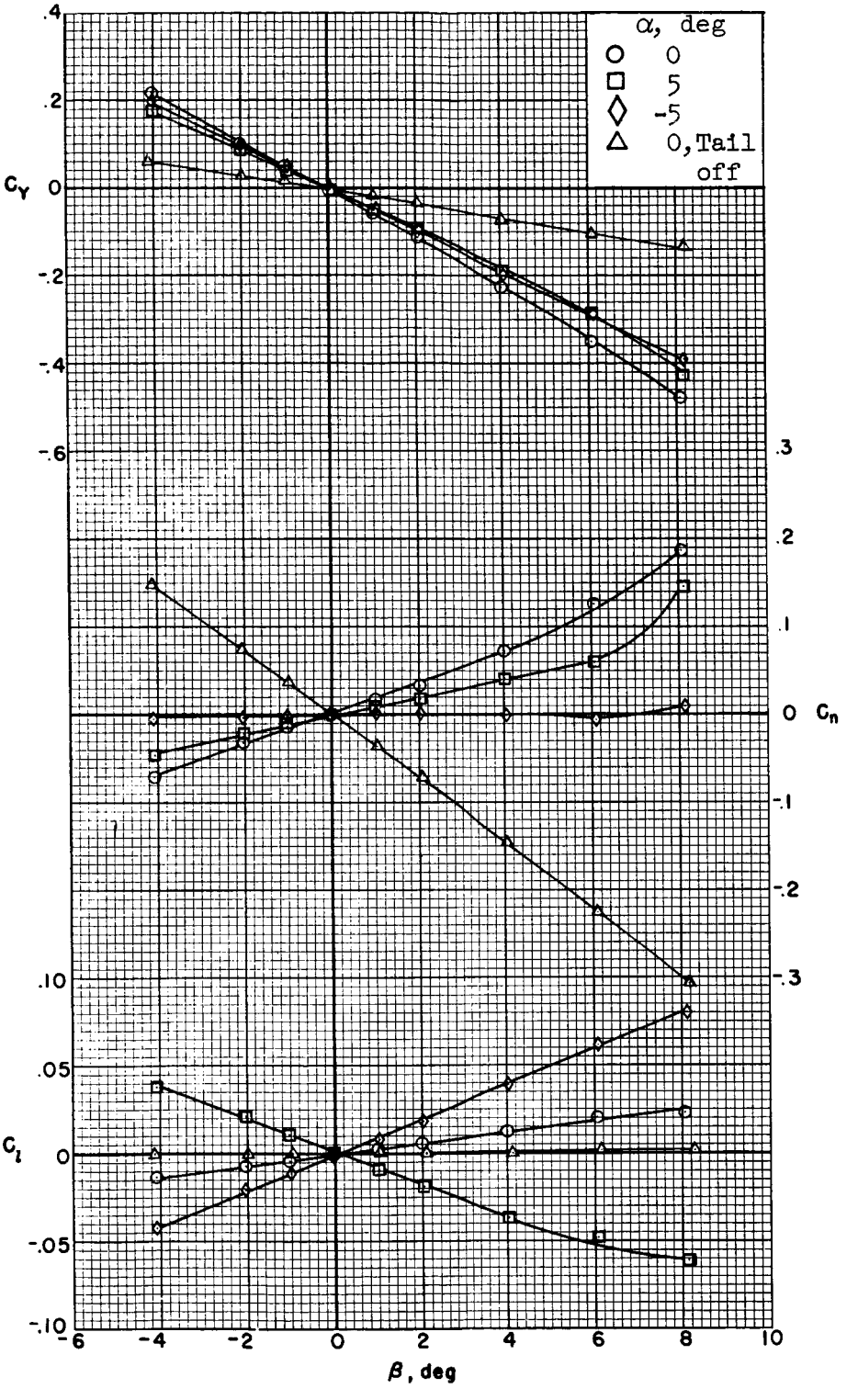

(b) $M_\infty = 0.80$

Figure 4.- Continued.

[redacted]

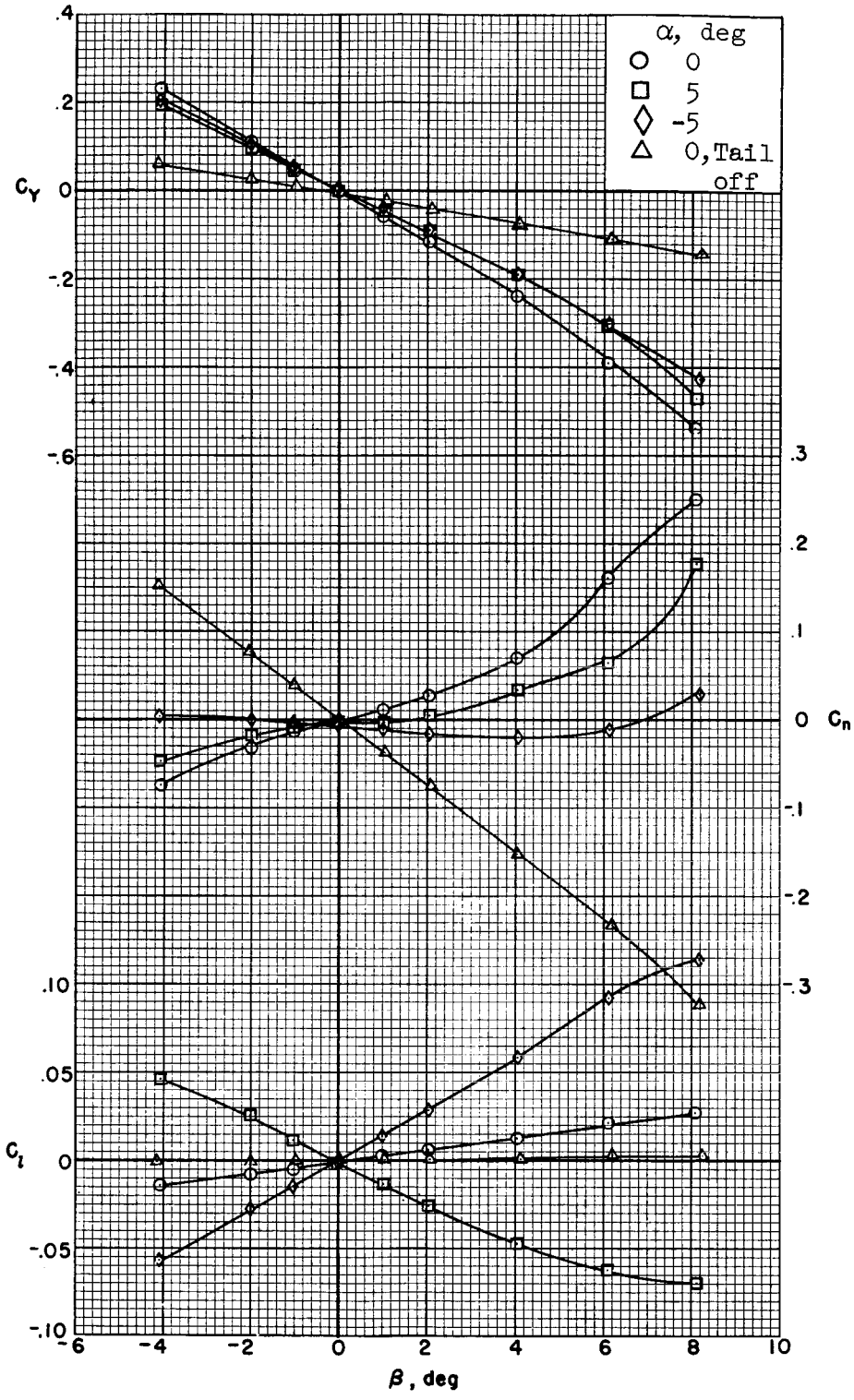

(c) $M_\infty = 0.90$

Figure 4.- Continued.

[redacted]

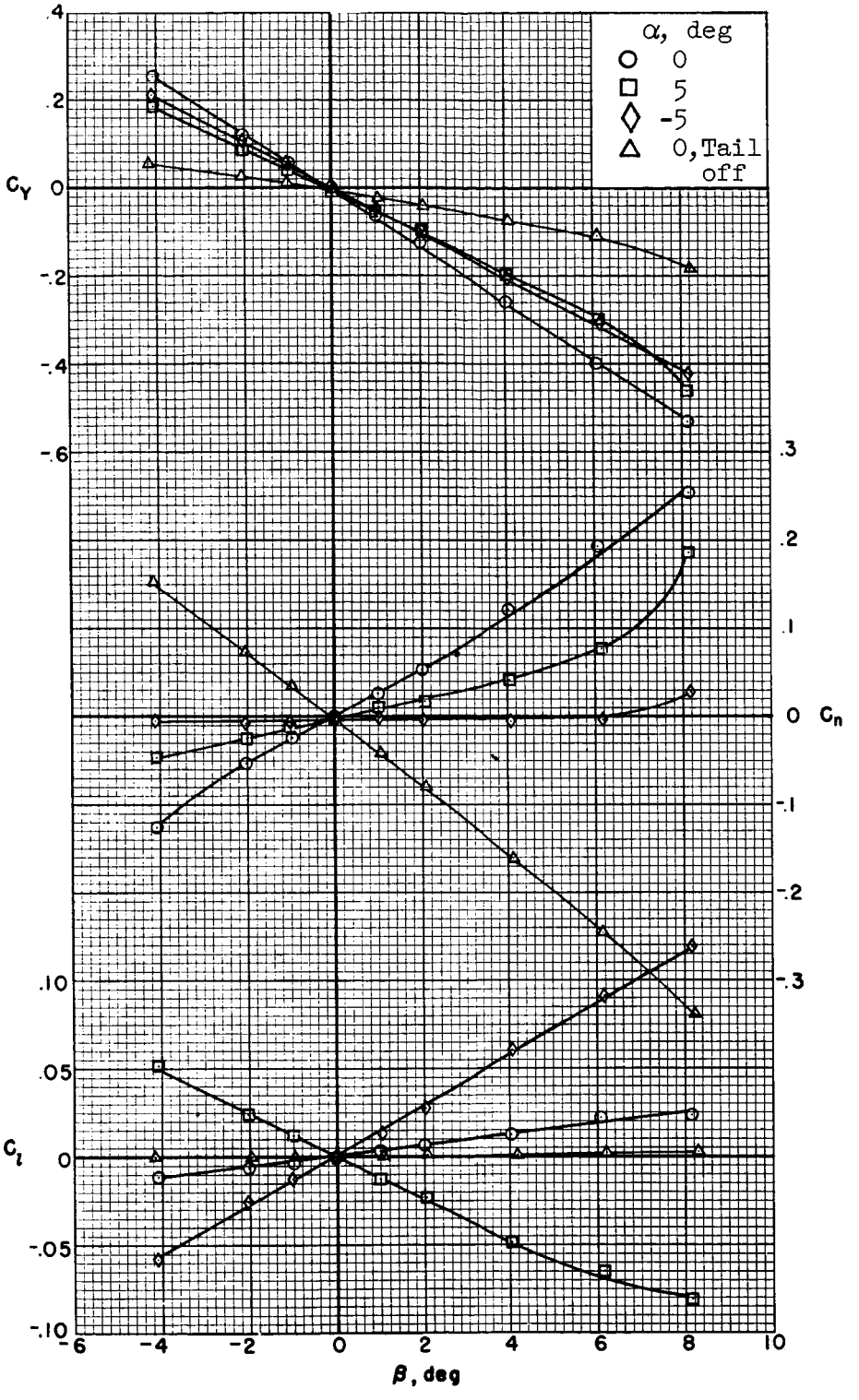

(d) $M_\infty = 1.00$

Figure 4.- Continued.

[redacted]

[redacted]

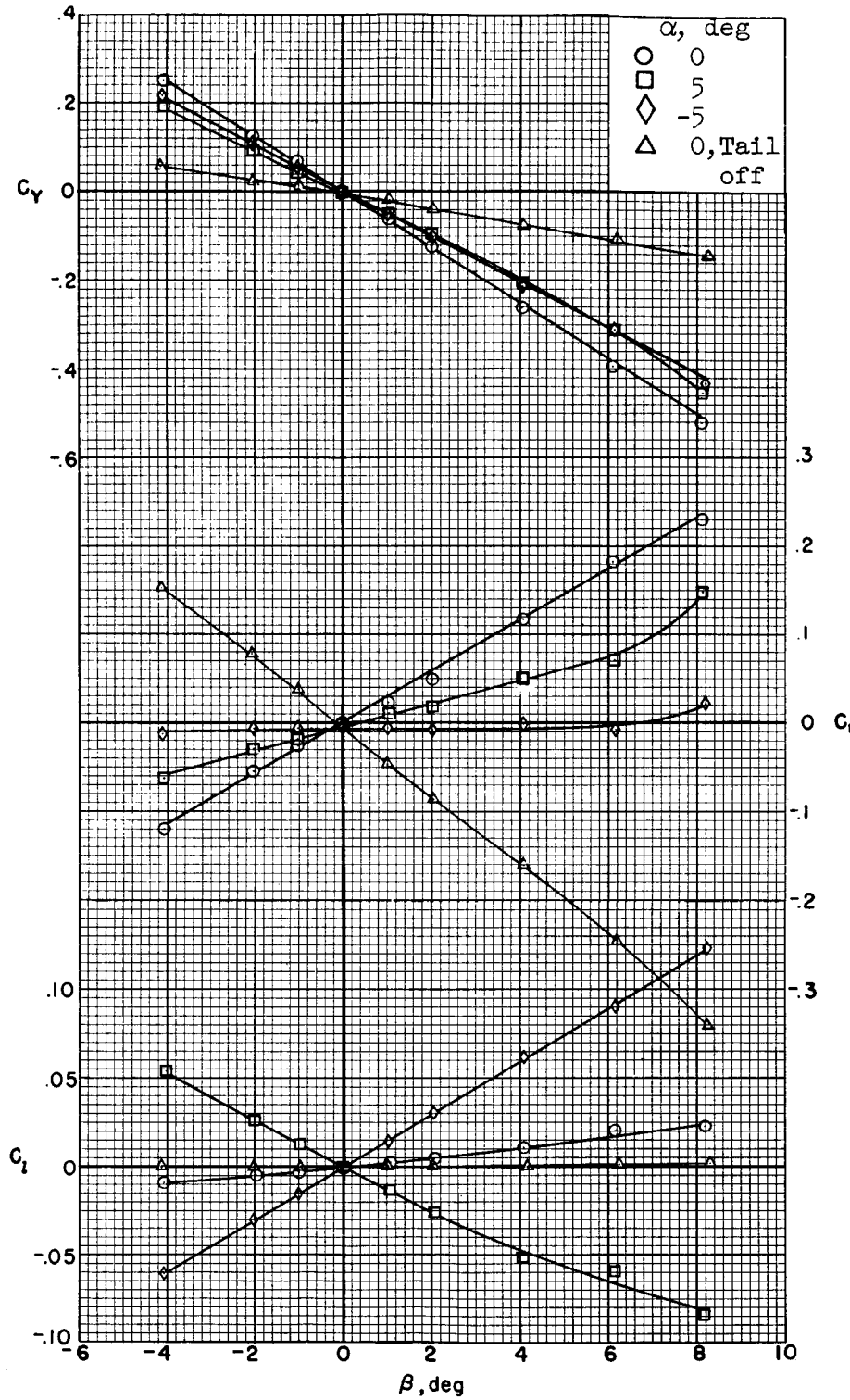

(e) $M_\infty = 1.10$

Figure 4.- Continued.

[redacted]

[redacted]

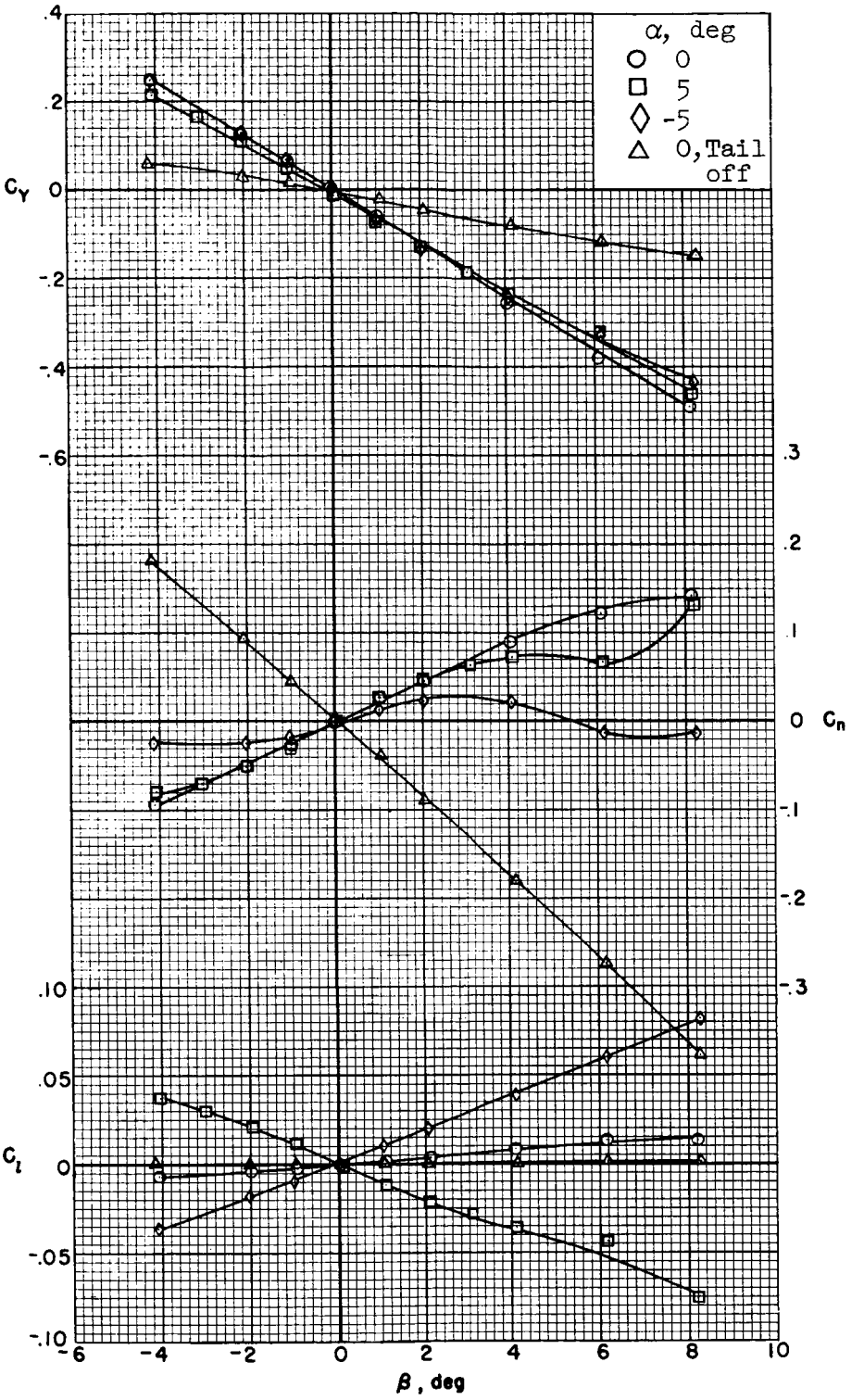

(f) $M_\infty = 1.30$

Figure 4.- Continued.

[redacted]

[redacted]

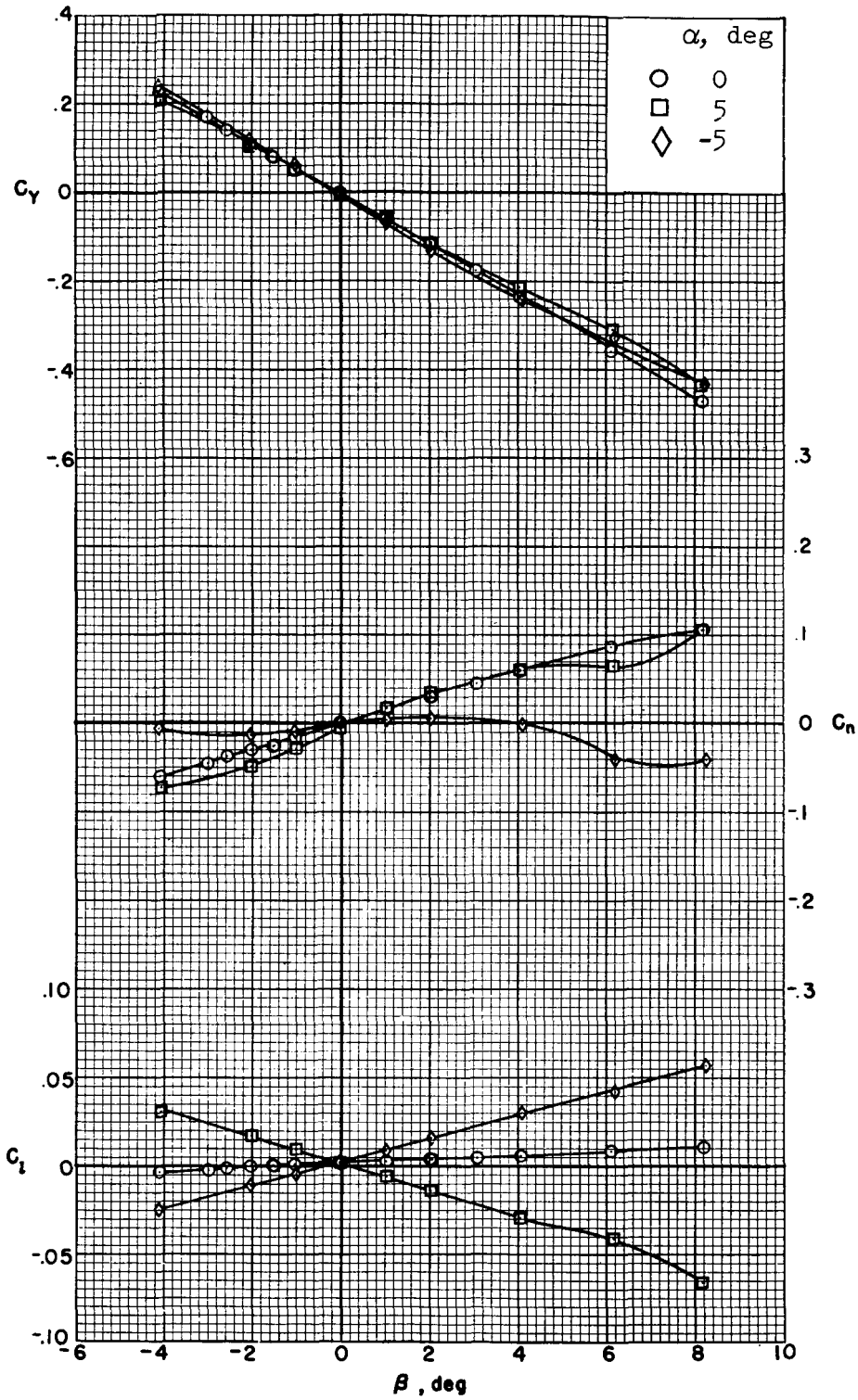

(g) $M_\infty = 1.40$

Figure 4.- Continued.

[redacted]

[redacted]

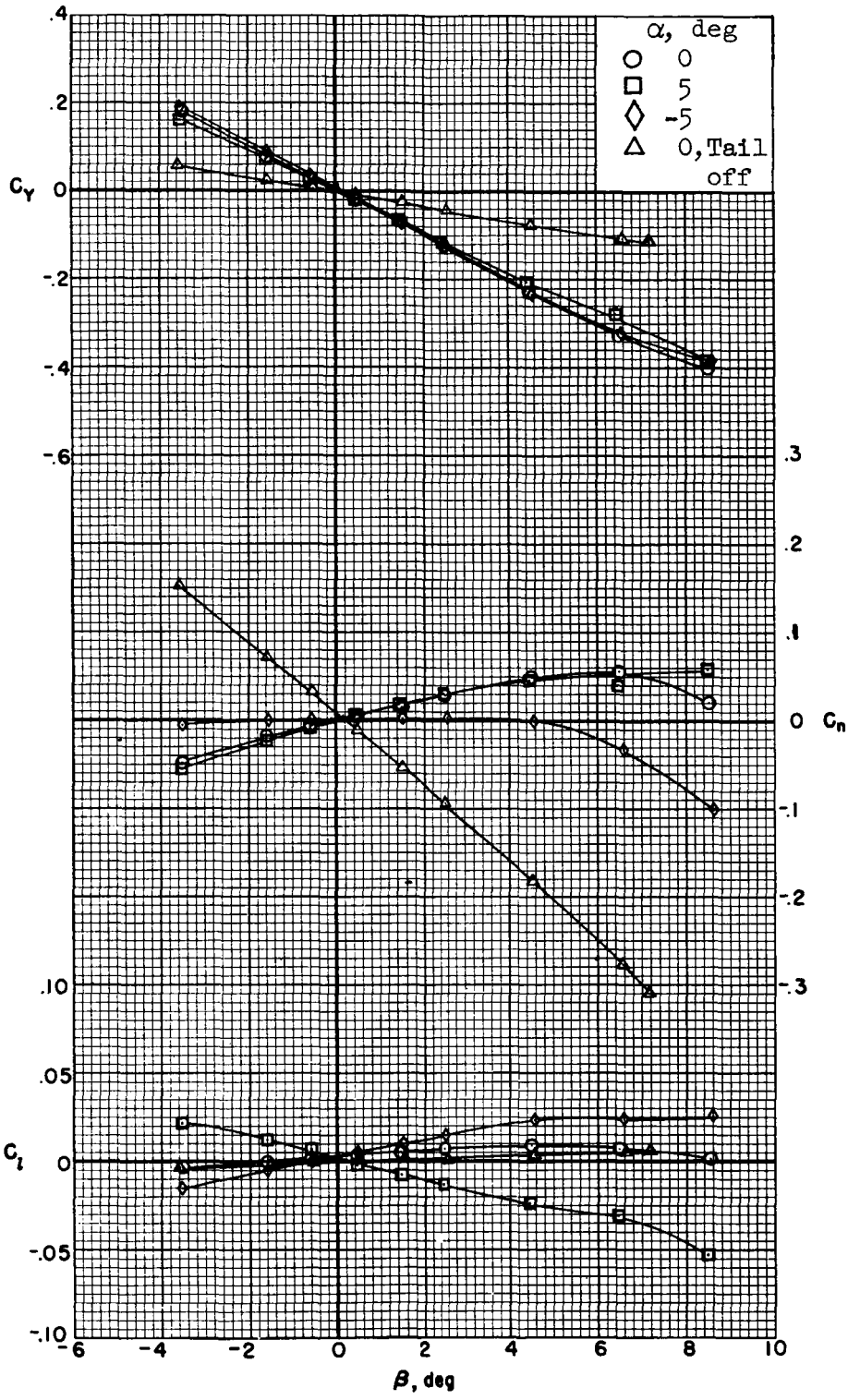

(h) $M_\infty = 1.55$

Figure 4.- Continued.

[redacted]

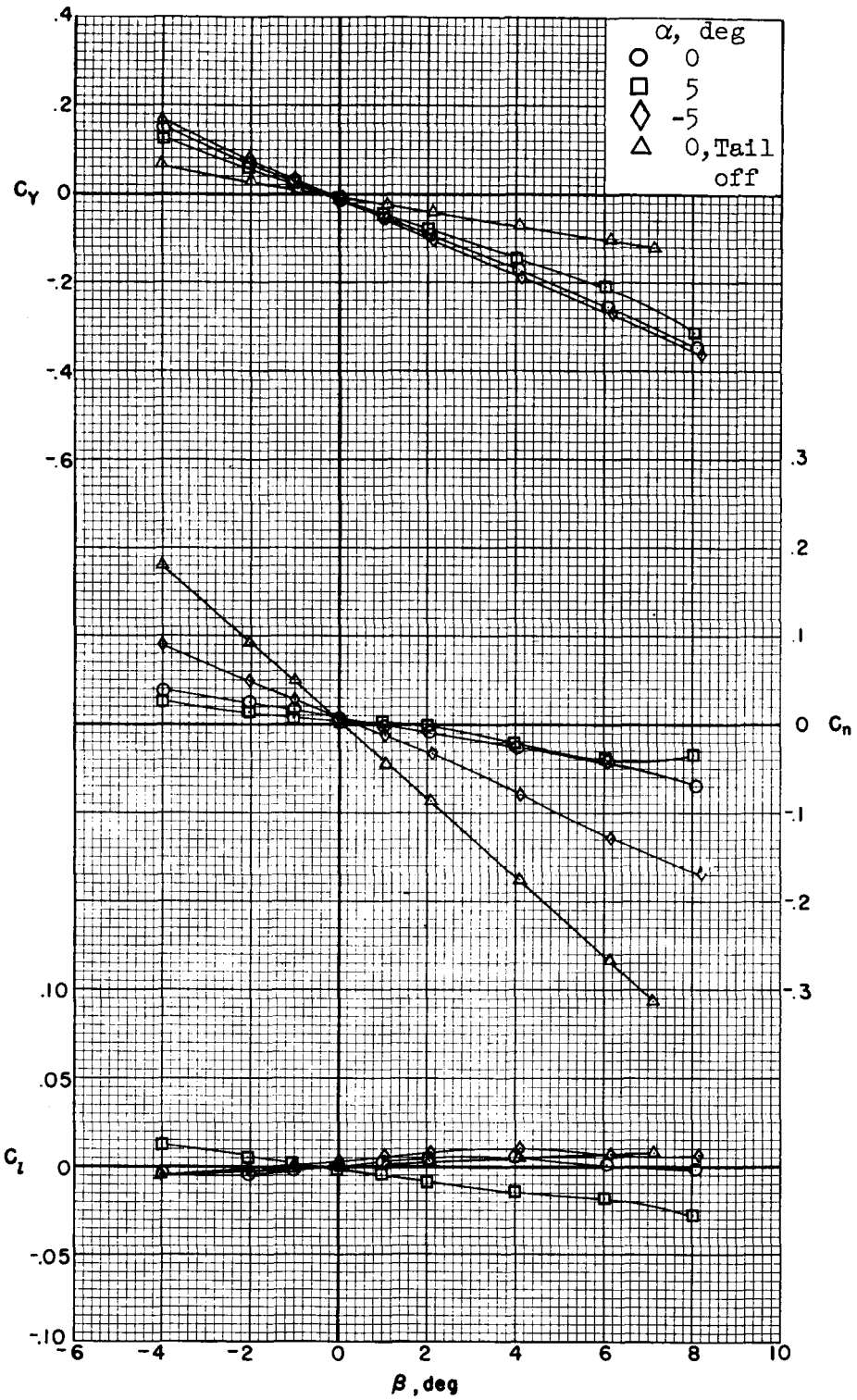

(i) $M_\infty = 2.01$

Figure 4.- Continued.

[redacted]

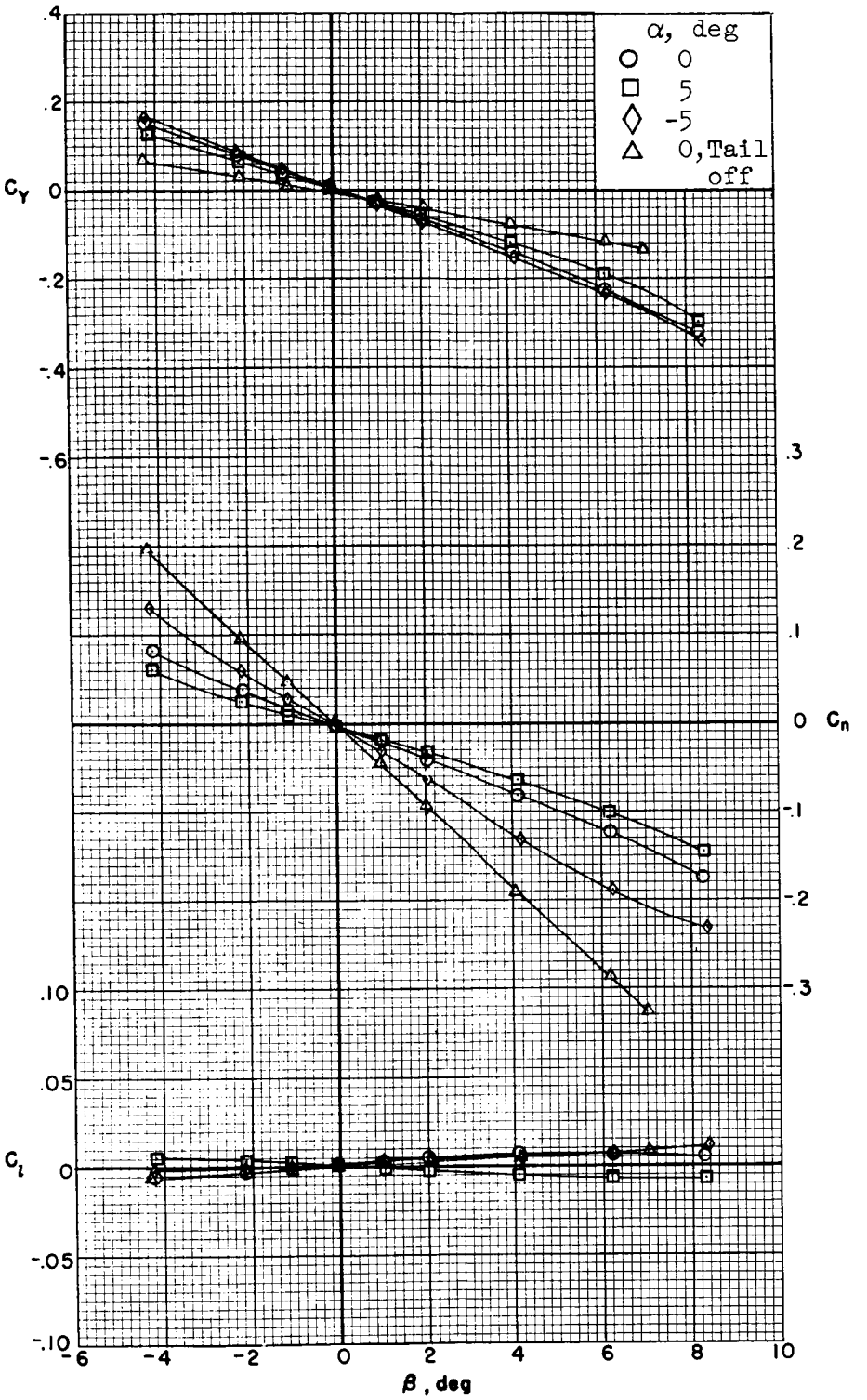

(j) $M_\infty = 2.48$

Figure 4.- Continued.

[redacted]

[redacted]

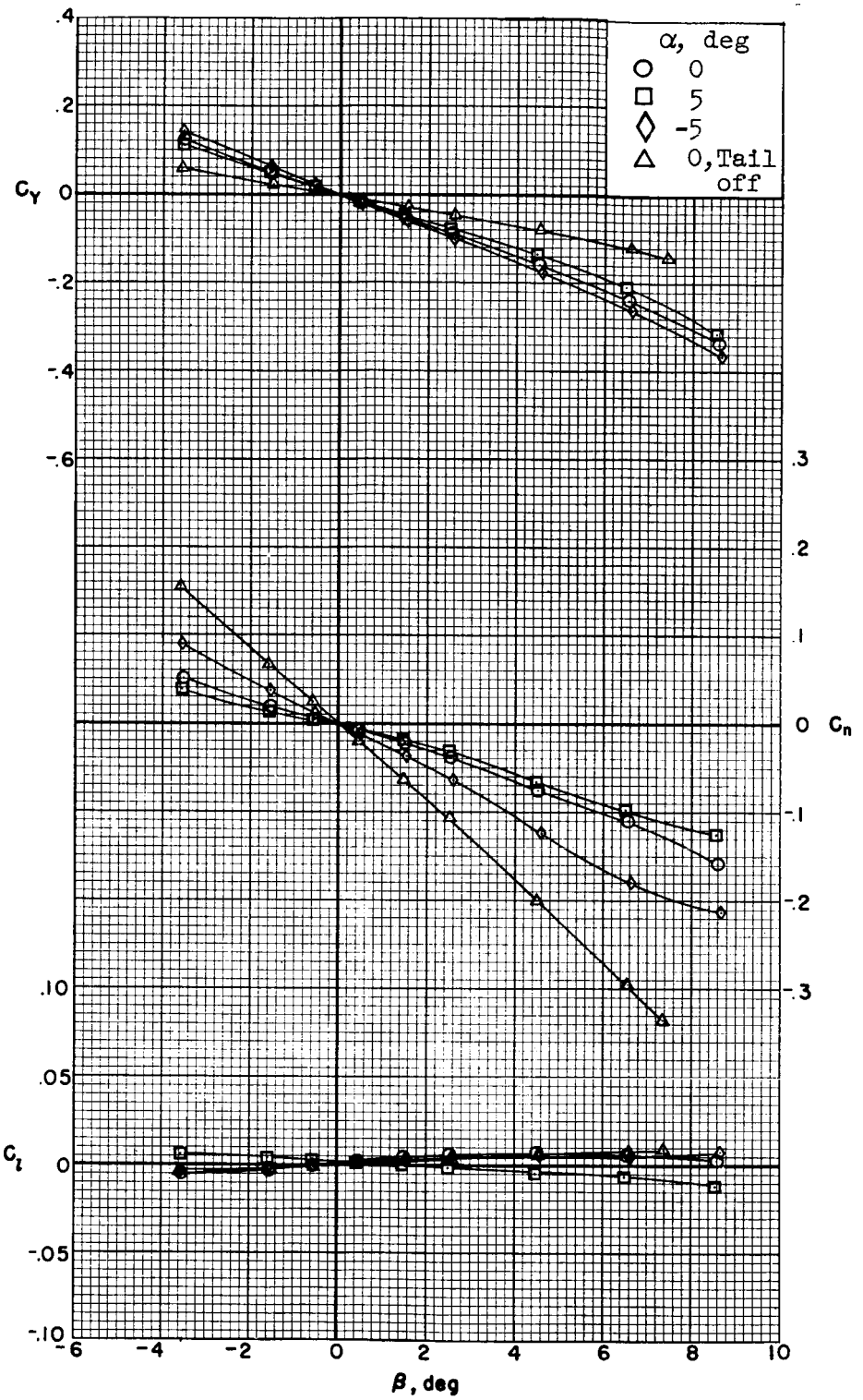

(k) $M_\infty = 2.51$

Figure 4.- Continued.

[redacted]

[redacted]

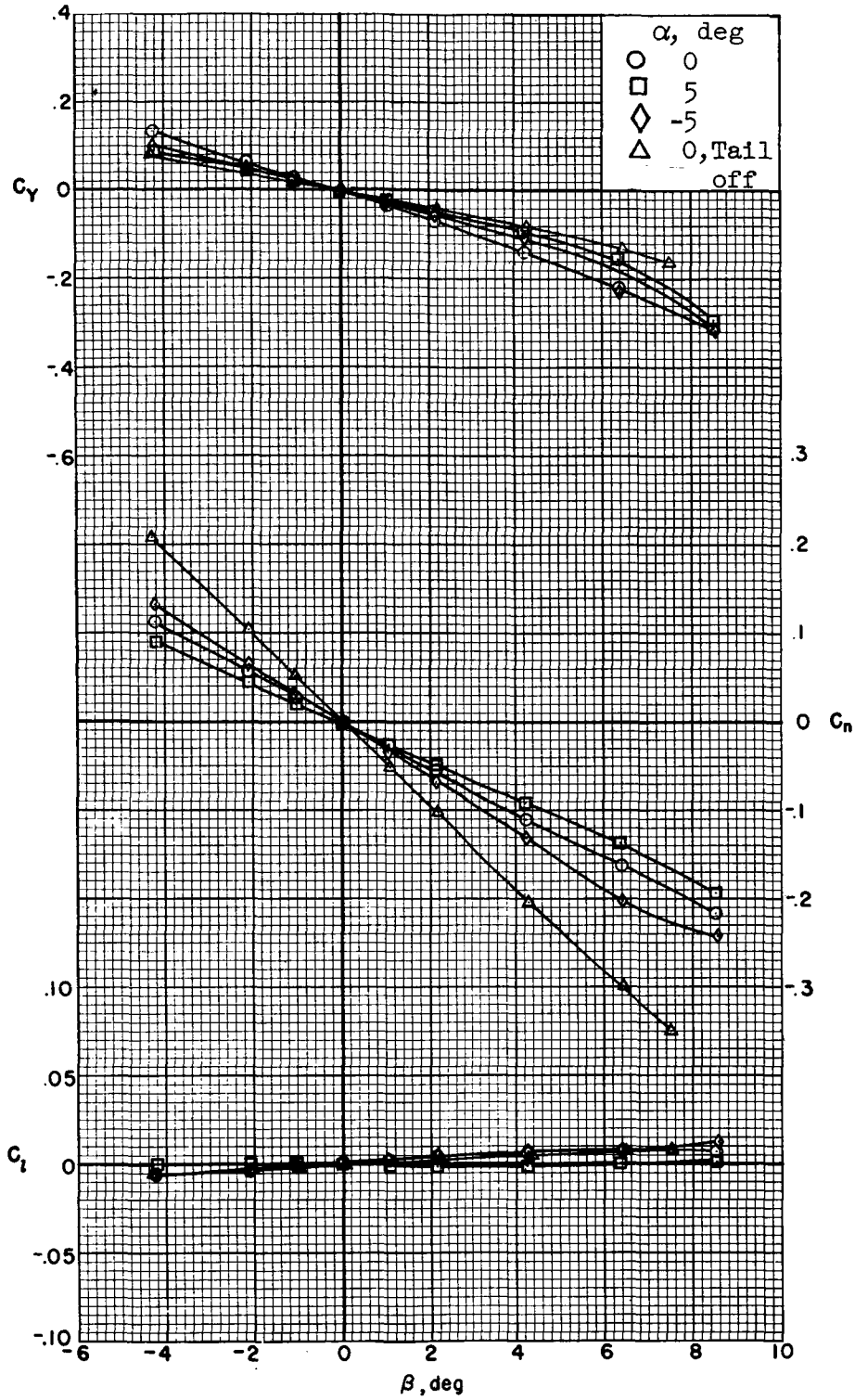

(1) $M_\infty = 3.05$

Figure 4.- Continued.

[redacted]

[redacted]

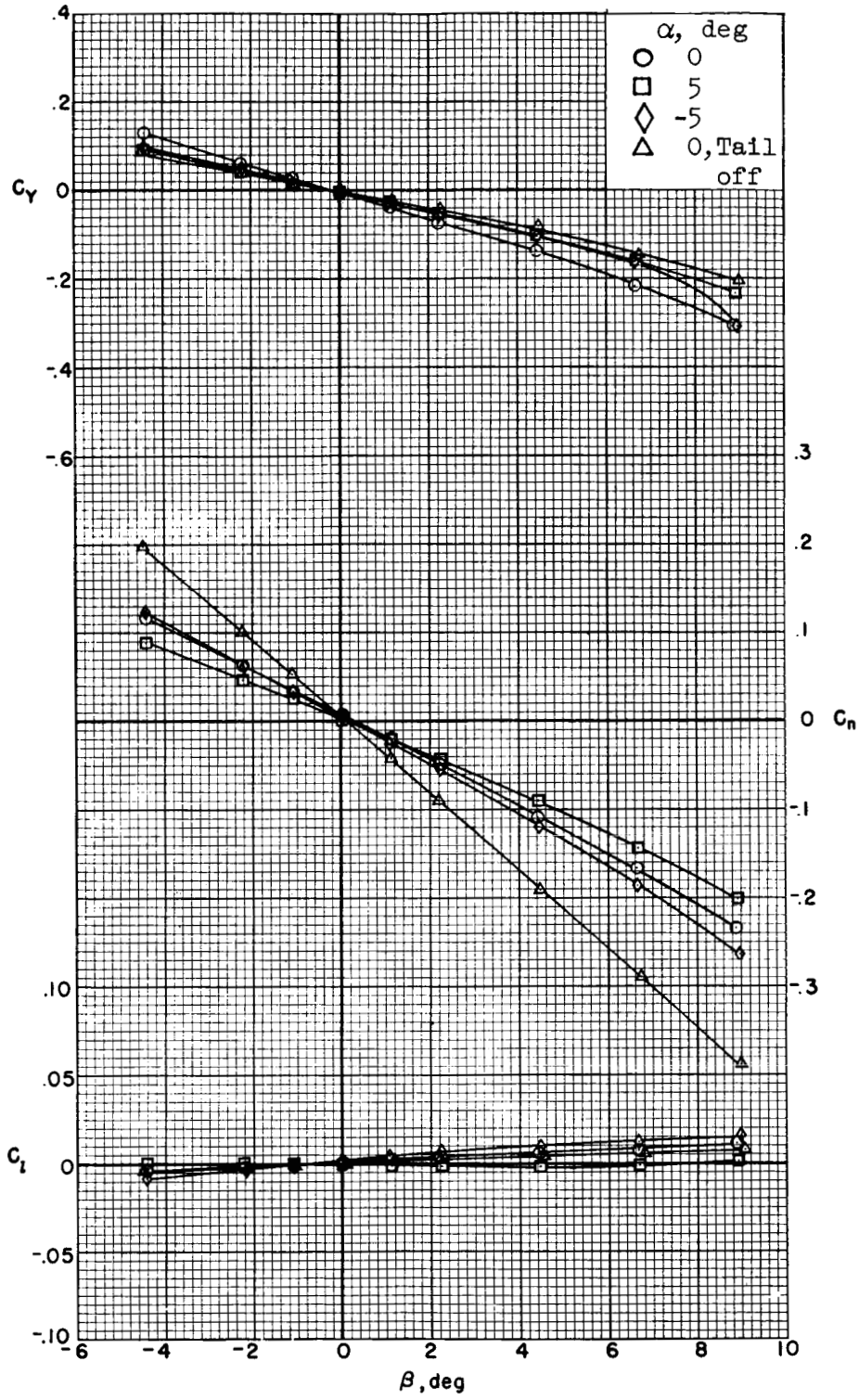

(m) $M_\infty = 3.52$

Figure 4.- Concluded.

[redacted]

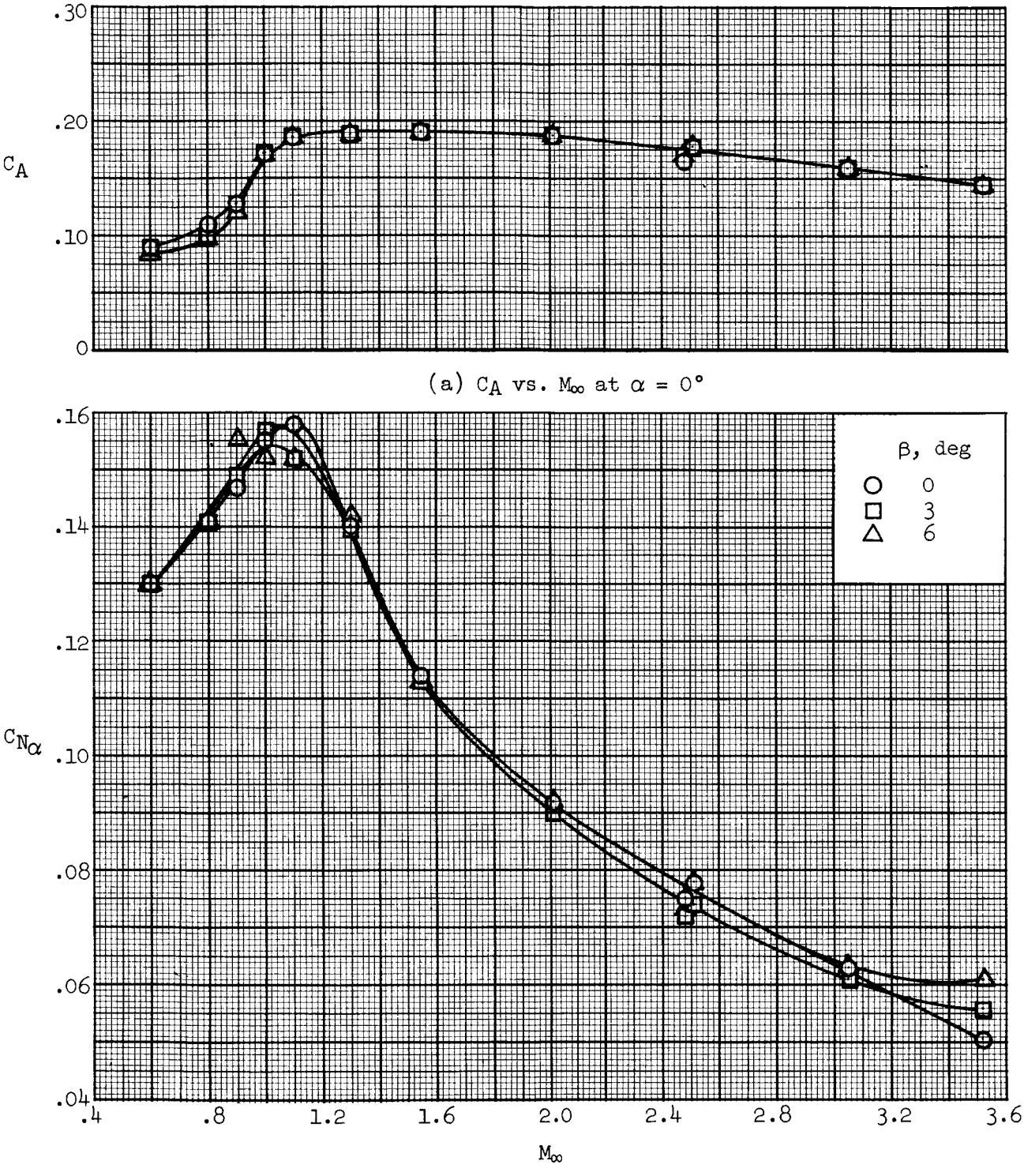

Figure 5.- The variation with Mach number of several aerodynamic coefficients of the vehicle.

[redacted]

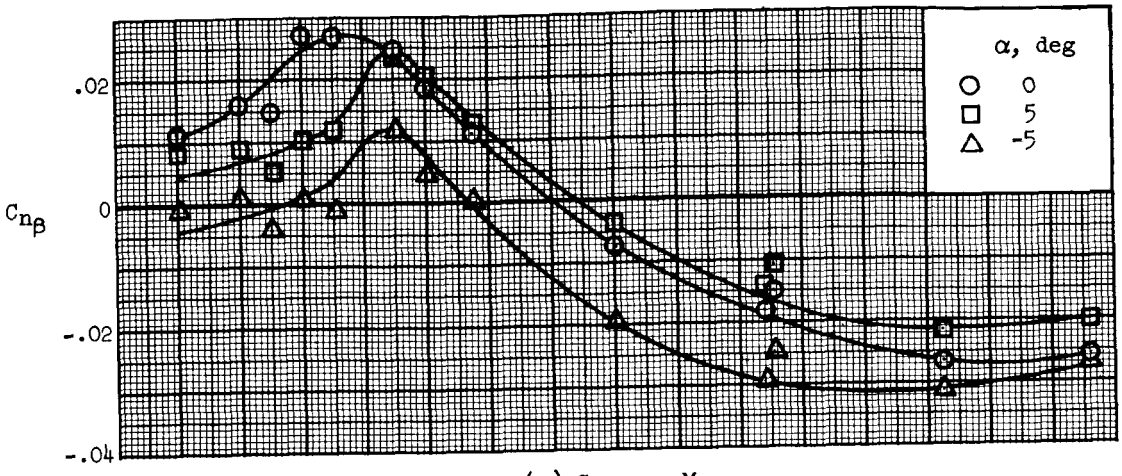

(c) C_{n_β} vs. M_∞

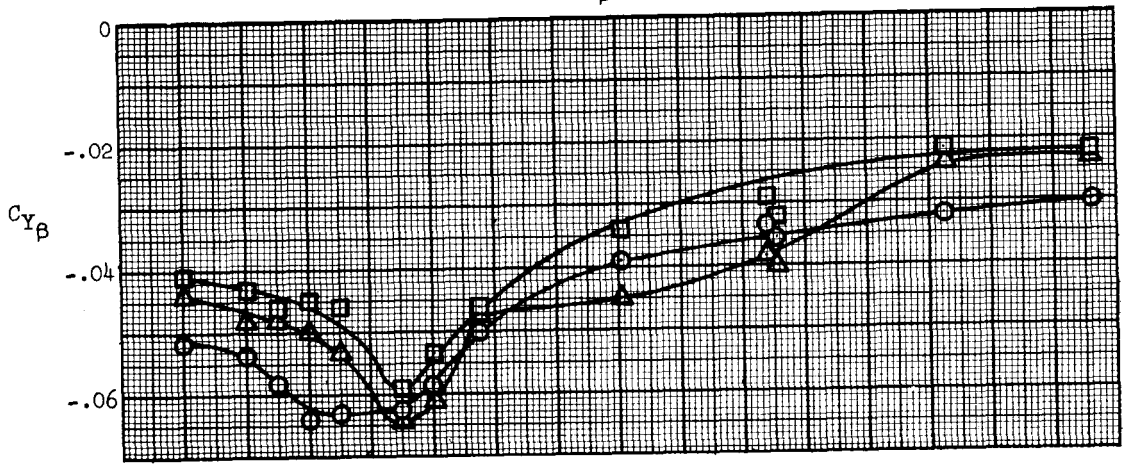

(d) C_{Y_β} vs. M_∞

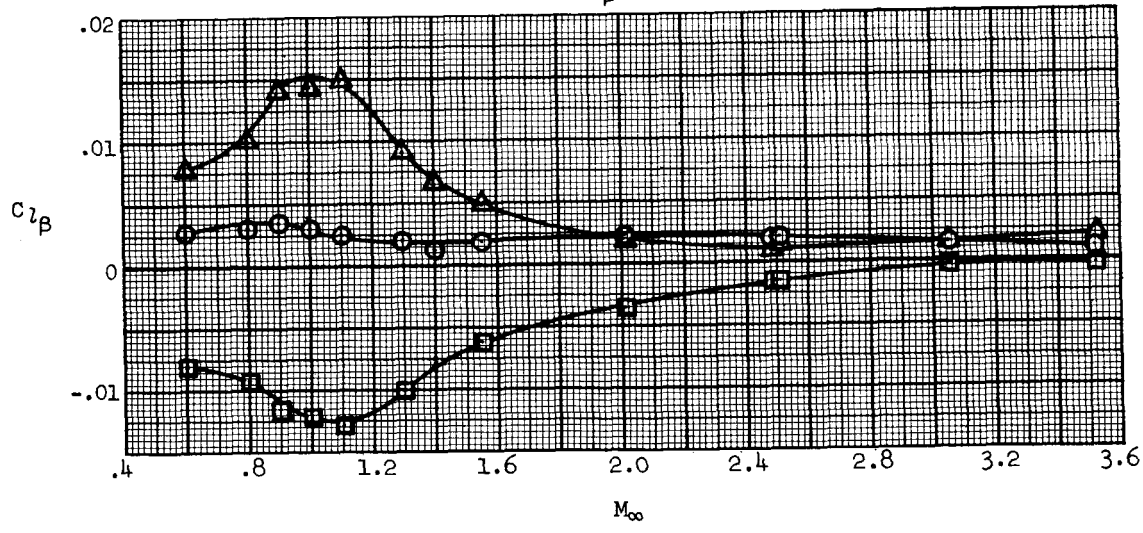

(e) C_{l_β} vs. M_∞

Figure 5.- Continued.

[redacted]

[redacted]

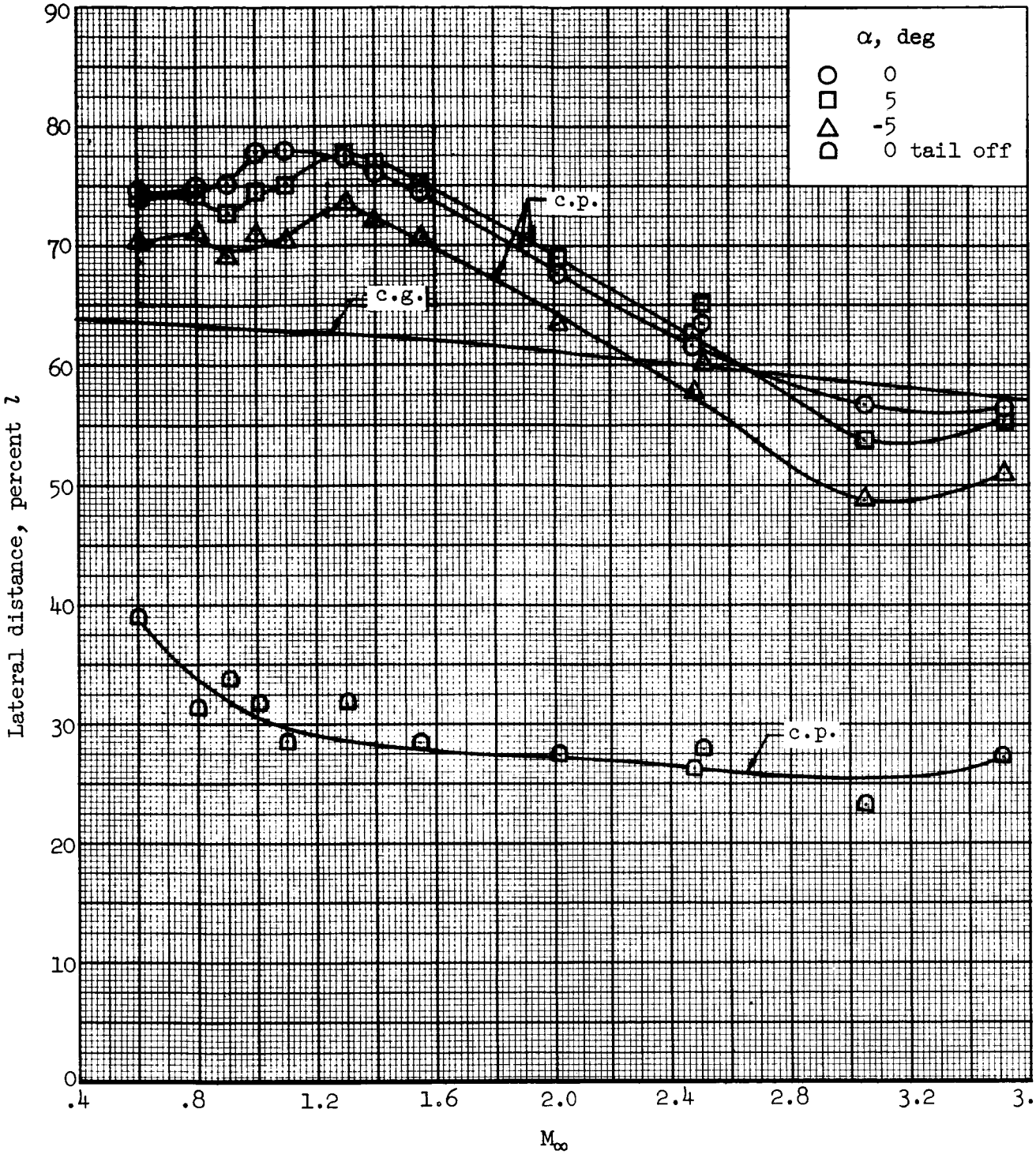

(f) Lateral center of pressure and center of gravity vs. M_∞.

Figure 5.- Continued.

[redacted]

[redacted]

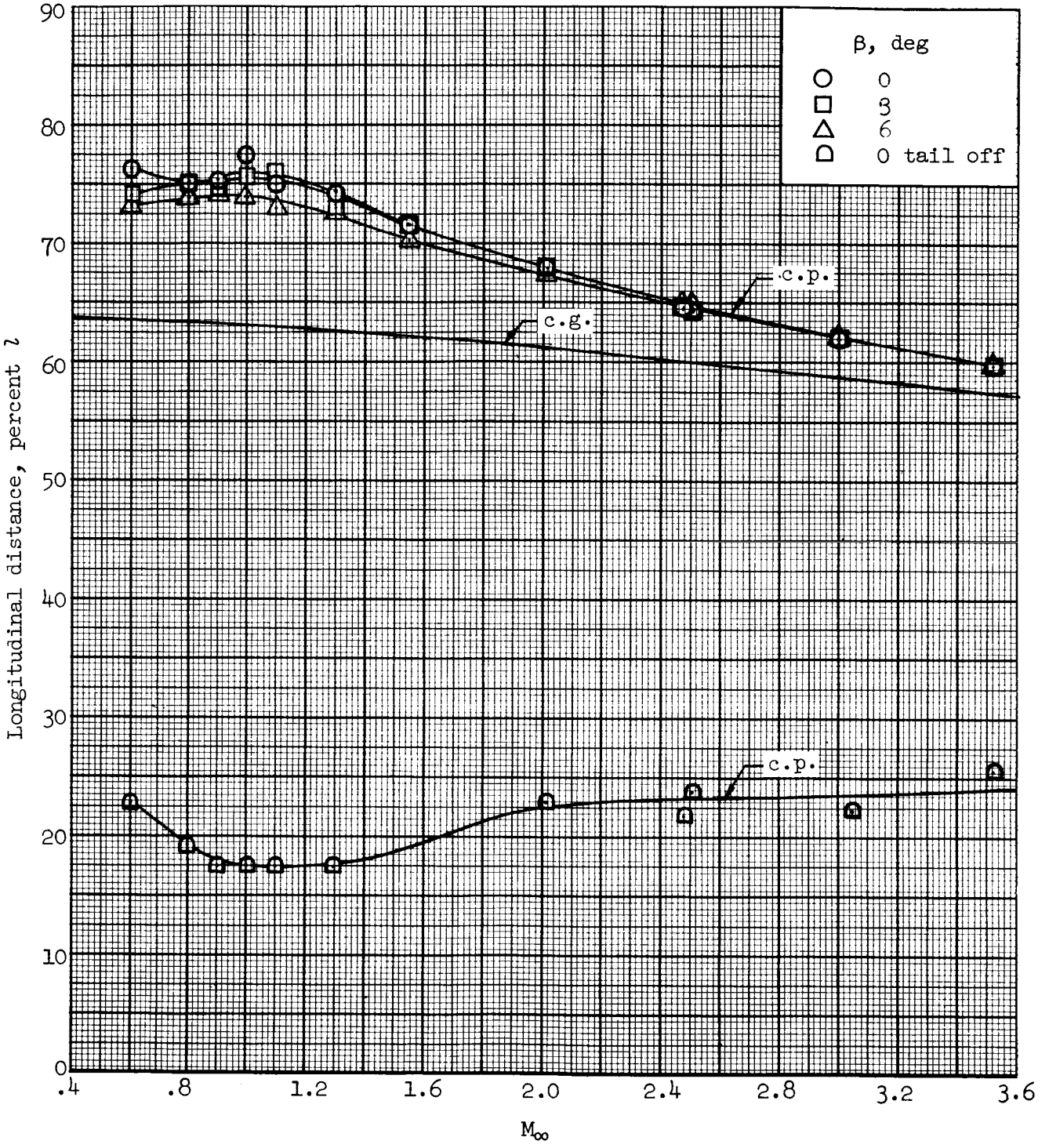

(g) Longitudinal center of pressure and center of gravity vs. M_∞.

Figure 5.- Concluded.

[redacted]

[redacted]

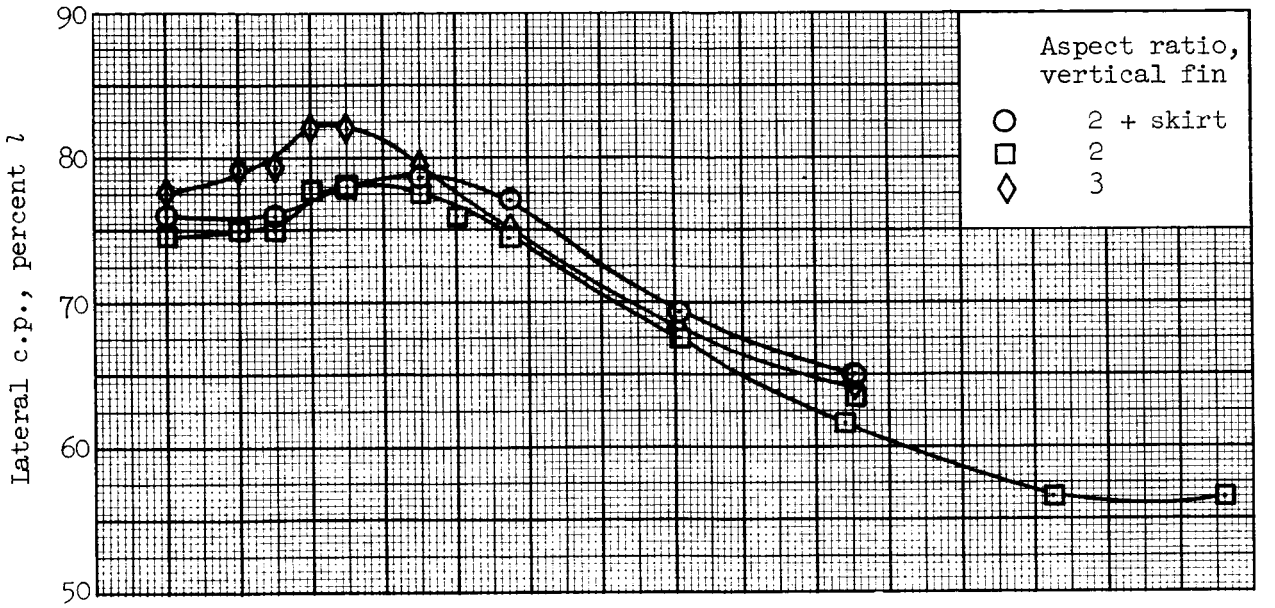

(a) Lateral center of pressure at $\alpha = 0^{\circ}$.

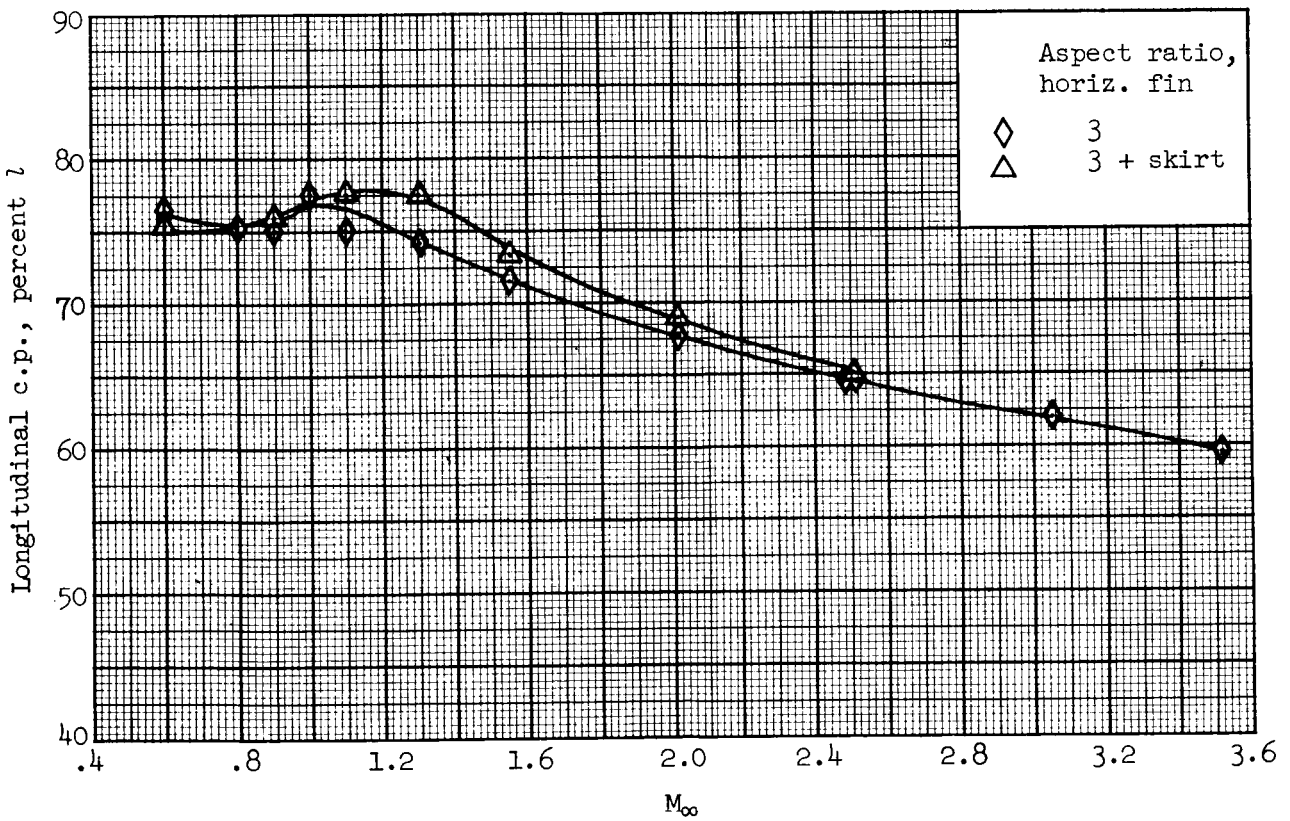

(b) Longitudinal center of pressure at $\beta = 0^{\circ}$.

Figure 6.- Effect of base skirt extension on the center of pressure as a function of Mach number.

[redacted]

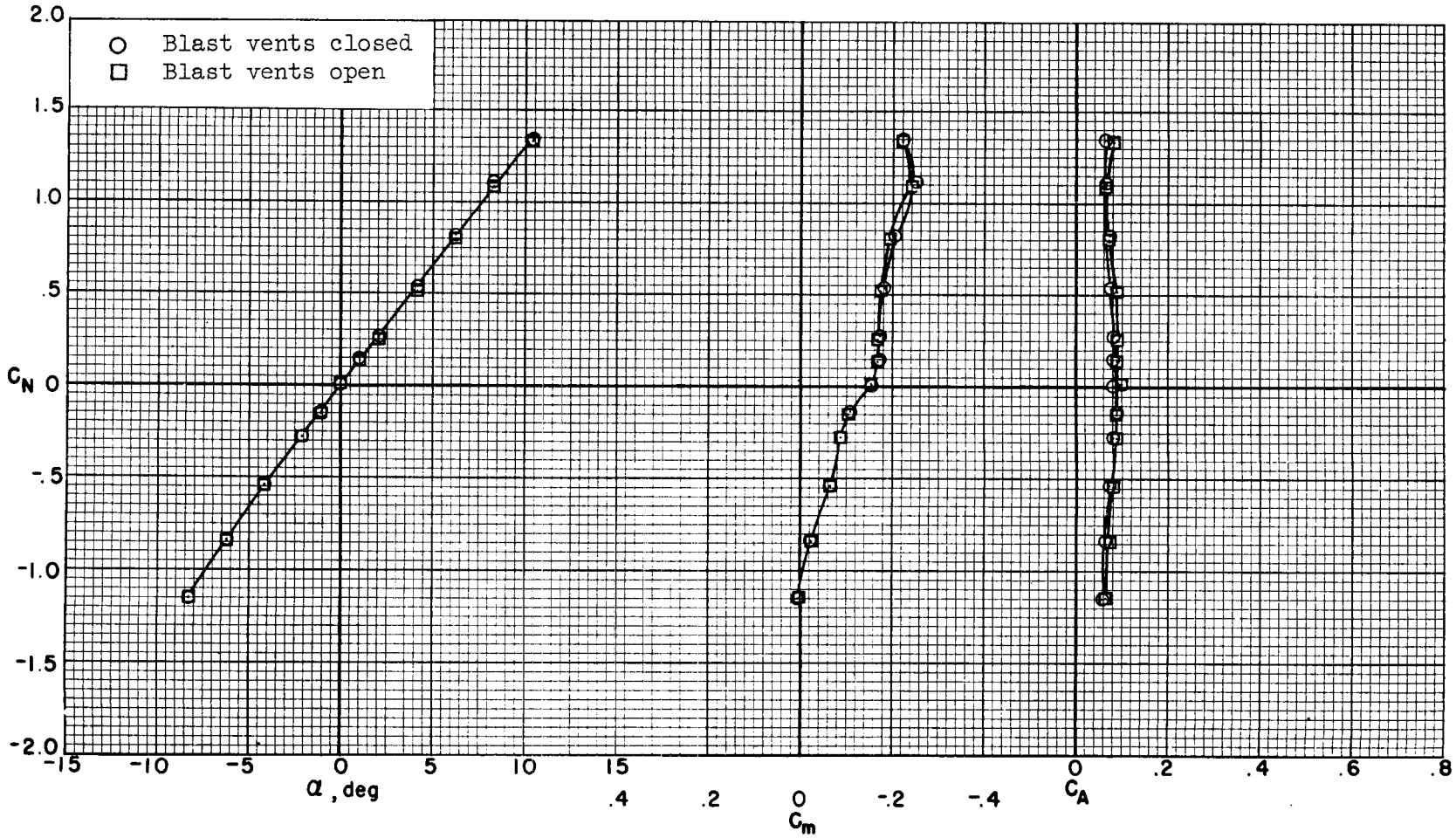

(a) $M_\infty = 0.60$

Figure 7.- Effect of blast vent openings on the longitudinal aerodynamic characteristics of the vehicle at $\beta = 0^\circ$ for several free-stream Mach numbers.

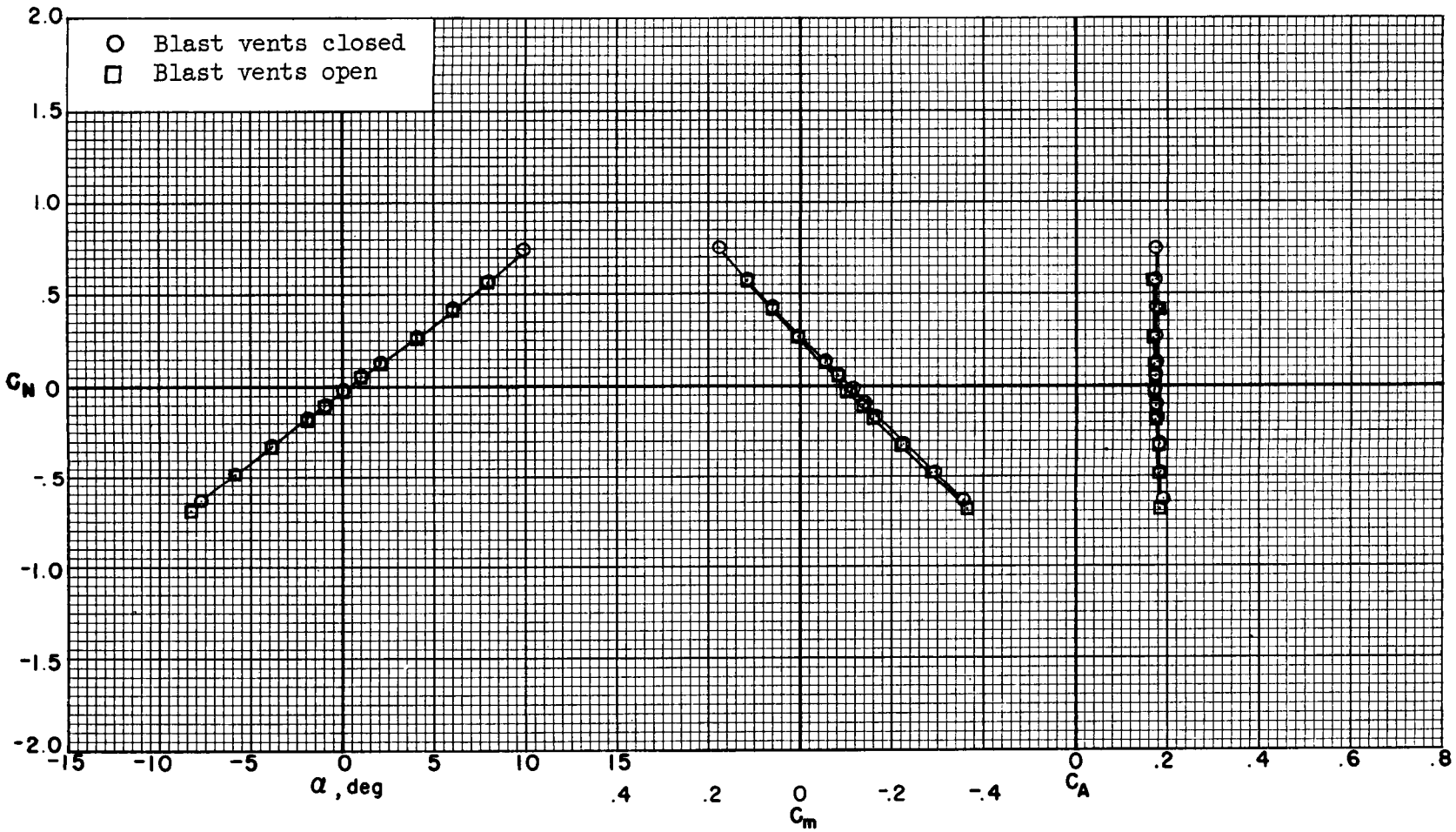

(b) $M_\infty = 2.51$

Figure 7.- Concluded.

[redacted]

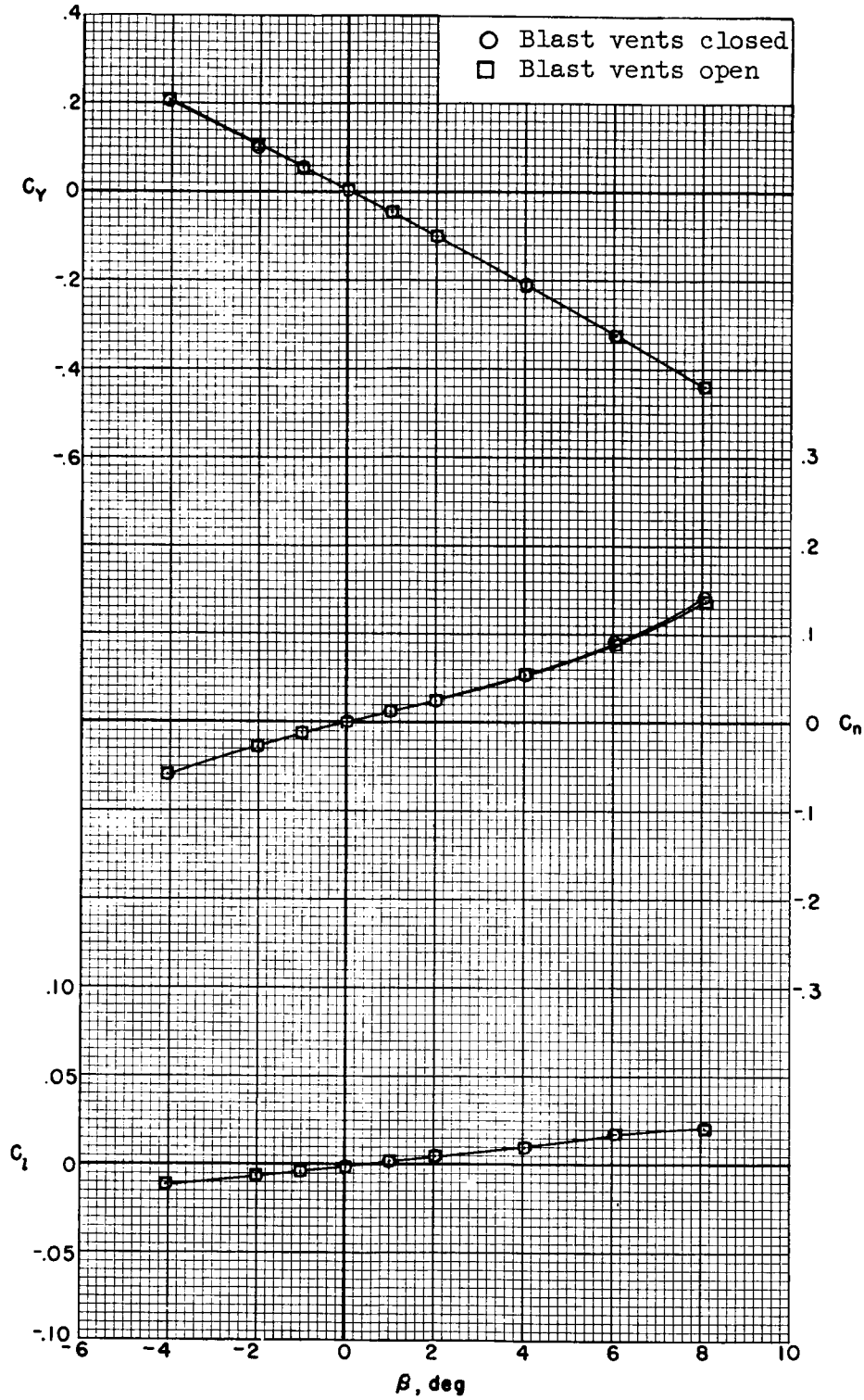

(a) $M_\infty = 0.60$

Figure 8.- Effect of blast vent openings on the lateral aerodynamic characteristics of the vehicle at $\alpha = 0^\circ$ for several free-stream Mach numbers.

[redacted]

[redacted]

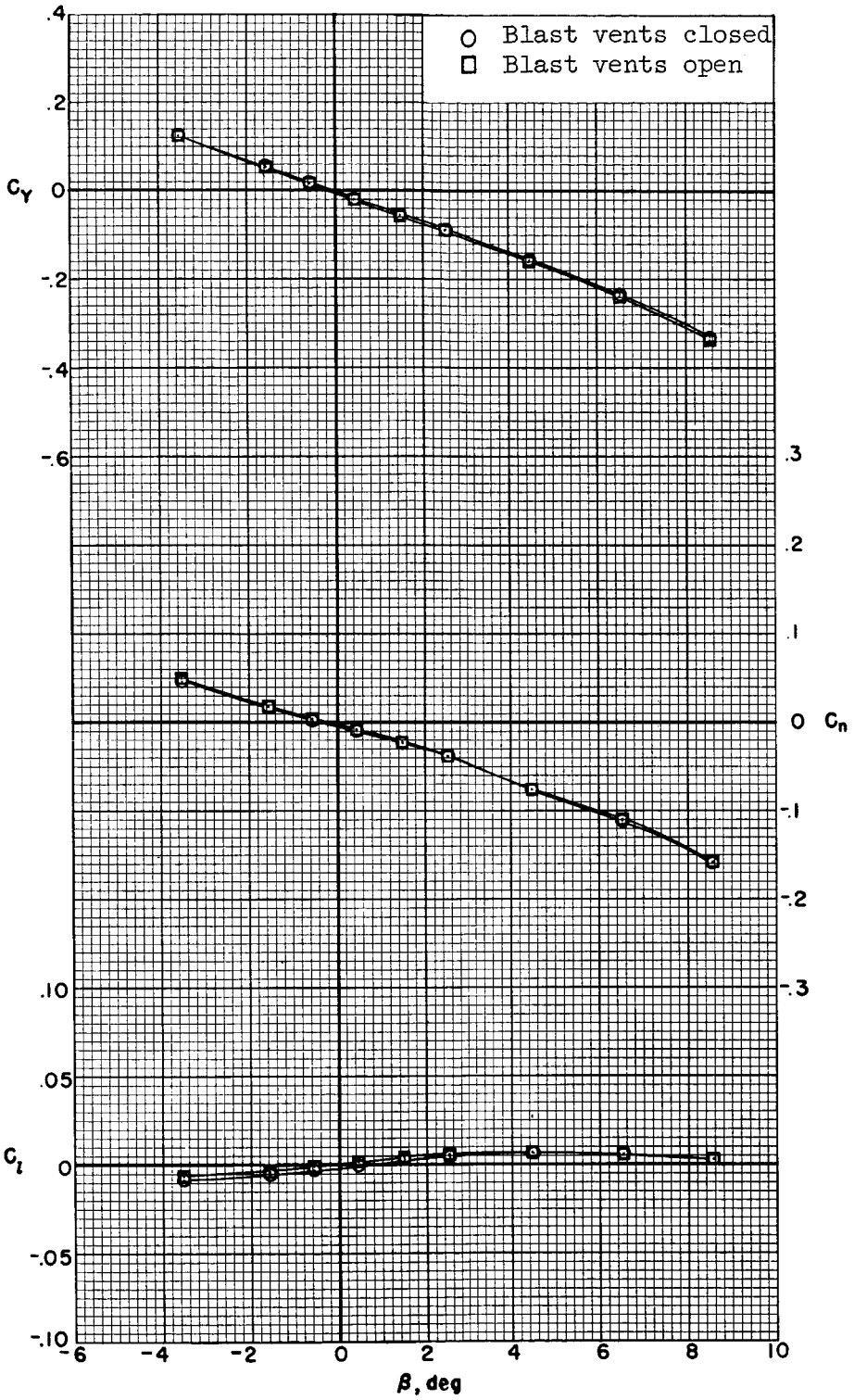

(b) $M_\infty = 2.51$

Figure 8.- Concluded.

[redacted]

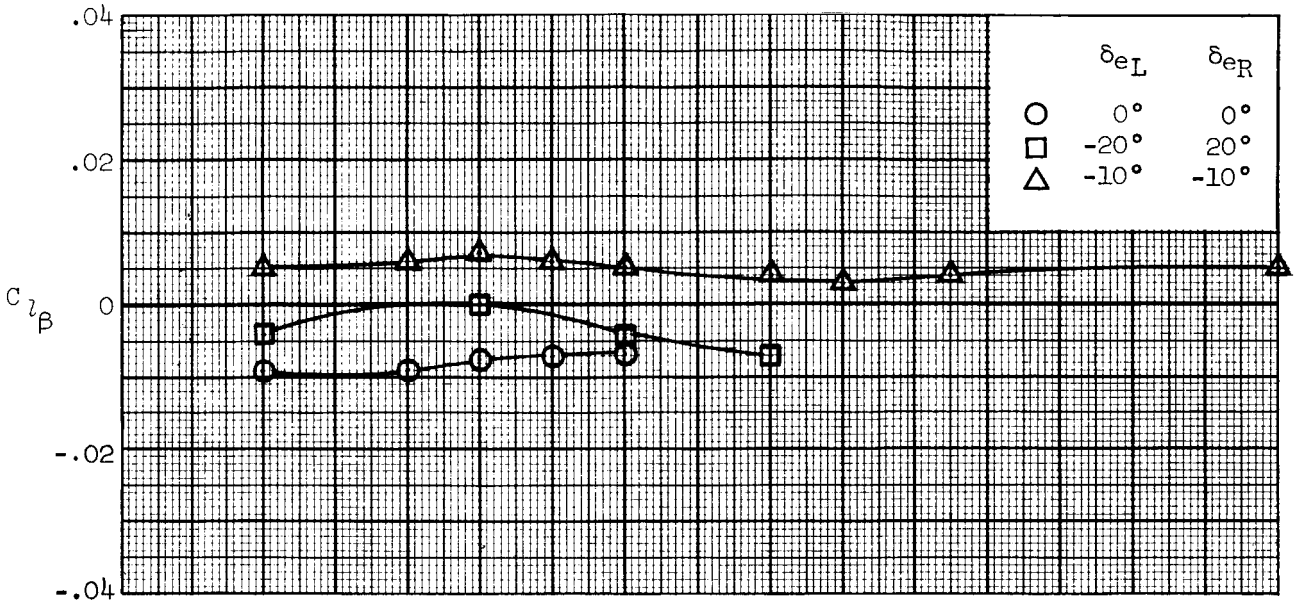

(a) Dihedral effect.

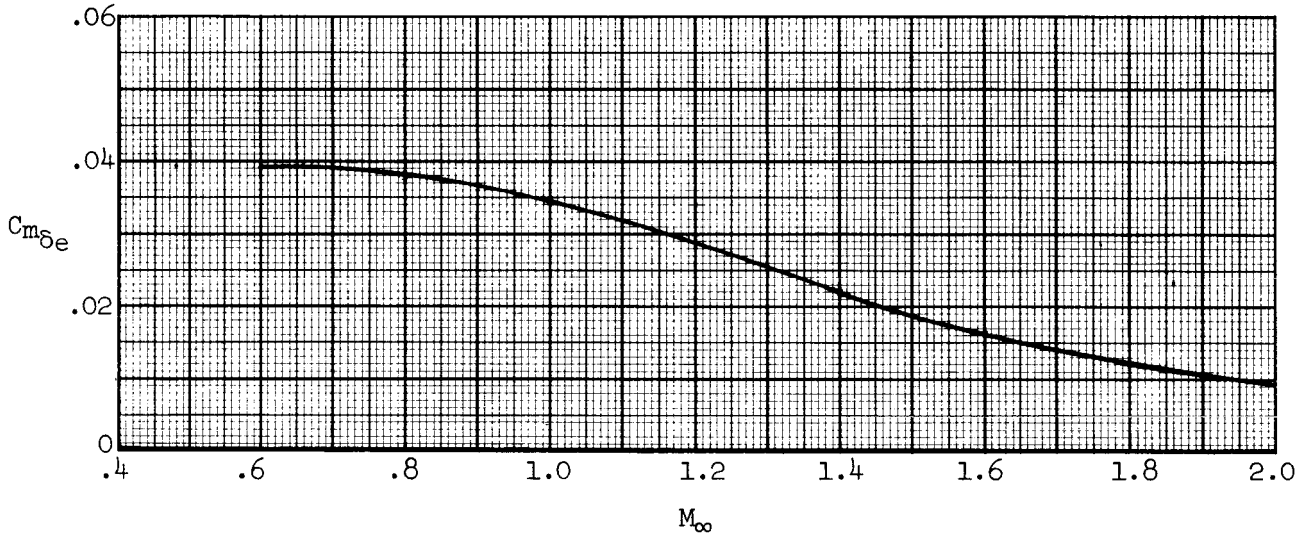

(b) Pitching-moment effectiveness.

Figure 9.- Effect of elevon deflection on the aerodynamic characteristics of the vehicle at 0° angle of attack.

[redacted]

[redacted]

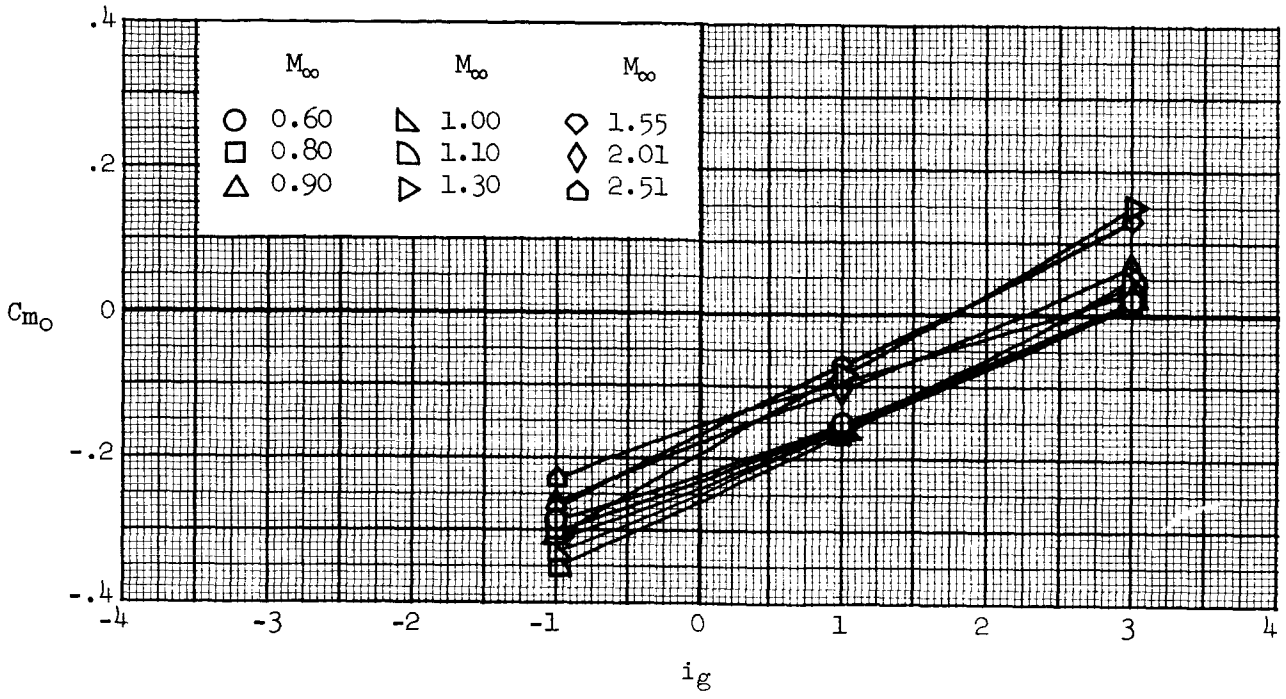

(a) C_{m_o} vs. i_g

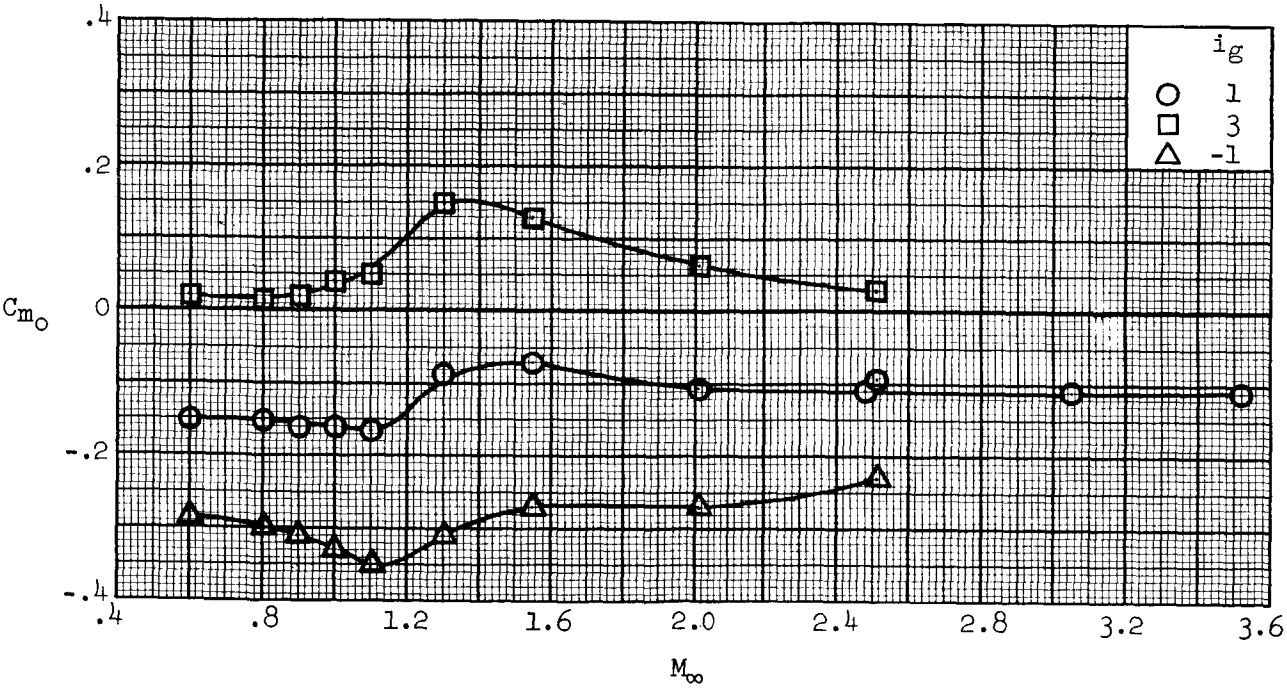

(b) C_{m_o} vs. M_∞

Figure 10.- Effect of glider-wing incidence on the pitching moment at zero normal force of the vehicle at $\beta = 0^\circ$.

[redacted]

[redacted]

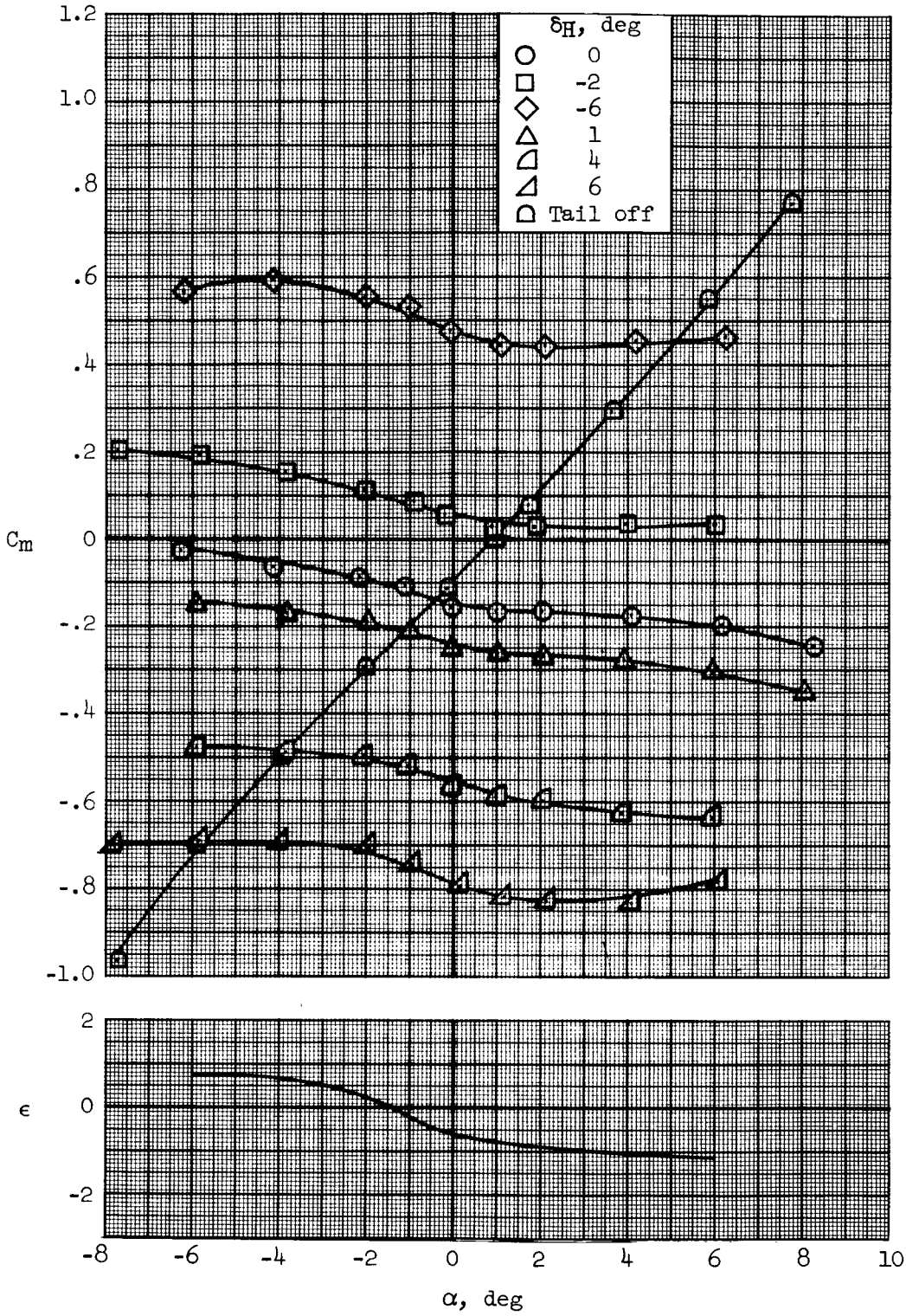

(a) $M_\infty = 0.60$

Figure 11.- Downwash characteristics of the vehicle at $\beta = 0^\circ$ for several free-stream Mach numbers.

[redacted]

[redacted]

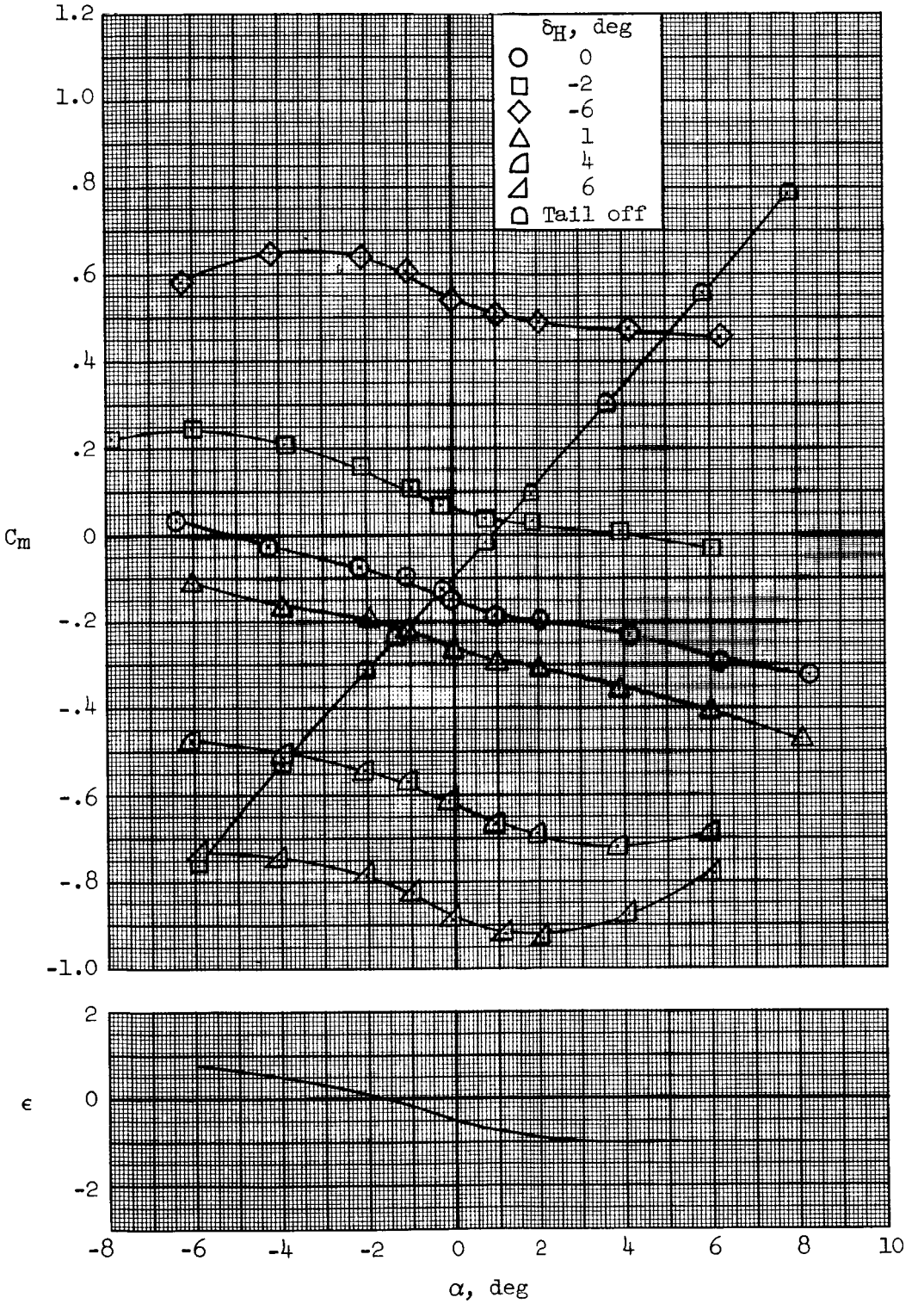

(b) $M_\infty = 0.80$

Figure 11.- Continued.

[redacted]

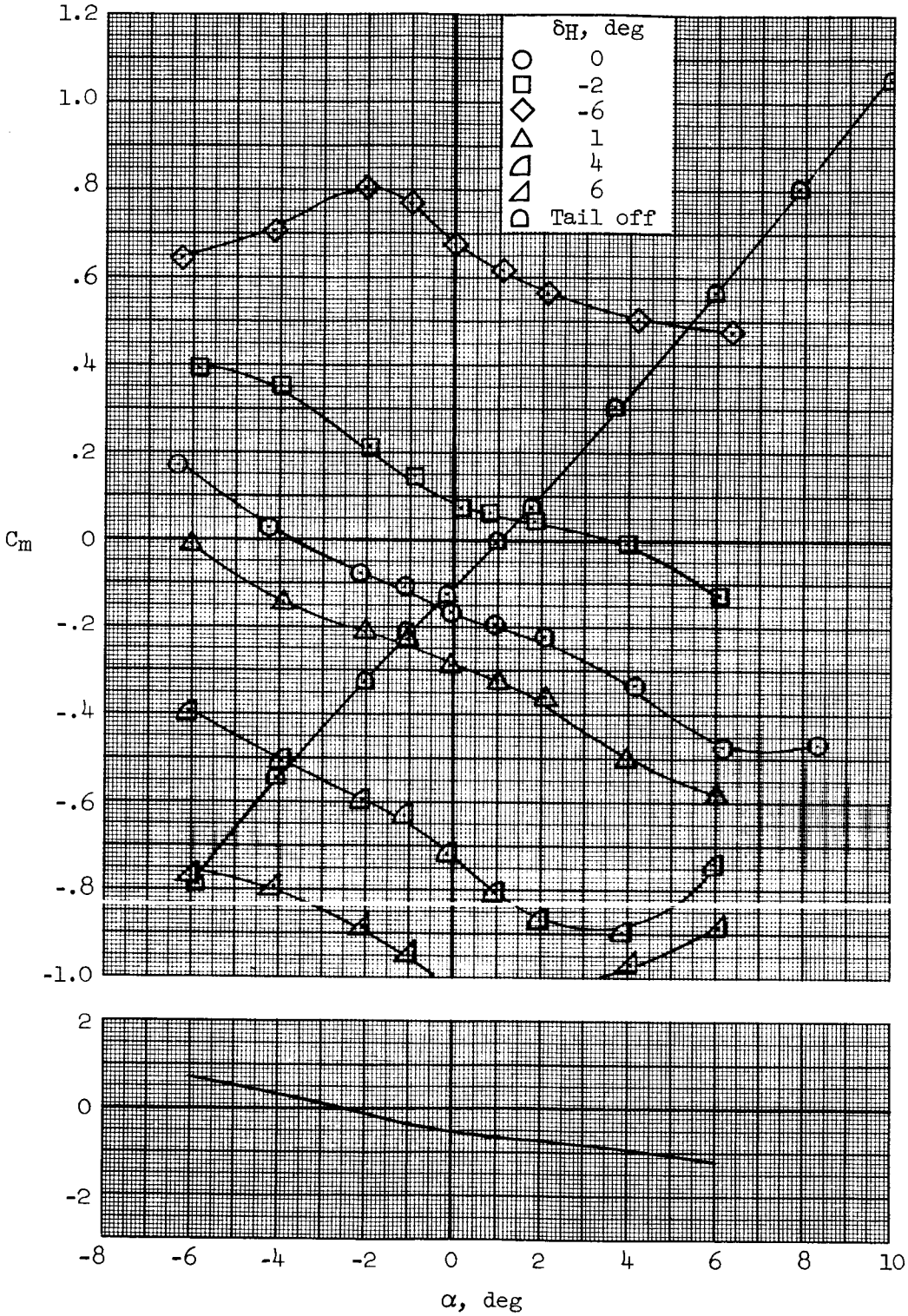

(c) $M_\infty = 0.90$

Figure 11.- Continued.

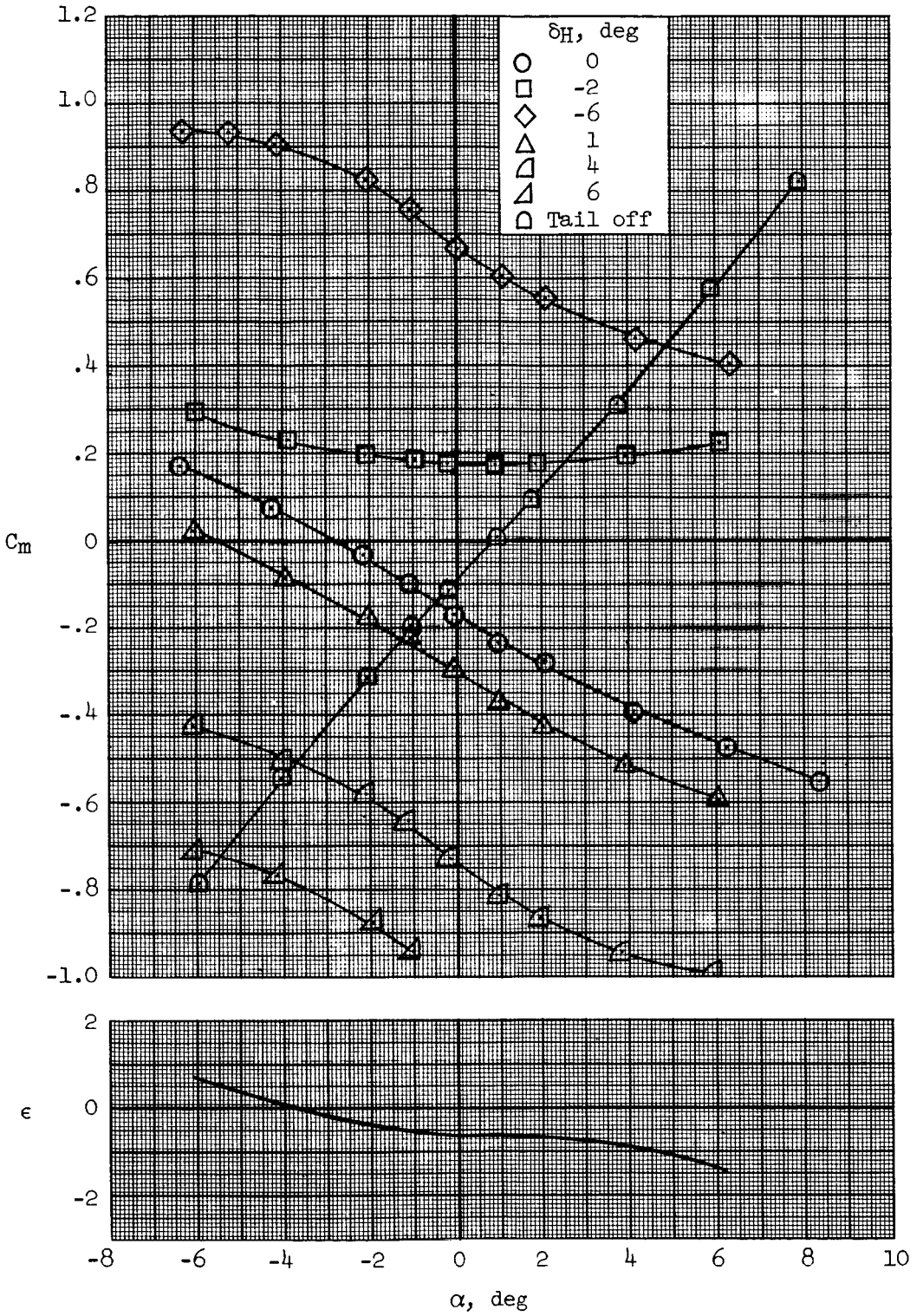

(d) $M_\infty = 1.00$

Figure 11.- Continued.

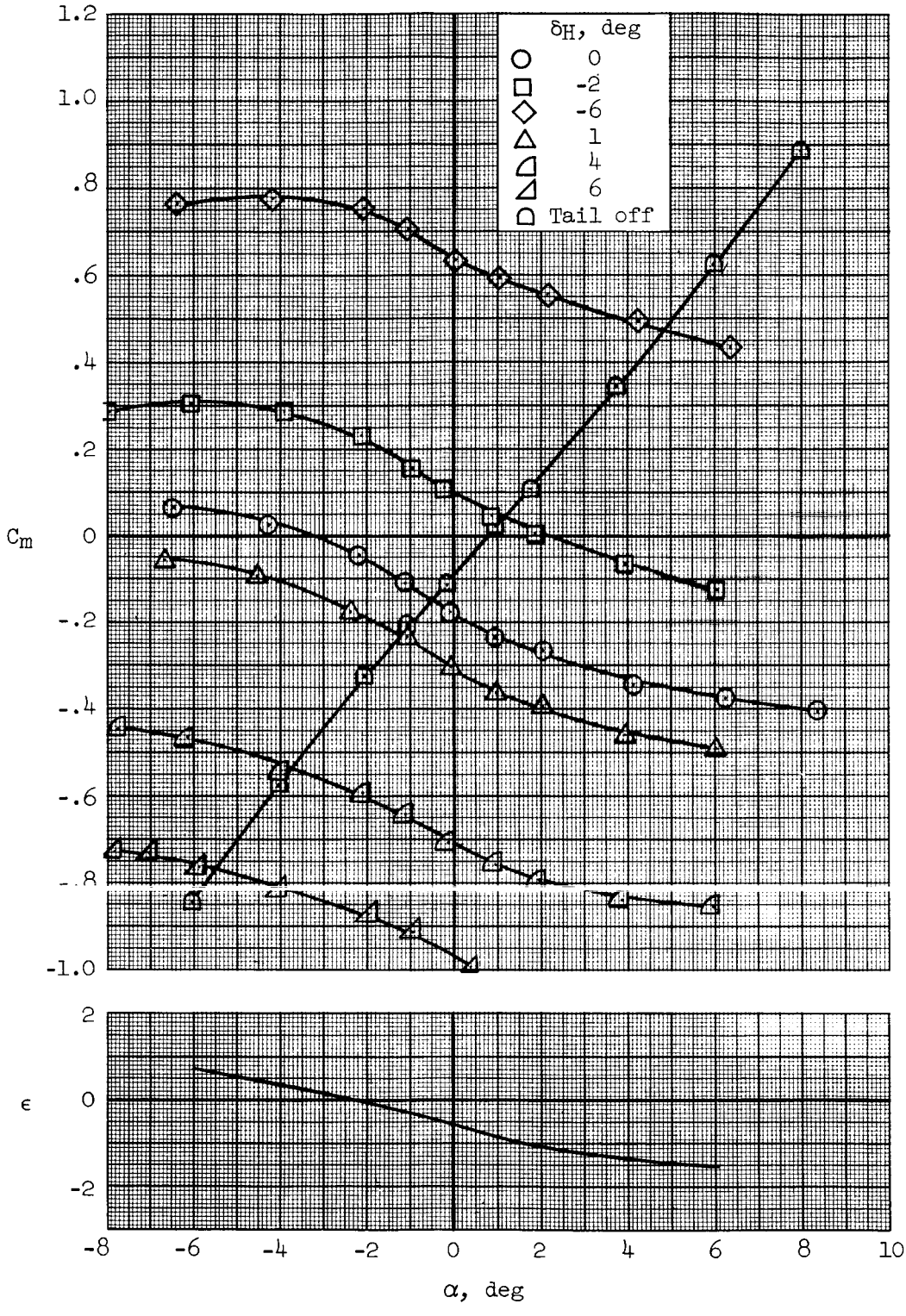

(e) $M_\infty = 1.10$

Figure 11.- Continued.

[redacted]

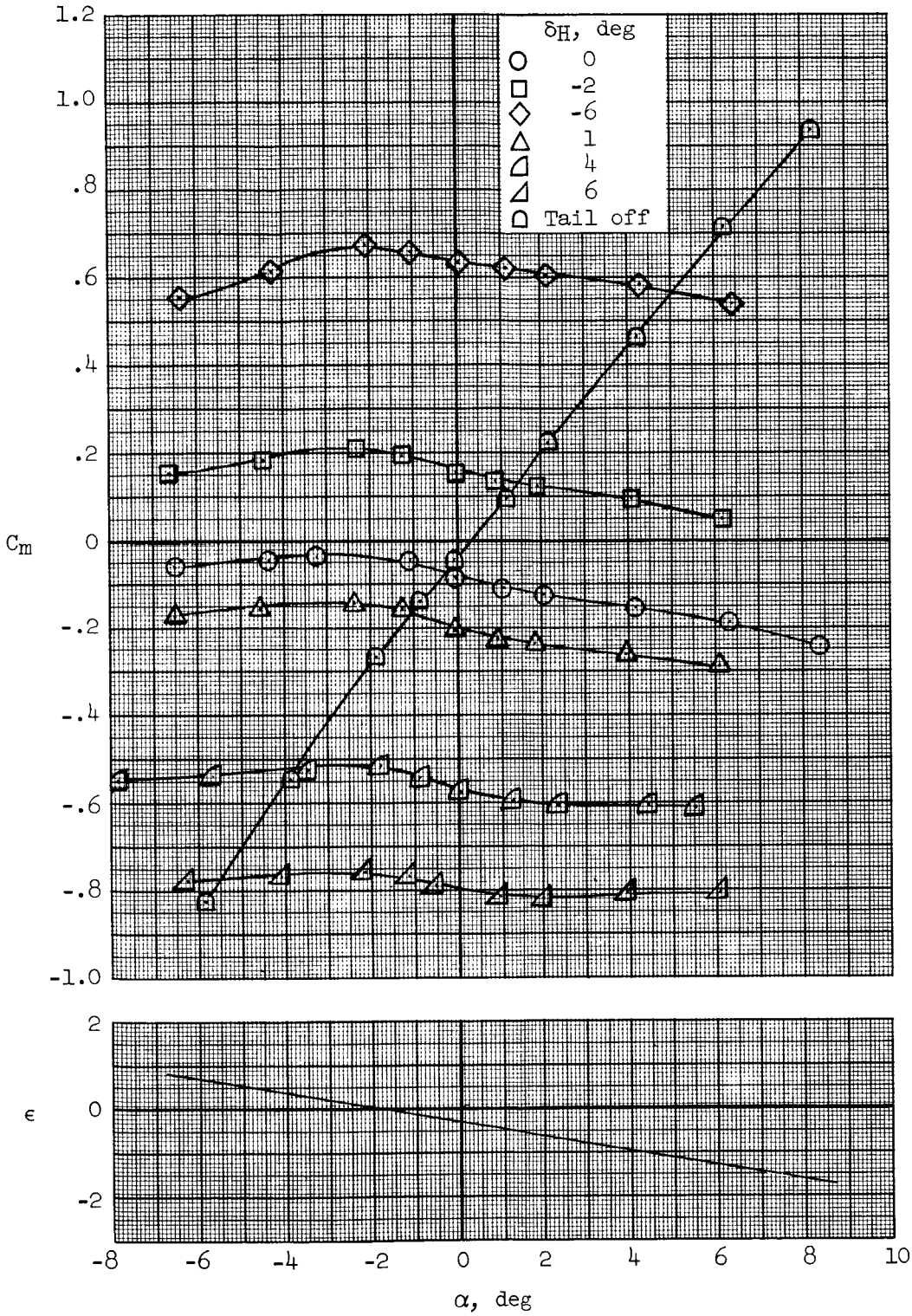

(f) $M_\infty = 1.30$

Figure 11.- Continued.

[redacted]

[redacted]

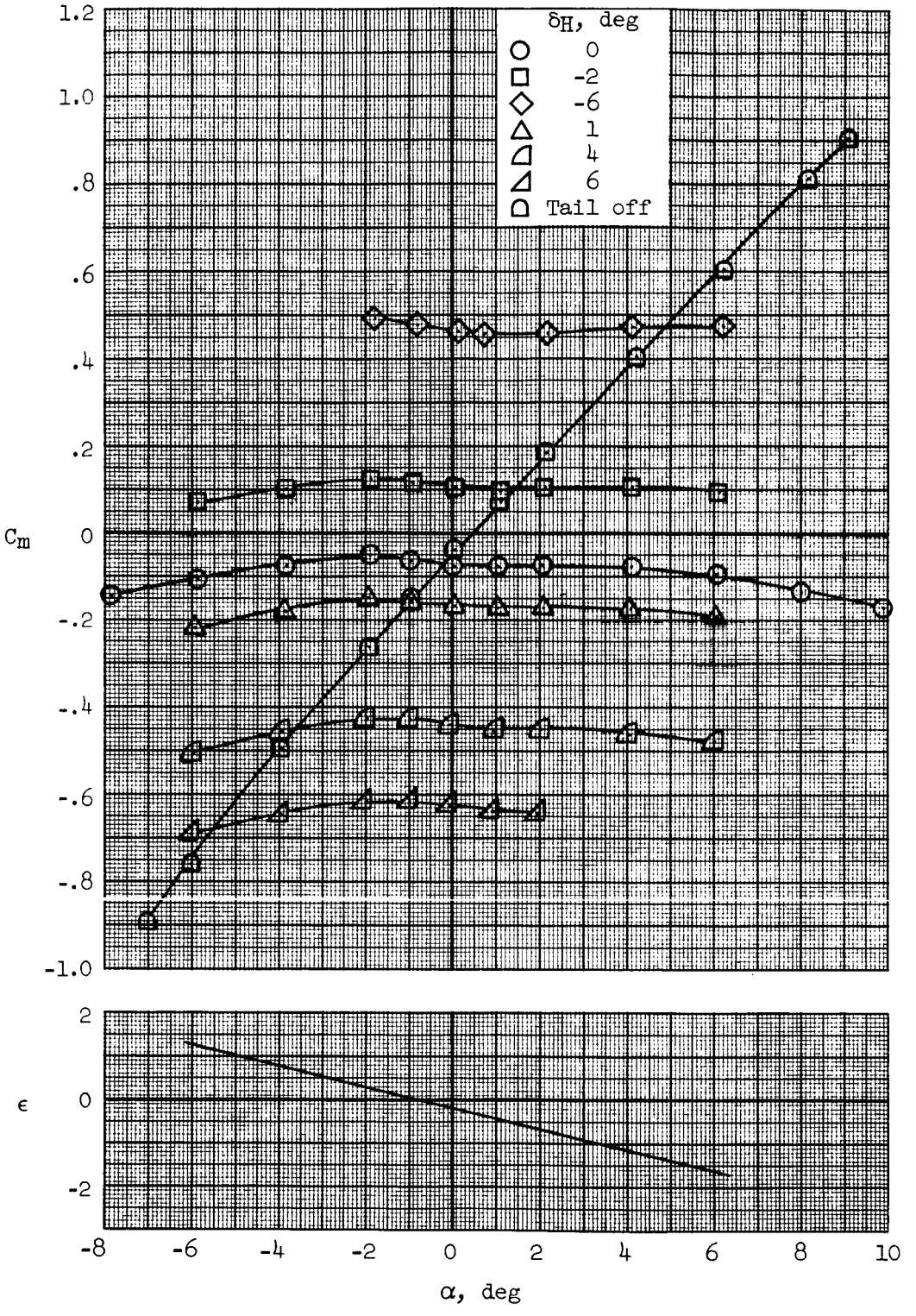

(g) $M_\infty = 1.55$.

Figure 11.- Continued.

[redacted]

[redacted]

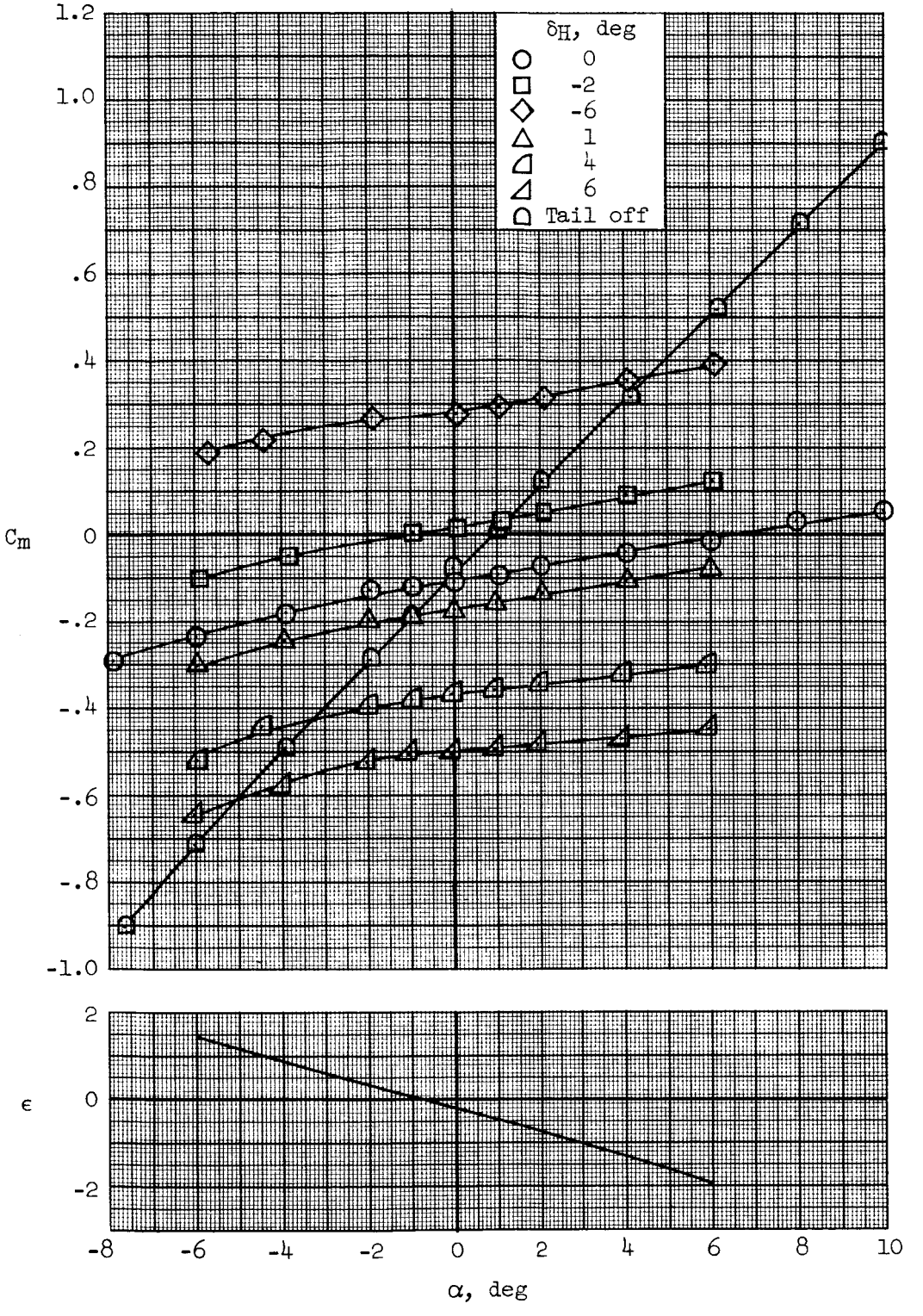

(h) $M_\infty = 2.01$

Figure 11.- Continued.

[redacted]

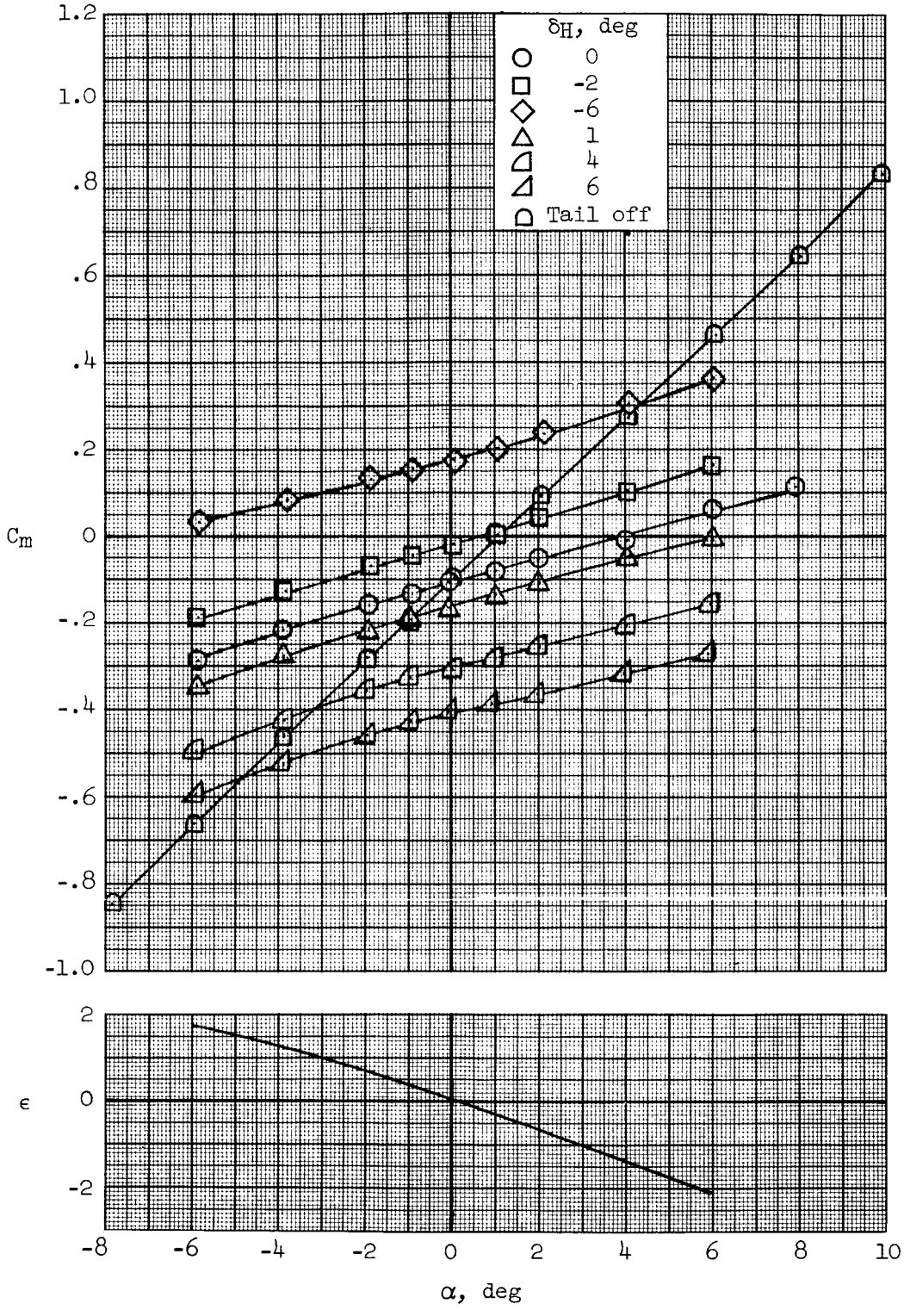

(i) $M_\infty = 2.51$

Figure 11.- Continued.

[redacted]

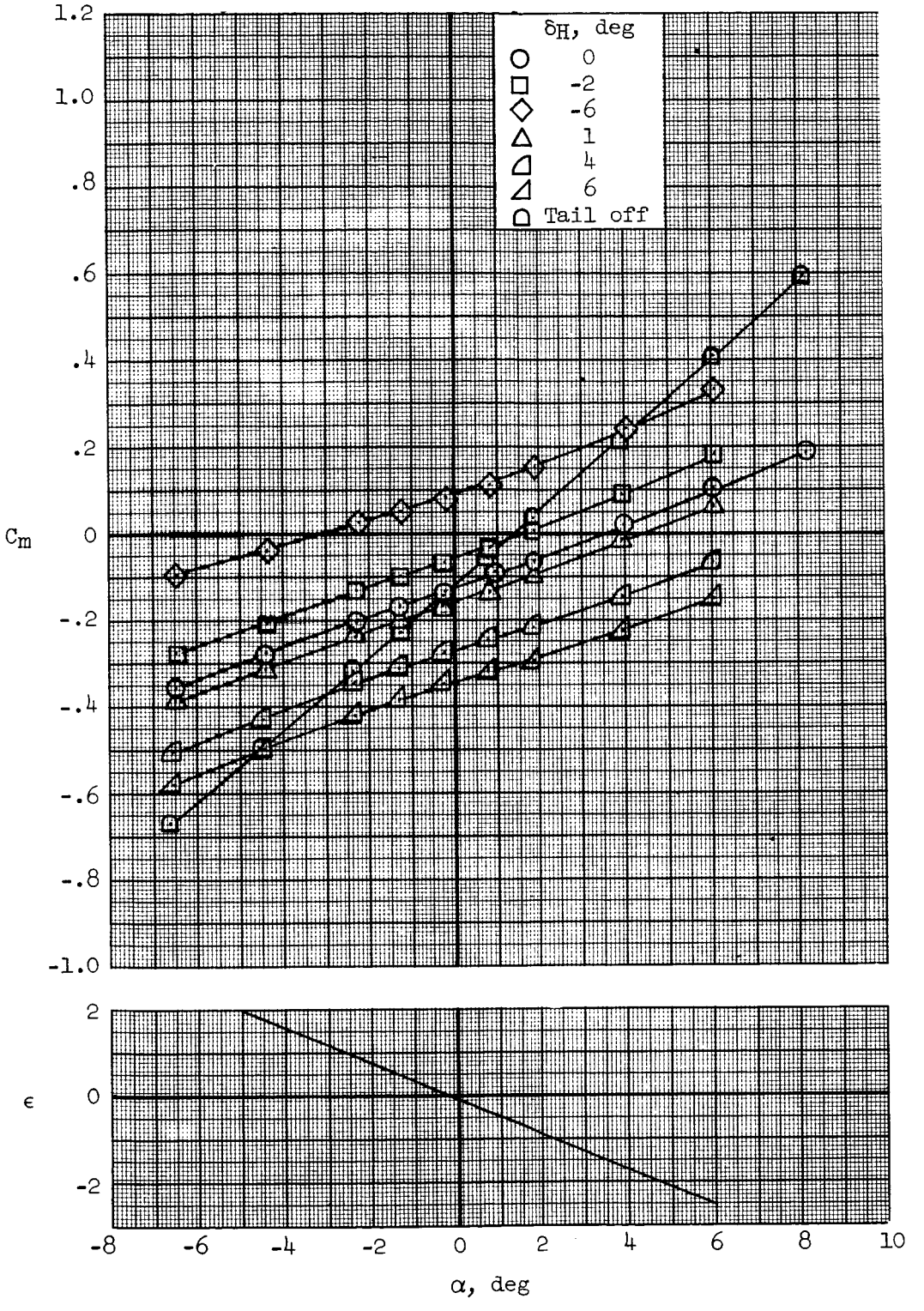

(j) $M_\infty = 3.05$

Figure 11.- Continued.

[redacted]

[redacted]

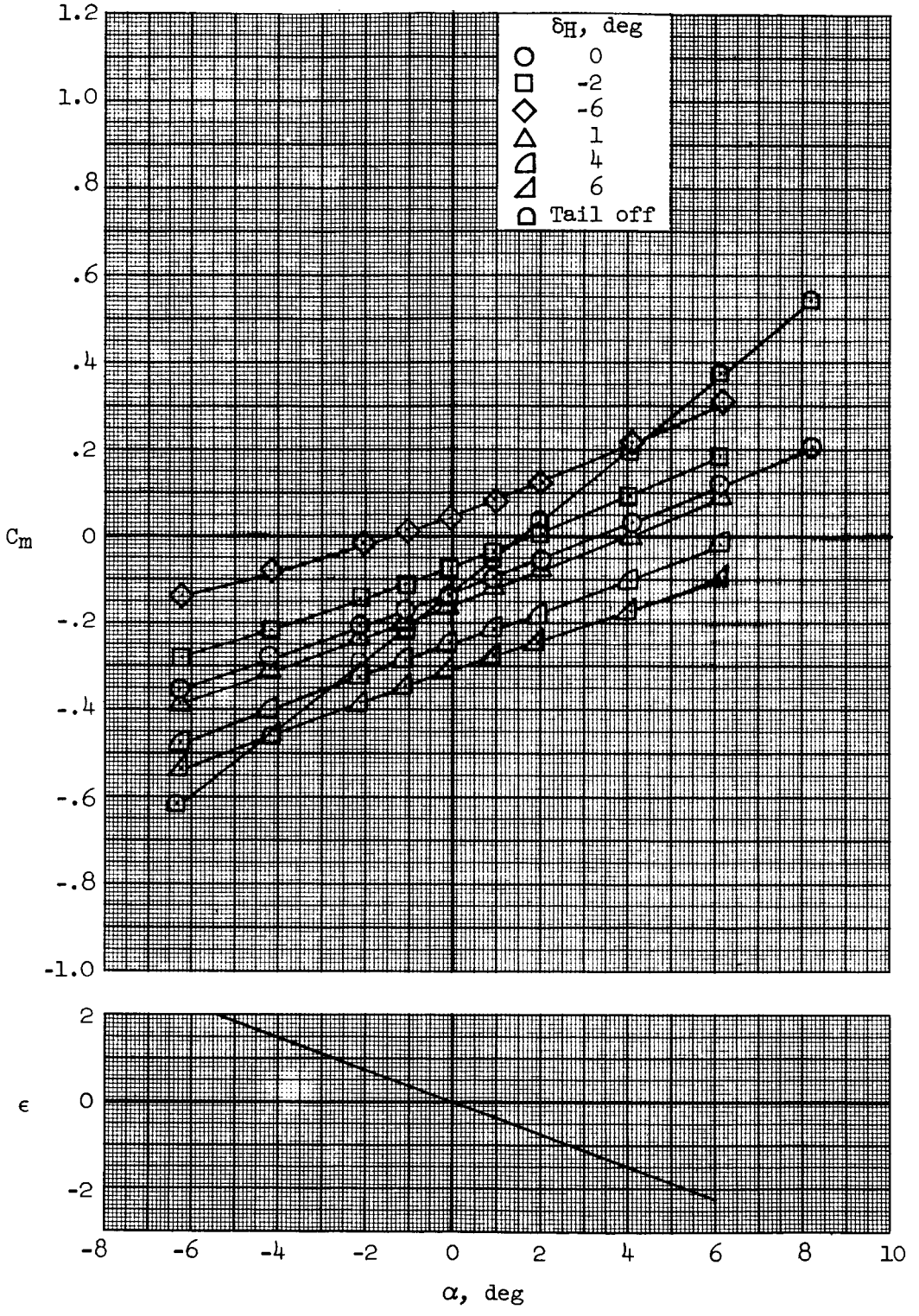

(k) $M_\infty = 3.52$

Figure 11.- Concluded.

[redacted]

[redacted]

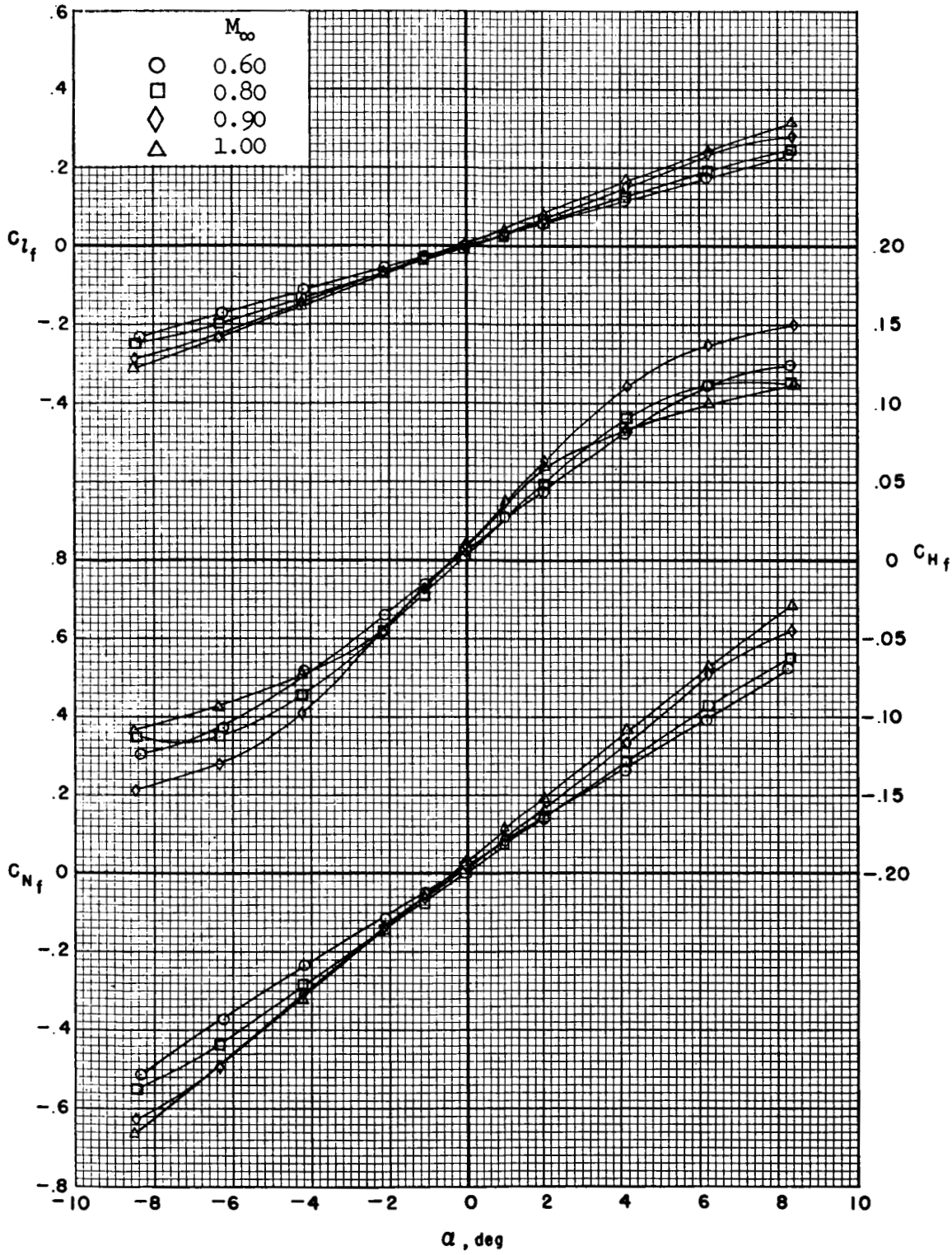

(a) M_∞ = 0.60 to 1.00

Figure 12.- Aerodynamic coefficients of the left horizontal booster fin at $\beta = 0°$ for several free-stream Mach numbers.

[redacted]

[redacted]

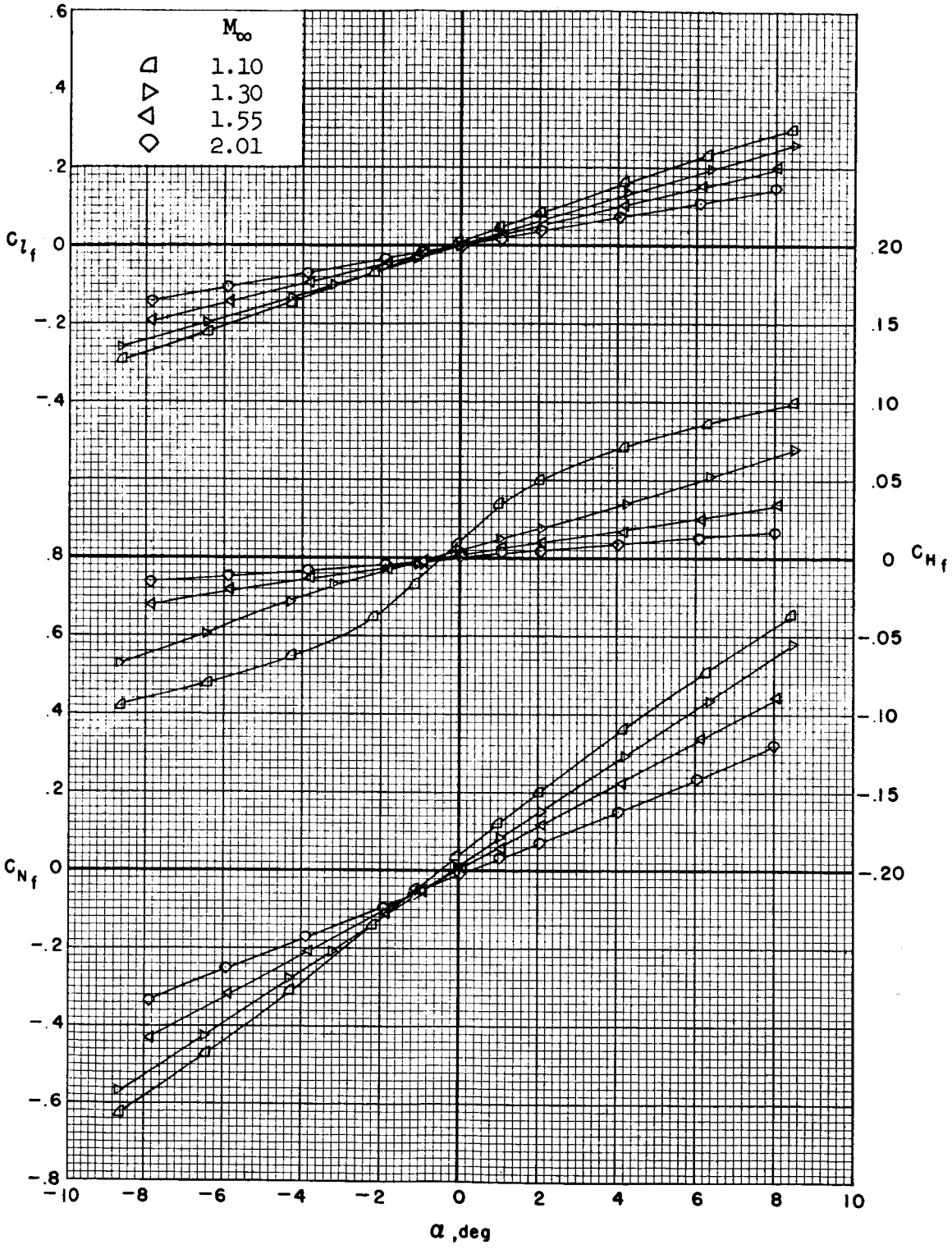

(b) M_∞ = 1.10 to 2.01

Figure 12.- Continued.

[redacted]

[redacted]

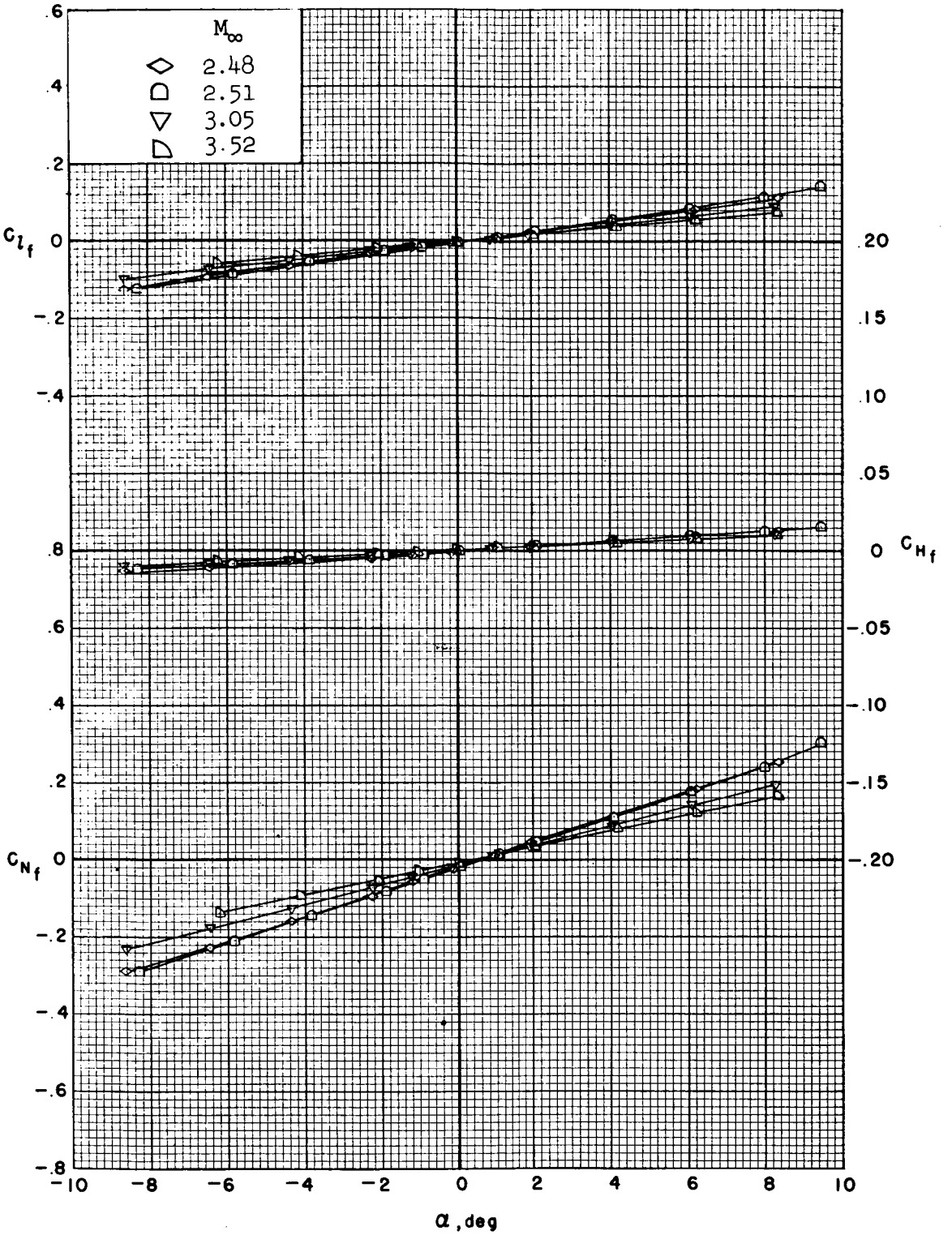

(c) M_∞ = 2.48 to 3.52

Figure 12.- Concluded.

[redacted]

[redacted]

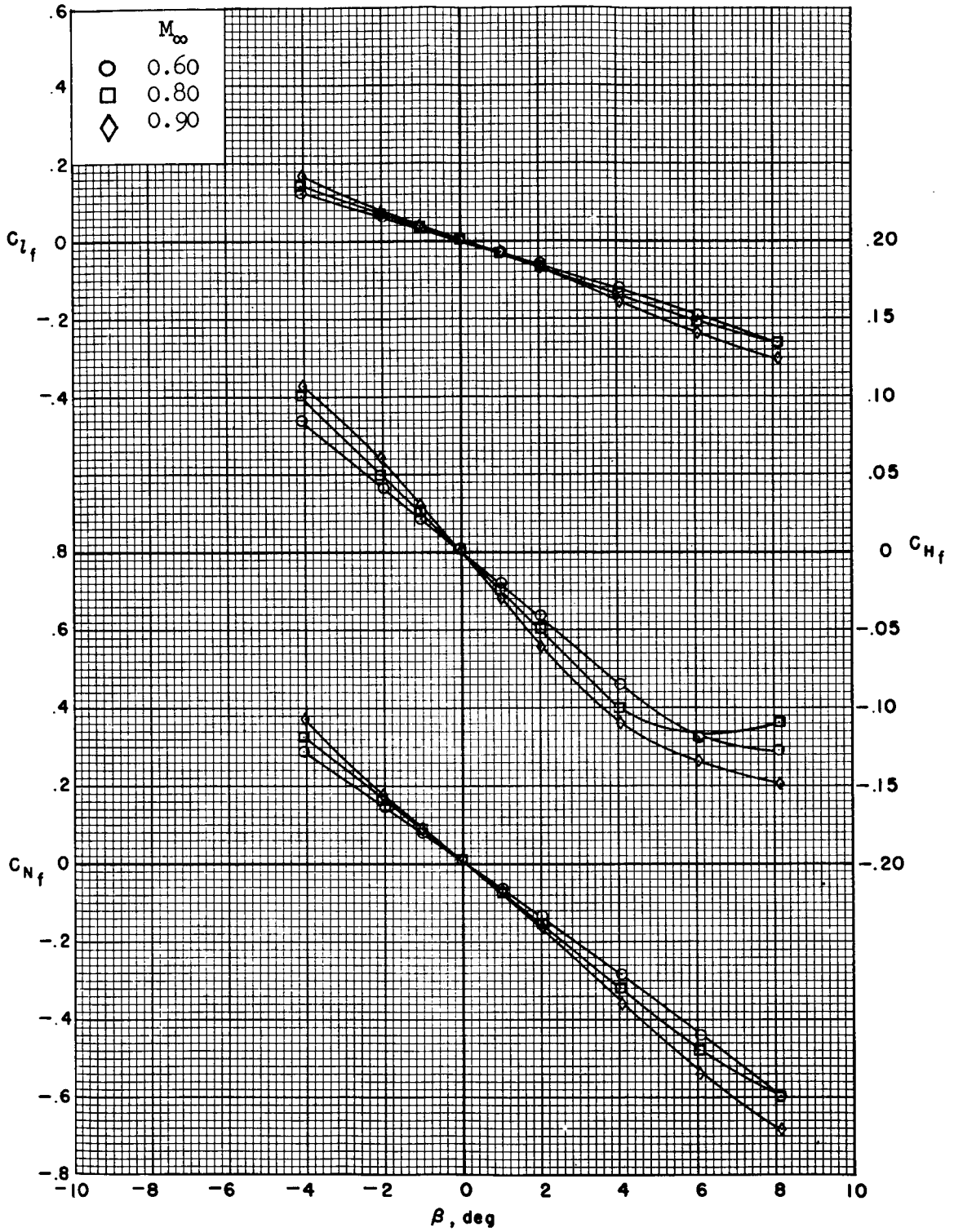

(a) M_∞ = 0.60 to 0.90

Figure 13.- Aerodynamic coefficients of the aspect ratio 3 upper vertical fin at $\alpha = 0°$ for several free-stream Mach numbers.

[redacted]

[redacted]

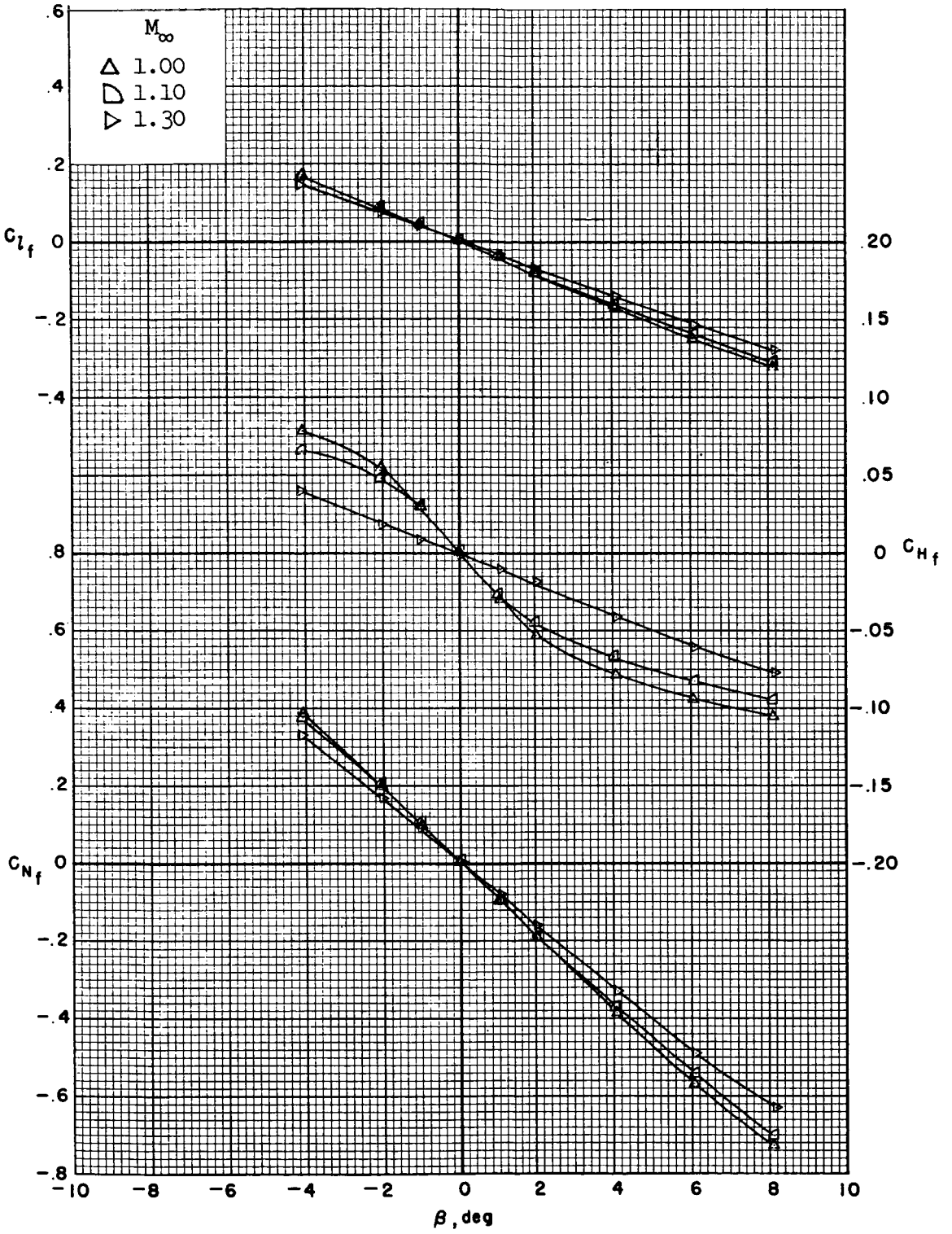

(b) M_∞ = 1.00 to 1.30

Figure 13.- Continued.

[redacted]

[redacted]

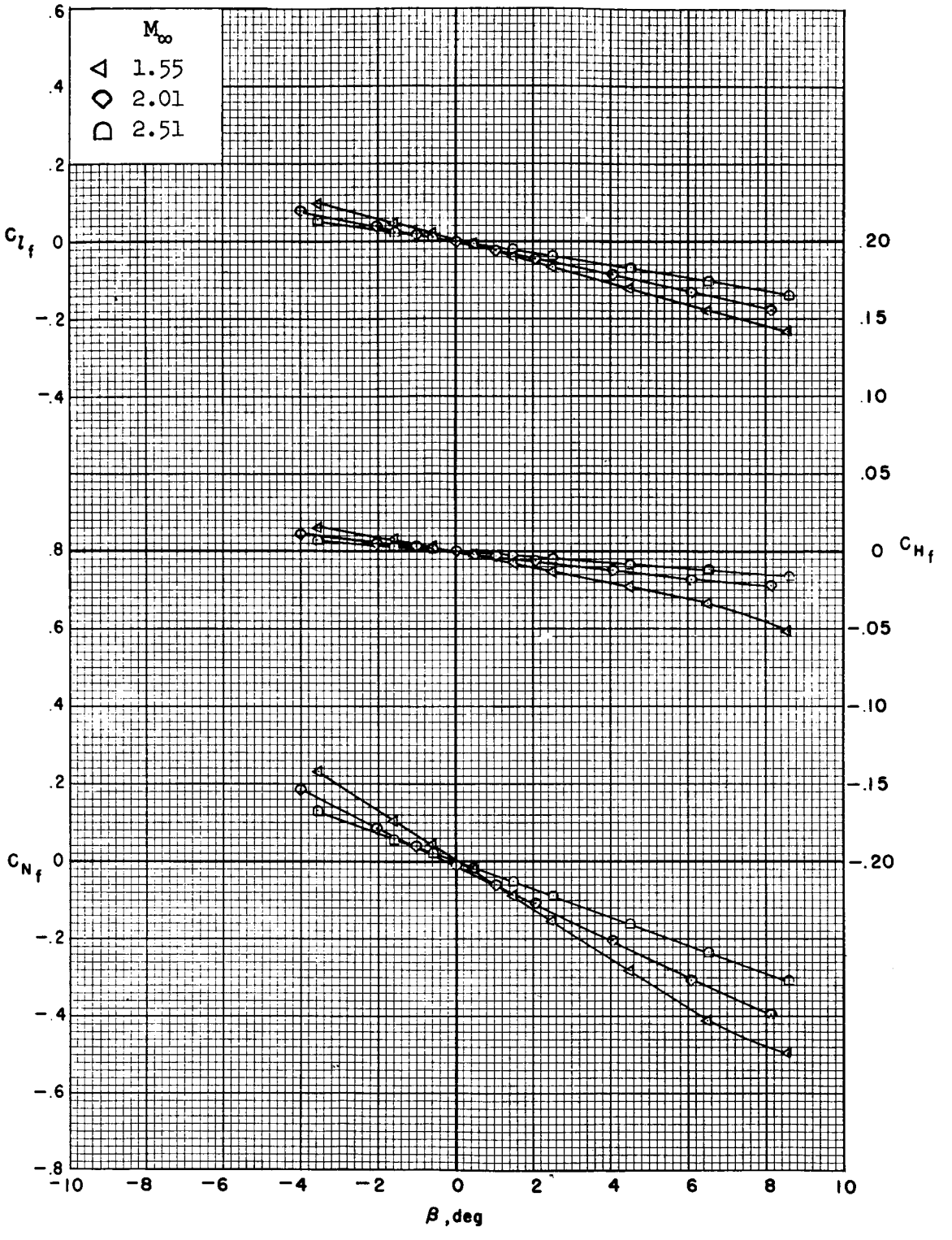

(c) M_∞ = 1.55 to 2.51

Figure 13.- Concluded.

[redacted]

[redacted]

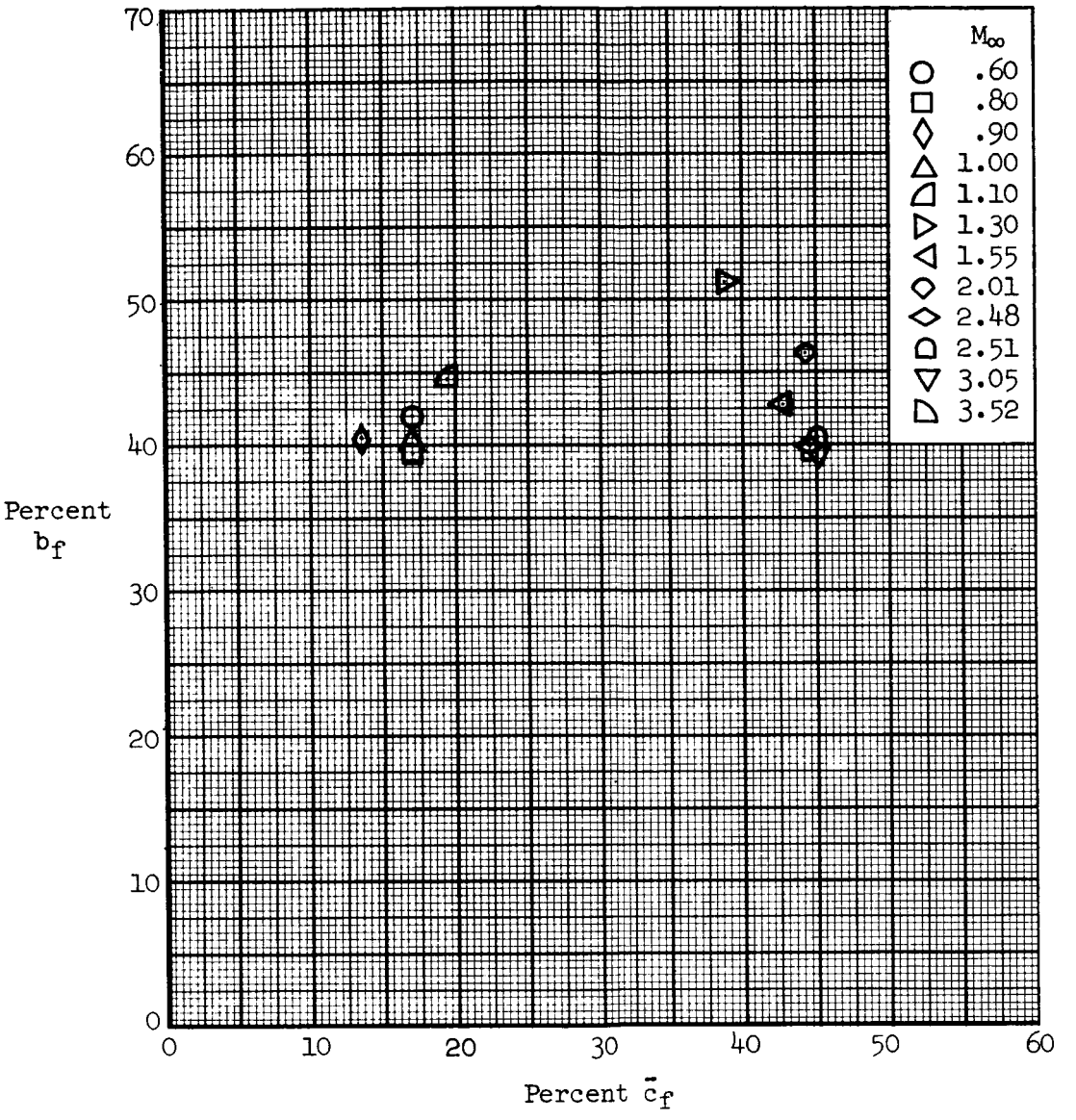

(a) $\beta = 0°$

Figure 14.- Location of center of pressure on the left horizontal booster fin at $\alpha = 0°$ for several free-stream Mach numbers and angles of sideslip.

[redacted]

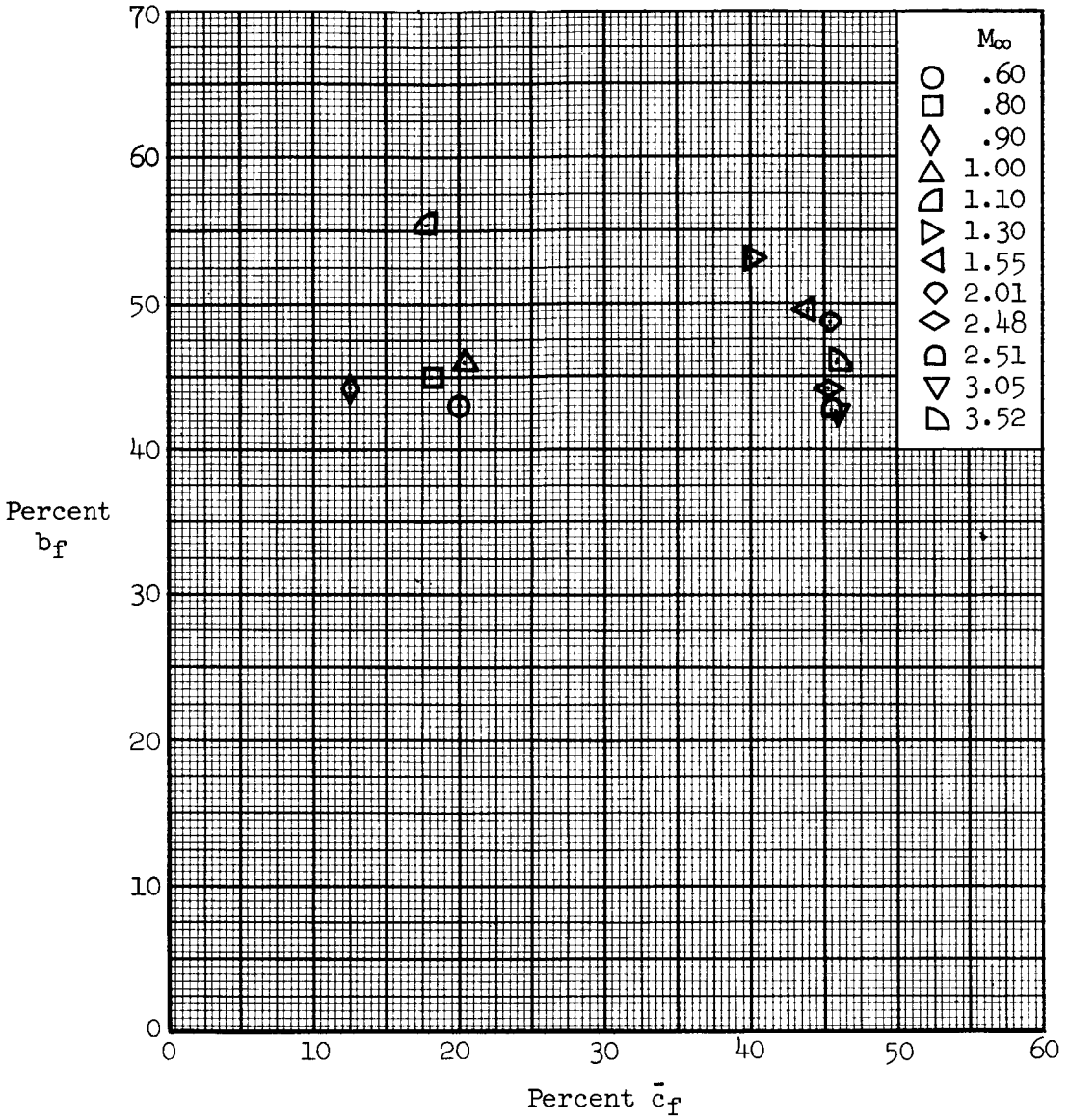

(b) $\beta = 3°$

Figure 14.- Continued.

[redacted]

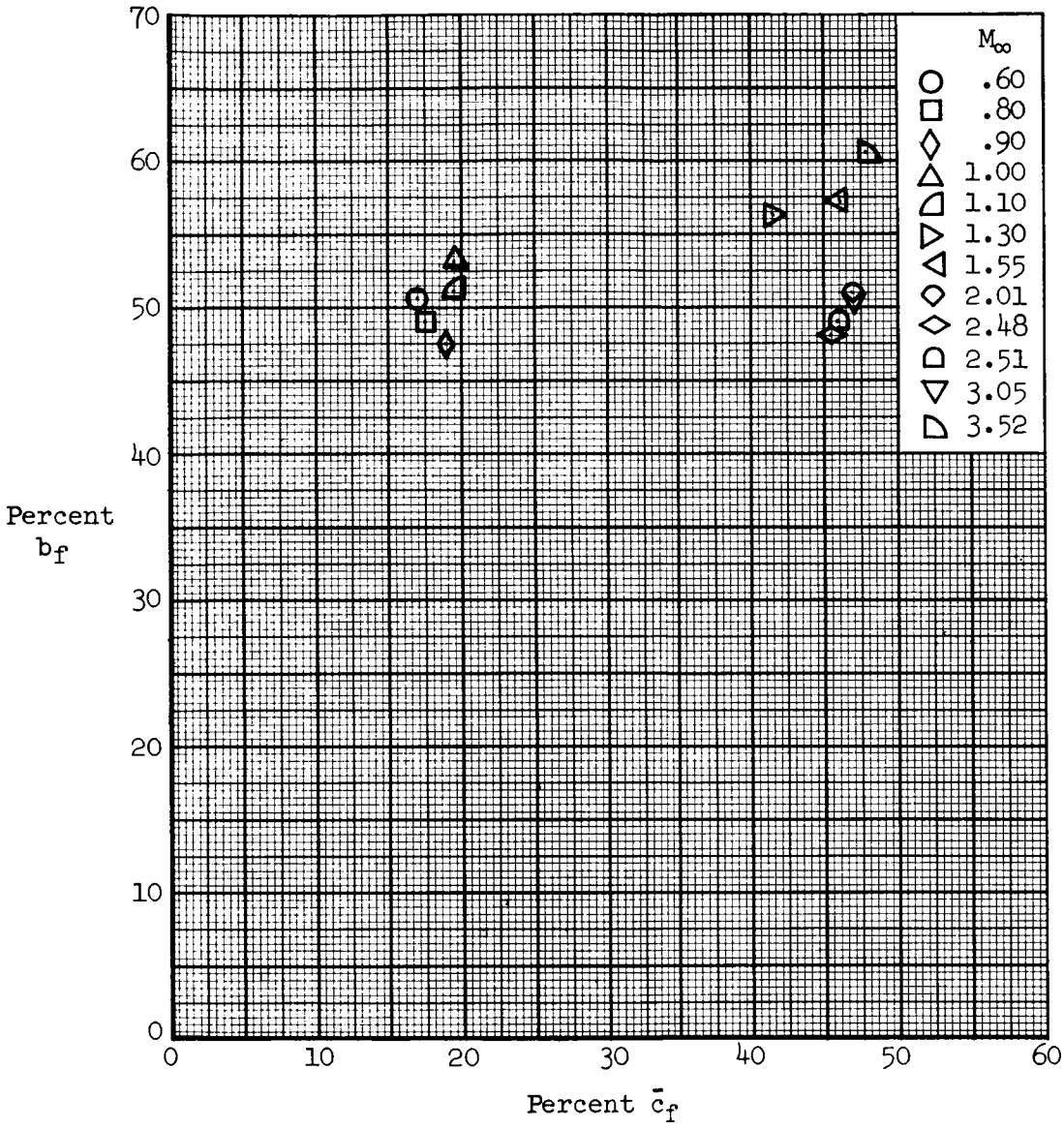

(c) $\beta = 6°$

Figure 14.- Concluded.

[redacted]

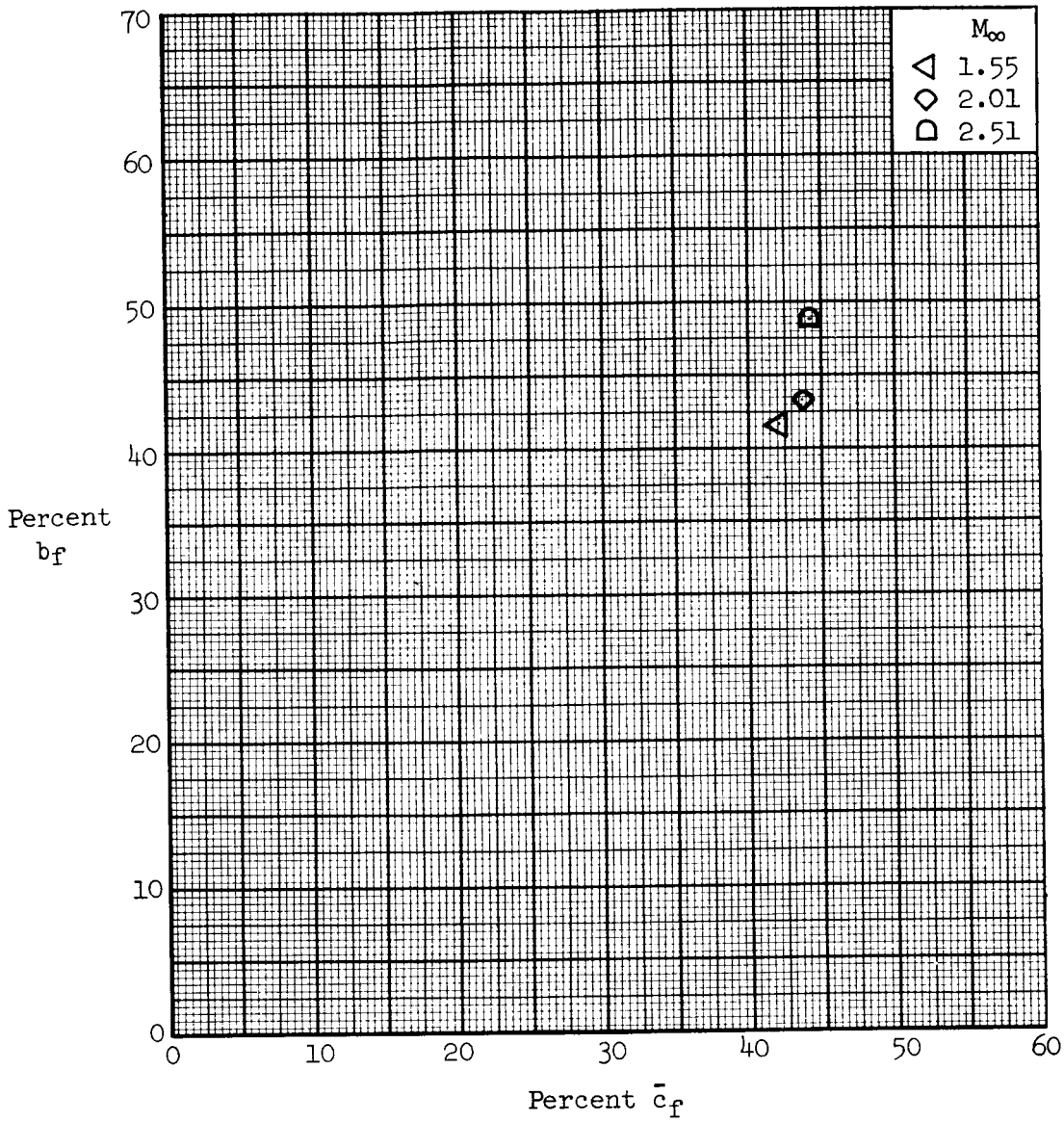

Figure 15.- Location of the center of pressure on the aspect-ratio-3 upper vertical booster fin at $\alpha = 0^\circ$, $\beta = 0^\circ$ for several free-stream Mach numbers.

NASA-Langley, 1964 A-626

[redacted]

"The aeronautical and space activities of the United States shall be conducted so as to contribute . . . to the expansion of human knowledge of phenomena in the atmosphere and space. The Administration shall provide for the widest practicable and appropriate dissemination of information concerning its activities and the results thereof."

—NATIONAL AERONAUTICS AND SPACE ACT OF 1958

NASA SCIENTIFIC AND TECHNICAL PUBLICATIONS

TECHNICAL REPORTS: Scientific and technical information considered important, complete, and a lasting contribution to existing knowledge.

TECHNICAL NOTES: Information less broad in scope but nevertheless of importance as a contribution to existing knowledge.

TECHNICAL MEMORANDUMS: Information receiving limited distribution because of preliminary data, security classification, or other reasons.

CONTRACTOR REPORTS: Technical information generated in connection with a NASA contract or grant and released under NASA auspices.

TECHNICAL TRANSLATIONS: Information published in a foreign language considered to merit NASA distribution in English.

TECHNICAL REPRINTS: Information derived from NASA activities and initially published in the form of journal articles.

SPECIAL PUBLICATIONS: Information derived from or of value to NASA activities but not necessarily reporting the results of individual NASA-programmed scientific efforts. Publications include conference proceedings, monographs, data compilations, handbooks, sourcebooks, and special bibliographies.

Details on the availability of these publications may be obtained from:

SCIENTIFIC AND TECHNICAL INFORMATION DIVISION

NATIONAL AERONAUTICS AND SPACE ADMINISTRATION

Washington, D.C. 20546

[redacted]